

RCA REVIEW

a technical journal

**RADIO AND ELECTRONICS
RESEARCH • ENGINEERING**

VOLUME XI,

JUNE 1950

NO. 2

RCA REVIEW

GEORGE M. K. BAKER
Manager

CHAS. C. FOSTER, JR.
Editorial Manager

SUBSCRIPTIONS:

United States, Canada, and Postal Union: One Year \$2.00, Two Years \$3.50, Three Years \$4.50
Other Countries: One Year \$2.40, Two Years \$4.30, Three Years \$5.70

SINGLE COPIES:

United States: \$.75 each. Other Countries: \$.85 each

Copyright, 1950, by RCA Laboratories Division, Radio Corporation of America

Published quarterly in March, June, September, and December by RCA Laboratories
Division, Radio Corporation of America, Princeton, New Jersey

Application for reentry as second class matter at the Post Office at Princeton,
New Jersey, under the act of March 3, 1879, is pending as a transfer
from the Post Office at New York, New York

RADIO CORPORATION OF AMERICA

DAVID SARNOFF, *Chairman of the Board*

FRANK M. FOLSOM, *President*

LEWIS MACCONNACH, *Secretary*

ERNEST B. GORIN, *Treasurer*

RCA LABORATORIES DIVISION

C. B. JOLLIFFE, *Executive Vice President*

RCA REVIEW

a technical journal

RADIO AND ELECTRONICS
RESEARCH • ENGINEERING

Published quarterly by

RADIO CORPORATION OF AMERICA
RCA LABORATORIES DIVISION

in cooperation with

RCA VICTOR DIVISION

RADIOMARINE CORPORATION OF AMERICA

RCA INTERNATIONAL DIVISION

RCA COMMUNICATIONS, INC.

NATIONAL BROADCASTING COMPANY, INC.

RCA INSTITUTES, INC.

VOLUME XI

JUNE 1950

NUMBER 2

CONTENTS

	PAGE
IN MEMORIAM—John G. Wilson	163
FOREWORD	<i>The Manager, RCA Review</i> 164
Studies of Thyatron Behavior, Part I—The Effect of Grid Resistance on the Recovery Time of Thyratrons	165
L. MALTER and E. O. JOHNSON	
Studies of Thyatron Behavior, Part II—A Study of the Effect of Grid Potential Variations During The Afterglow Period Upon the Recovery Time of Thyratrons	178
E. O. JOHNSON and L. MALTER	
A New Ultra-High-Frequency Television Transmitter	190
J. R. BENNETT and L. S. LAPPIN	
Ultra-High-Frequency Antenna and System for Television Trans- mission	212
O. O. FIET	
General Description of Receivers for the Dot-Sequential Color Tele- vision System Which Employ Direct-View Tri-Color Kinescopes..	228
Program Control Console For International Program Service	233
S. H. SIMPSON, JR., R. E. HAMMOND and M. P. REHM	
An Analysis of the Sampling Principle of the Dot-Sequential Color Television System	255
A Study of Cochannel and Adjacent-Channel Interference of Television Signals, Part II—Adjacent-Channel Studies	287
Stabilization of Wide-Band DC Amplifiers for Zero and Gain	296
E. A. GOLDBERG	
A Feedback-Controlled Calibrator For Phonograph Pickups	301
J. G. WOODWARD	
RCA TECHNICAL PAPERS	310
ADDENDUM	312
AUTHORS	313

RCA Review is regularly abstracted and indexed by *Industrial Arts Index*, *Science Abstracts* (I.E.E.-Brit.), *Engineering Index*, *Electronic Engineering Master Index*, *Abstracts and References* (*Wireless Engineer*-Brit. and *Proc. I.R.E.*) and *Digest-Index Bulletin*.

RCA REVIEW

BOARD OF EDITORS

Chairman

C. B. JOLLIFFE

RCA Laboratories Division

M. C. BATSEL

RCA Victor Division

G. L. BEERS

RCA Victor Division

H. H. BEVERAGE

RCA Laboratories Division

I. F. BYRNES

Radiomarine Corporation of America

D. D. COLE

RCA Victor Division

O. E. DUNLAP, JR.

Radio Corporation of America

E. W. ENGSTROM

RCA Laboratories Division

A. N. GOLDSMITH

Consulting Engineer, RCA

O. B. HANSON

National Broadcasting Company, Inc.

E. A. LAPORT

RCA International Division

C. W. LATIMER

RCA Communications, Inc.

H. B. MARTIN

Radiomarine Corporation of America

H. F. OLSON

RCA Laboratories Division

D. F. SCHMIT

RCA Victor Division

S. W. SERLEY

RCA Laboratories Division

G. R. SHAW

RCA Victor Division

R. E. SHELBY

National Broadcasting Company, Inc.

S. M. THOMAS

RCA Communications, Inc.

G. L. VAN DEUSEN

RCA Institutes, Inc.

A. F. VAN DYCK

RCA Laboratories Division

I. WOLFF

RCA Laboratories Division

V. K. ZWORYKIN

RCA Laboratories Division

Secretary

GEORGE M. K. BAKER

RCA Laboratories Division

REPUBLICATION AND TRANSLATION

Original papers published herein may be referenced or abstracted without further authorization provided proper notation concerning authors and source is included. All rights of republication, including translation into foreign languages, are reserved by RCA Review. Requests for republication and translation privileges should be addressed to *The Manager*.

IN MEMORIAM JOHN G. WILSON

It is with deep regret that *RCA Review* announces the death of John G. Wilson, Executive Vice President in charge of the RCA Victor Division, Radio Corporation of America. Mr. Wilson died suddenly at his home in Wynnewood, Pa., on June 1, 1950.

To an extent little realized outside the industry because of his abhorrence for personal publicity, Mr. Wilson was a potent force in the advancement of radio, television, acoustic and electronic science.



A firm believer in the close integration of engineering, manufacturing and merchandising, Mr. Wilson brought boldly courageous support during his six-year association with RCA Victor to forward-looking research, product design and technical service which would open mass markets for the developments of the laboratory. The commercial success of television is in no small measure due to his brilliant leadership and infectious enthusiasm.

Mr. Wilson would have been fifty years old in August. Born in Alma, Illinois, he rose to the position of executive head of the RCA Victor Division after 30 years of successful experience in the fields of finance and merchandising. In June, 1944, he joined the RCA Victor Division as administrator of accounts and finance, and a year later was advanced to Operating Vice President. In 1947, Mr. Wilson was elected Vice President and General Manager, succeeding in January, 1949, to the position of Executive Vice President.

Mr. Wilson's guidance and inspiration will be greatly missed but he left behind him a great strength, tremendous accomplishments and a host of friendships whose force for progress will endure for many, many years.

FOREWORD

TWO additional volumes in the *RCA Technical Book Series* are currently under preparation. These books, *TELEVISION, Volume V* and *TELEVISION, Volume VI*, together cover the period 1947 to June of 1950. It is expected that they will be ready for distribution sometime in August of this year.

With the appearance of these books, the *RCA Technical Book Series* will consist of twelve volumes:

TELEVISION, Vol. I 1933-1936	RADIO AT ULTRA-HIGH FREQUENCIES, Vol. I 1930-1939
TELEVISION, Vol. II 1936-1937	RADIO AT ULTRA-HIGH FREQUENCIES, Vol. II 1940-1947
TELEVISION, Vol. III 1938-1941	FREQUENCY MODULATION, Vol. I—1936-1947
TELEVISION, Vol. IV 1942-1946	RADIO FACSIMILE, Vol. I 1938
TELEVISION, Vol. V 1947-1948	ELECTRON TUBES, Vol. I 1935-1941
TELEVISION, Vol. VI 1949-1950	ELECTRON TUBES, Vol. II 1942-1948

The *RCA Engineering Book Series* volume—*PATENT NOTES FOR ENGINEERS*—originally published in 1947 has been revised in accordance with the new regulations of the United States Patent Office. This second edition of *PATENT NOTES FOR ENGINEERS* will be ready for distribution sometime in July of this year.

Further information on these volumes and on other material published by RCA Review may be obtained by writing to:

RCA Review
Radio Corporation of America
RCA Laboratories Division
Princeton, New Jersey

June 15, 1950

The Manager, RCA Review

STUDIES OF THYRATRON BEHAVIOR*

Part I.—The Effect of Grid Resistance on the Recovery Time of Thyratrons

BY

L. MALTER AND E. O. JOHNSON

Research Department, RCA Laboratories Division,
Princeton, N. J.

Summary—This paper is the first of a series describing results of studies of various aspects of thyatron behavior. The purpose of this part is to explain the role of grid resistance in recovery of grid control following the interruption of a discharge. A picture is presented of the processes which occur during the post-discharge (or afterglow) period and of the manner in which recovery of grid control is effected.

It is known that the Recovery Time of thyratrons increases with increasing value of grid resistance. It is shown that a common conception that this is due to decreased rate of deionization with increasing grid resistance is erroneous. On the contrary, the positive ion current to the grid (and consequently, deionization) is shown to be essentially independent of grid resistance and voltage. The increase of Recovery Time, in the presence of grid resistance, is due to a delayed return of the grid voltage to its bias value.

Recovery Time is demonstrated to depend upon the value of the instantaneous grid potential and in no appreciable way upon the course of the grid potential during the period following the interruption of the discharge unless an abrupt change in grid potential occurs shortly before recovery.

INTRODUCTION

IN A THYRATRON, firing can be prevented when a positive potential is applied to the anode, by the simultaneous application of a sufficiently negative potential to the grid. If the grid bias is decreased, the tube will fire when the bias crosses the so-called control characteristic curve. After the tube is fired, making the grid more negative than the value corresponding to the control characteristic does not result in an interruption of the discharge. The grid is said to have "lost control". During the discharge the negative grid surrounds itself with a positive ion sheath.¹ This sheath shields the surrounding plasma from the influence of the grid. Varying the potential of the grid merely serves to change the sheath thickness slightly without influencing the discharge in any fundamental fashion.

* Decimal Classification: R337.12.

¹ P. K. Hermann, "Über Entionisierung und Wiederzundung Gittergesteuerter Gasentladungs Gefasse," *Archiv. fur Elektrotechnik*, Vol. 30, pp. 555-580, 1936.

In order to enable the grid to recapture control, it is necessary to interrupt the discharge by dropping the anode potential below a definite value. After the interruption of the discharge, a finite time must elapse before the grid recaptures control. To determine whether the grid has recaptured control a signal is applied to the plate to determine whether the tube will fire. The time it takes for the grid to recapture control is here designated as the "Recovery Time" (hereinafter denoted by T_R).*

It is well known that at fixed bias, T_R increases with the magnitude of the grid resistance R_g . The common conception of the mechanism whereby this result is produced appears to be in error. It is commonly believed that:

1. Deionization,† and consequently recovery, is speeded up by making the grid more negative.
2. Large values of R_g make the grid voltage return to its bias value more slowly, thus resulting in a decrease of the positive ion current and a slowing down of the deionization.

Thus, Germeshausen² states: "Deionization . . . can be accelerated by applying a negative grid bias to pull the ions to the grid. . . . The time required to remove the ions depends on the degree of ionization, which is a function of the bias voltage, and on the impedance in series with this voltage."

Ostendorf³ states: "The values of the grid resistance and grid bias battery are important in determining the rate of ion loss."

Shepherd⁴ states: "The deionization by a negative grid is proportional to the negative grid potential."

* The quantity herein referred to as "Recovery Time", is usually designated by the term "Deionization Time". These studies however, indicate that recovery of grid control may occur when intense ionization is still present in the tube. This makes the term Deionization Time definitely unsuitable. This paper conforms to the notation of Hermann¹ who recommends the use of the term Recovery Time (Freiwerdezeit) in the sense in which it is used here, and the term Deionization Time (Entionizierungszeit) to denote the time it takes the tube to return to the state it was in just before firing. (Studies here show that there is a sharply defined Deionization Time.)

† "Deionization" is understood to be the decrease of ion and electron density in the tube plasma following the interruption of a discharge. Deionization in thyratrons is generally due to diffusion of ions and electrons to walls and electrodes.

² PULSE GENERATORS, edited by G. N. Glasoe and J. V. Lebacqz; Chapter 8, "The Hydrogen Thyatron" by K. J. Germeshausen, p. 354, McGraw-Hill Book Company, Inc., New York, N. Y., 1948.

³ W. Ostendorf, "Entionisierung von Stromrichtern," *Elektrotechnische Zeitschrift*, Vol. 59, pp. 87-89, January, 1938.

⁴ W. G. Shepherd, "Deionization Considerations in a Harmonic Generator Employing a Gas-Tube Switch," *Proc. I.R.E.*, Vol. 31, pp. 66-74, February, 1943.

In contrast with the above, the following statement appears in the paper by Hermann¹: "During deionization, a plasma of decreasing density is present. The density is independent of electrode potentials."

As will be seen below, experiment indicates that Hermann's statement is in much closer agreement with the facts than those of the other authors, whose conclusions appear to be based upon inadequate data or on a misinterpretation of existing data. Thus, a conception of the effect of grid resistance upon T_R is required, which fits in with the observations that the deionization of the tube, and the positive-ion current to the grid, are essentially independent of the value of the grid voltage and of the grid resistance. A picture consistent with all the observations will be presented.

CONSIDERATIONS REGARDING RECOVERY TIME

Fundamental studies of the behavior of a decaying plasma following the interruption of a gas discharge have led to a formulation of the conditions necessary for recovery. When the discharge in a thyatron is interrupted, the tube is substantially completely suffused with a plasma (a region of practically equal ion and electron density). As the plasma decays, i.e., as the ionization diminishes, it does so in a manner whereby the plasma retains its plasma-like characteristics. This is accomplished primarily by an equal rate of loss of electrons and ions by diffusion to the walls and electrodes.

If the grid is negative with respect to the plasma, it will surround itself with a positive ion sheath. As the plasma decays, the sheath thickness increases. The positive-ion current to the grid is determined by the rate at which ions diffuse out of the plasma into the sheath. Since the sheath area surrounding the grid varies only slightly with grid potential, one would expect the positive-ion current to the grid to be almost (but not quite) independent of grid potential.⁵ This in turn implies that the density of ionization in the plasma will be practically uninfluenced by the grid potential.

As the plasma decays, the sheath around the negative grid increases in thickness until it finally extends across the grid opening or openings.⁶ When this occurs the residual plasmas in the anode and cathode spaces become independent and can assume different potentials. During the decay the net rate of loss of electrons and ions from each of these

⁵ I. Langmuir and H. M. Mott-Smith, "Studies of Electric Discharges in Gases at Low Pressures," *General Electric Review*, Vol. 27, pp. 449-455, 538-548, 616-623, 762-771, 810-820, 1924.

⁶ W. Koch, "Experimental Demonstration of the Existence of Ion Sheaths at Electrodes of Rectifiers During Deionization," *Zeit. fur Tech. Physik*, Vol. 17, p. 446, 1936.

plasmas must be equal. This condition is satisfied in the anode-grid region, by the plasma assuming a potential slightly positive with respect to the anode.⁶ This prevents the excessive loss of electrons due to their higher velocities. In the cathode-grid region where the plasma is in contact with a copious electron emitter, the plasma normally goes slightly negative with respect to the cathode, in order to satisfy the net loss equality condition. If a positive potential is now applied to the anode, the plasma potential in the grid-anode region will almost instantaneously assume a value slightly positive with respect to the anode, leading to a potential distribution through the tube as shown in Figure 1. The tube now behaves like a thyatron with reduced spacings, the "effective cathode" being at A and the "effective anode" at B. Whether or not the tube fires depends closely on whether or not a thyatron with cathode at A, anode at B, and grid at G, and with the potentials as shown in Figure 1 will refire. As time progresses, the grid sheath expands, forcing A and B farther away from the grid. Thus, the effective refiring geometry varies in the fashion that one would expect, to explain the observed results that T_R increases with anode refiring voltage and with increasing negative grid voltage. Ultimately, as the grid sheath expands, the control ratio gets larger approaching as a limit the control ratio of the unfired tube.

This picture, which was developed independently in this laboratory and which will be presented fully in a forthcoming paper was subsequently found to be similar to one presented by Romanowitz.⁷

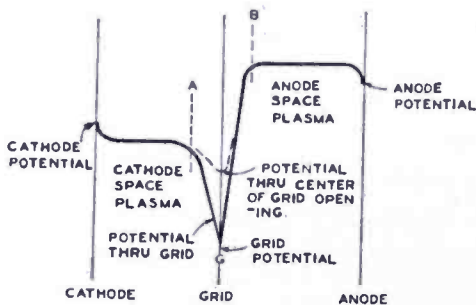


Fig. 1 — Potential distribution in thyatron during afterglow.

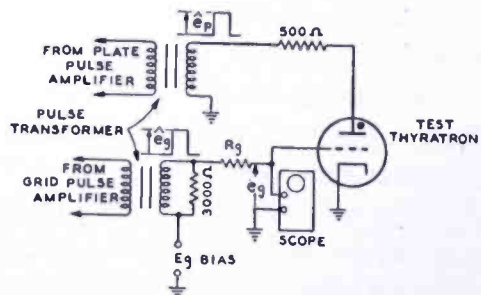


Fig. 2 — Test circuit for studying grid current during afterglow.

METHOD FOR MEASUREMENT OF GRID CURRENT DURING AFTERGLOW

The measurements were all made on a commercial thyatron containing mercury vapor and argon. The circuit employed is shown in Figure 2. The circuit shown in Figure 2 is merely the tail end of

⁷ H. A. Romanowitz, "Measurements, Analysis, and Statistical Nature of Deionization Time in a Mercury Vapor Thyatron," Engineering Experiment Station Bulletin, University of Kentucky, Vol. 2, No. 2, December, 1947.

complex circuitry developed in these laboratories for the study of T_R and plasma decay. With it one can vary the electrode potentials in desired fashions and study the consequent current flow to electrodes and probes as a function of time.

To fire the tube, the plate and grid were subjected simultaneously to 7-microsecond pulses. The anode pulse, \hat{e}_p , was 800 volts and the grid pulse, \hat{e}_g , was 135 volts. These are the values when the tube is unfired. They drop to lower values on firing. The plate current during the pulse was 600 milliamperes. The pulse repetition rate was 60 per second.

After each pulse, the anode potential would ordinarily go about 20 volts negative and then return to ground potential in about 100 microseconds. The insertion of a damping diode across the plate pulse transformer reduced the negative overshoot to about 1.5 volts. This had no effect on the observed data. This is in accord with extended observations⁸ that varying anode potential does not ordinarily affect the rate of plasma decay.

The grid circuit is driven by a cathode follower. The initial indicial admittance of the cathode follower output shunted by the 3000-ohm resistor across the grid pulse transformer is about 1800 ohms. The indicial admittance decays with a time constant of about 100 microseconds. These figures are such that, with the values of R_g employed in the tests, the effect of the grid drive circuit may be neglected during the decay period. For all practical purposes, the effective value of the grid circuit resistance is given by the value of R_g employed.

During the discharge and the following decay period the grid voltage was measured as a function of time by means of the oscilloscope as shown. From these measurements and from the values of R_g , the grid current at any instant could be determined.

The first set of measurements was made by varying R_g while holding E_g constant at -40 volts. The oscillograms are shown in Figure 3.

The second set of measurements was taken by varying E_g and holding R_g constant at 26,000 ohms. The results are shown in Figure 4.

In all the work, the tube was first permitted to run for at least 15 minutes before taking data, in order to insure temperature equilibrium.

While the data here taken and presented all apply to the commercial thyatron studied, additional tests on other commercial and experimental thyratrons further confirm the conclusions drawn.

⁸ J. R. Cance, "Note on the Deionization Times of Gas-Filled Thyratrons," *Jour. Sci. Instr.*, Vol. 23, p. 50, March 1946.

ANALYSIS OF EXPERIMENTAL GRID-CURRENT MEASUREMENTS

Series 1 — E_g Constant

Consider first the data shown in Figure 3. For these cases E_g was held constant at -40 volts while R_g was varied. The e_g curves have the form shown in Figure 5.

It was found in each case that, in the initial flat region present after interruption of the discharge, the grid (within limits of measurement) was at cathode potential. After a time $\approx T$, the grid potential drops off exponentially to the bias value of -40 volts. From Figure 5 it is seen that

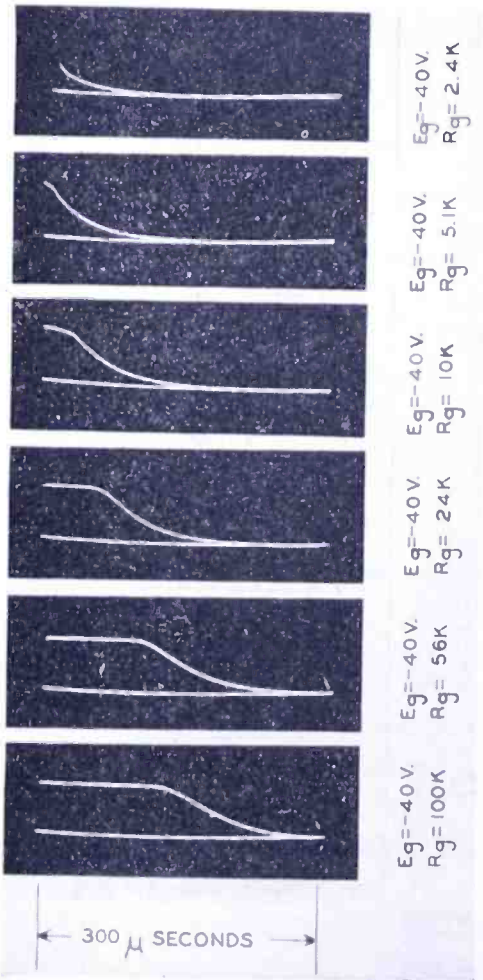


Fig. 3—Grid voltage pattern during afterglow.

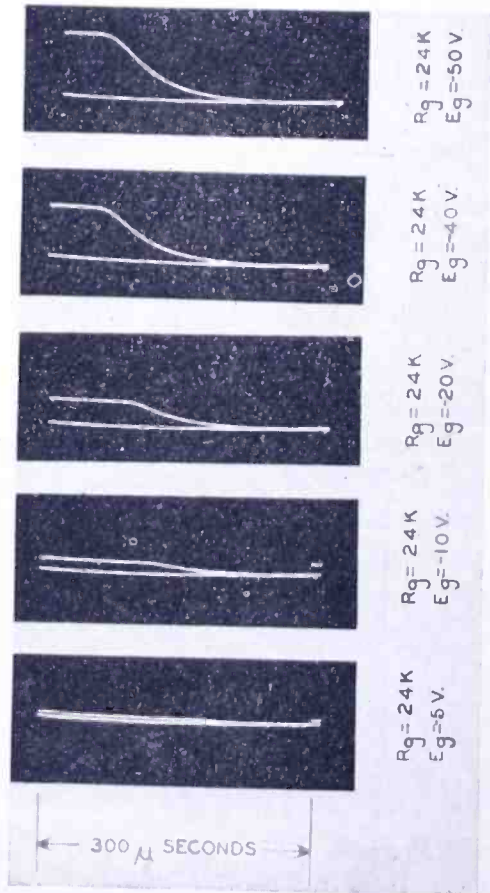


Fig. 4—Grid voltage pattern during afterglow.

$$e_g = [-40 - i_g R_g] \text{ volts.} \tag{1}$$

Therefore
$$|i_g| = \left(\frac{e_g + 40}{R_g} \right) \text{ amperes.} \tag{2}$$

It is thus seen that $|i_g| = 40/R_g$ along the flat portion of the grid-voltage characteristic (where $e_g = 0$) and then decays. i_g was computed for the decaying portions of characteristics of the various curves of Figure 3. The results are plotted as a function of time in Figure 6. It is seen that i_g can be expressed in the form

$$i_g = i_{g0} e^{-\frac{t}{\tau}}, \tag{3}$$

where the ion-current decay constant, τ , is 52 microseconds, and $i_{g0} = 6.0$ milliamperes.* It would appear from a cursory analysis that the grid current is due to positive ions and is constant until $t \approx T$ and then decays exponentially. The following hypothesis is offered instead. The positive-ion grid current is initially 6.0 milliamperes and decays exponentially with the time constant τ . However, when

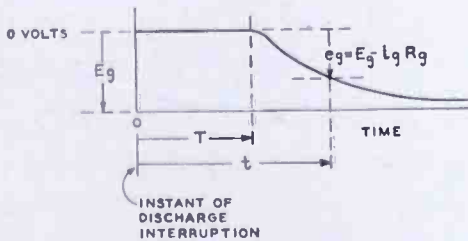


Fig. 5—Detailed grid voltage pattern during afterglow.

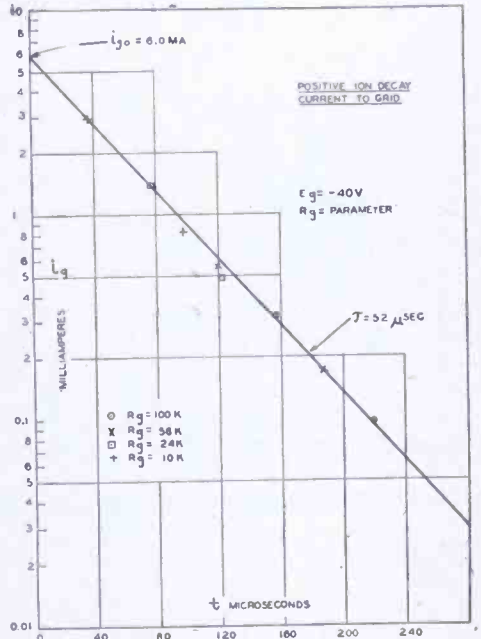


Fig. 6 — Positive-ion grid current during afterglow.

$$i_{gp} R_g > 40 \text{ volts,}$$

where i_{gp} is the positive-ion grid current, the grid tends to collect electrons in addition to the positive ions. This occurs when $t < T$. The collection of electrons tends to prevent the grid potential from going highly positive. The actual electron current to the grid, i_{ge} , assumes a value such that the grid potential assumes a stable value close to cathode potential. If the electron current tends to increase above this value, the grid potential decreases thus returning the electron current and, in consequence, the grid potential to their original values. When i_{gp} decreases below the value $40/R_g$, the grid can go negative. The

* Careful measurements show that the decay is initially more rapid than that corresponding to τ . However, this transition period following the interruption of the discharge is, as a rule, so brief (several microseconds), that it does not influence the results or conclusions here presented.

electron current then rapidly drops to zero, and the grid current is now entirely made up of positive ions. The current behavior is as shown in Figure 7.

It is thus seen that along the flat portion of the grid-voltage characteristic,

$$i_g = i_{gp} - i_{ge}. \quad (4)$$

On the decaying portion of the characteristic,

$$i_g = i_{gp}. \quad (5)$$

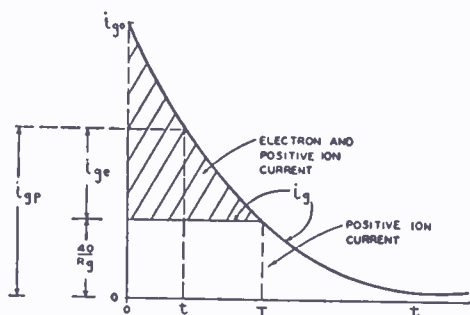


Fig. 7 — Electron and positive-ion decay curves during afterglow.

across the effective grid resistance $(R_g)_{eff}$ is about 20 volts. Thus

$$i_{g0} = \frac{20}{(R_g)_{eff}}. \quad (6)$$

Now $(R_g)_{eff}$ must be greater than 2400 ohms, since the indicial admittance of the grid drive circuit is appreciable at low values of t . The initial indicial admittance is about 1800 ohms. Thus $(R_g)_{eff}$ must lie between 2400 ohms and $2400 + 1800 = 4200$ ohms. Using both extremes one finds that i_{g0} must lie between 4.8 and 8.3 milliamperes. It is seen that this result is in good agreement with the value of 6.0 milliamperes obtained above by the extrapolation of the current decay characteristic to zero time.

Series 2 — R_g Constant

In this series, R_g was held constant at 24,000 ohms and grid-voltage characteristics were obtained during the decay period for $E_g = -5, -10, -20, -30, -40,$ and -50 volts. The oscillograph traces are shown in Figure 4. The portions of the characteristic wherein E_g is returning to its bias value were analyzed in the same manner as for the pre-

ceding case, to yield the values of the positive-ion grid current i_{gp} . In this case, i_{gp} is given by

$$|i_{gp}| = \frac{-E_g + e_g}{24,000} \text{ amperes.} \tag{7}$$

In Equation (7), E_g and e_g are either negative or zero at all times. The values for i_g as a function of time for the various values of E_g are plotted in Figure 8. It is seen that in this case, i_{gp} decays exponentially with a time constant of 49 microseconds and that i_{g0} (intercept on t axis), is equal to 6.3 milliamperes. These are in excellent agreement with the values obtained in Series 1 where it was found that $\tau = 52$ microseconds; $i_{g0} = 6.0$ milliamperes.

It is thus concluded that the positive-ion current to the grid follows an exponential decay law during the afterglow period after the interruption of the discharge, and that this positive-ion current is practically *uninfluenced* by the value of the negative grid potential and of the grid resistance. During a portion of the afterglow period, the grid may be substantially at cathode potential. During this time the grid collects both electrons and positive ions.

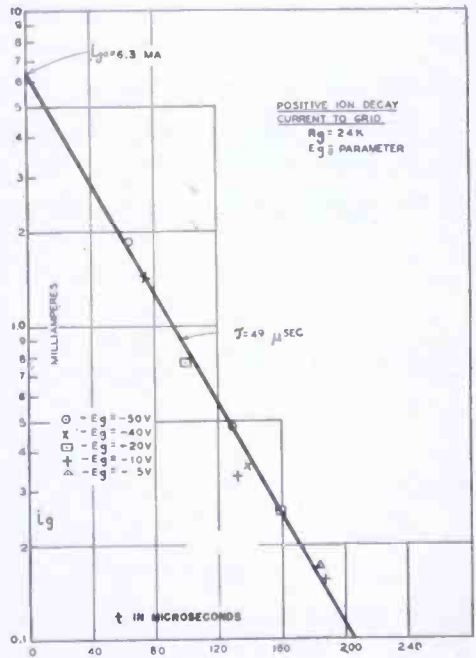


Fig. 8 — Positive-ion grid current during afterglow.

EFFECT OF GRID RESISTANCE ON RECOVERY TIME

It is now possible to explain the observed fact, that at fixed bias, the recovery time increases with increasing grid resistance. The situation appears to be as simple as this: The presence of the grid resistance delays the return of the grid voltage to the bias value. Thus the recovery time that one measures is that corresponding (at least in part) to the grid voltage e_g at the instant when grid recovery occurs. The question arises as to whether T_R may depend not only upon the instantaneous value of e_g but upon the prior history of e_g . Previous studies (to be described in Part II of this series) had already demonstrated that T_R is, to the first order, independent of the prior history

of e_g . (An exception occurs when the grid potential changes abruptly shortly before the application of the test plate pulse used to check as to whether or not recovery has occurred.) It was felt desirable, nevertheless, to confirm this conclusion for the case herein studied, i.e., when R_g itself affects the course of grid potential following the interruption of a discharge. The test setup for studying the positive-ion decay also permitted an independent study of this matter.

A block diagram of the equipment employed is shown in Figure 9. Using the output circuit of Figure 2, the tube was fired by simultaneous pulse applications to grid and plate. The grid-voltage characteristic was observed on a scope. At a later (and variable) time the plate alone was pulsed. The time position of this pulse was increased until the tube just recovered. When the tube had not recovered, the grid-voltage course was as shown in Figure 10. If recovery has occurred, the grid-voltage course is as shown in Figure 11 with a small capacitive spike showing where the plate pulse is applied. e_g is measured on the scope at the instant recovery occurs.

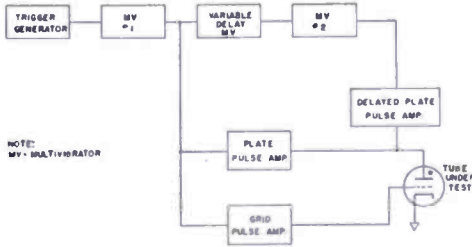


Fig. 9—Block diagram of Recovery Time test set.

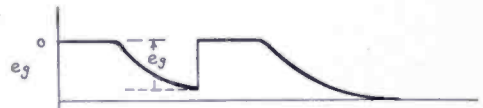


Fig. 10—Grid-voltage pattern when tube has not recovered.



Fig. 11—Grid-voltage pattern when tube has recovered.

Recovery Time data were taken on a standard commercial thyratron at the following values of R_g : 0; 39,000; 62,000; 240,000; and 680,000 ohms. The bias was varied between -10 and -80 volts for each value of R_g . In each case T_R determinations were made with two values of initial grid pulse; one just sufficient to fire the tube and the other at $\hat{e}_g = 135$ volts. Previous studies had shown that these yield slightly different values of T_R due, it is believed, to the fact that in the latter case the discharge occurs to the grid as well as to the anode, thus resulting in a somewhat higher plasma density at the beginning of the afterglow. The magnitude of the firing plate pulse, e_{p1} , was 400 volts, and that of the test plate pulse, e_{p2} , was 160 volts. Both pulses were 7 microseconds in length.

The results are plotted in Figure 12. Within experimental error,

the Recovery Time is seen to be a function of the grid voltage at the instant of recovery and not upon the prior history of the grid voltage. The effect of grid resistance on recovery is secondary. It merely serves to delay the return of the grid voltage to a value which permits recovery. In this test the grid-potential changes are sufficiently slow that the conditions in the tube are always essentially in a state of quasi-equilibrium. Consequently the exception mentioned above (for the case wherein the grid potential changes abruptly shortly before the application of the test plate pulse), does not apply.

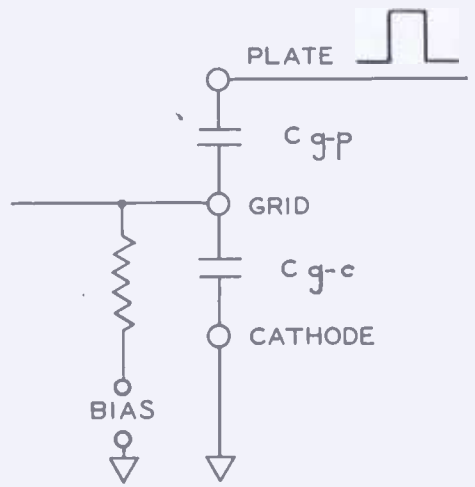
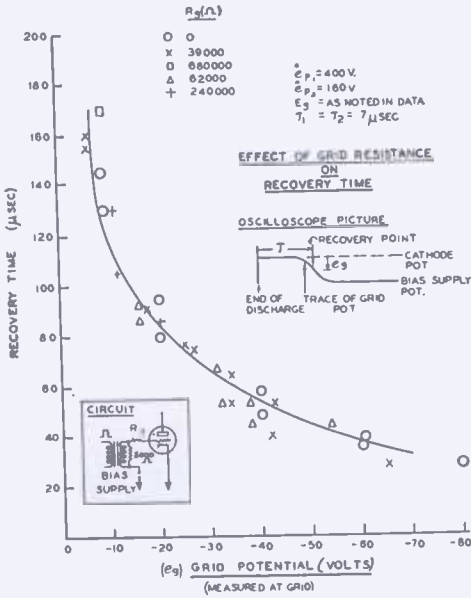


Fig. 12—Recovery Time characteristic of thyatron as function of grid potential.

Fig. 13 — Equivalent circuit of thyatron and grid resistor.

COMBINED EFFECTS OF INTERELECTRODE CAPACITANCE AND GRID RESISTANCE ON RECOVERY TIME

At very large values of grid resistance another effect appears which contributes to increase in T_R . This can best be explained by reference to Figure 13 which shows an equivalent circuit for the thyatron and its grid resistor. The application of a pulse to the plate causes the appearance on the grid of an additional signal as shown in Figure 14. The positive spike e_g' due to the plate pulse results in a change in the actual grid voltage. Its effect on the firing is undoubtedly quite complex being connected with such a little known matter as the ionization time of a thyatron when in a partially ionized state. If R_g is sufficiently large, then e_g' and t can both become sufficiently large so that the actual grid voltage is appreciably raised, over so great a portion of the plate pulse that T_R is appreciably lengthened. In actual prac-

tice, where the anode signal is often sinusoidal, the presence of large R_g will result in the appearance of large induced sinusoidal signals on the grid. This will make itself felt by a lower value for the upper limiting frequency of operation of the thyatron. A decrease of C_{p-g} can obviate the deleterious effect of increasing R_g on the upper frequency limit of operation.

In the case of these studies, the value of e_v' was always so small that it had no appreciable influence on the data, thus in no wise affecting the conclusion that Recovery Time is essentially a function of the actual

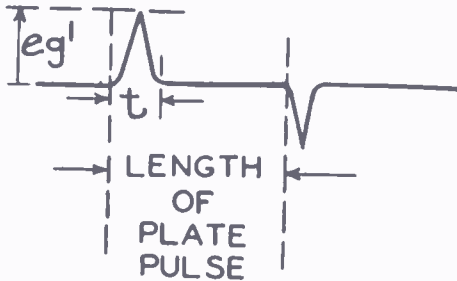


Fig. 14 — Capacitive signal on thyatron grid due to rectangular plate pulse.

grid potential at the instant of recovery (provided the grid potential is not changed shortly before the application of the plate repulse).

SUMMARY AND CONCLUSIONS

Studies were made of the grid-voltage and current characteristics of a commercial thyatron for different values of grid resistance and bias, during the period following the interruption of a discharge. It was found that, in general, the grid voltage stays close to cathode potential for a length of time dependent upon the values of bias and grid resistance, and then decays exponentially towards the bias value. The observed results can be explained in terms of a picture according to which both electron and positive-ion current flow to the grid. The positive-ion current decays with time from the instant of interruption of the discharge and is independent of the grid bias or resistance. If the potential drop across the grid resistor due to the positive-ion current exceeds the bias value, then electron current also flows to the grid. The electron current is of a magnitude just sufficient to hold the grid substantially at cathode potential. This condition holds until the positive-ion current has decayed to a value such that the potential drop across the grid resistor due to the positive-ion current is equal to the bias value. Beyond this point the electron current rapidly falls to zero and the grid potential returns to the bias value along an exponential curve. The increased Recovery Time when a grid resistor is present is accounted for by the delayed return of the grid voltage to its bias value.

Measurements were made of the Recovery Time along the decaying portion of the grid-voltage characteristic for various values of grid resistor and bias. These were compared with values obtained at very low values of grid resistor in which case the grid voltage returned to its bias value in a few microseconds. In all cases it was found that the Recovery Time depended essentially upon the instantaneous value of the actual grid voltage and not at all upon the prior history of the grid voltage during the plasma decay period. Under special conditions which are not representative of usual thyatron operation the conclusion stated in the preceding sentence is not valid. Experiments describing these special studies are presented in Part II of this series.

STUDIES OF THYRATRON BEHAVIOR*

Part II—A Study of the Effect of Grid Potential Variations During the Afterglow Period upon the Recovery Time of Thyratrons

BY

E. O. JOHNSON AND L. MALTER

Research Department, RCA Laboratories Division,
Princeton, N. J.

Summary—It is shown that the Recovery Time of thyratrons is dependent upon the course of the grid potential during the period following the interruption of a discharge, only if the grid potential experiences a sudden change during some time interval just preceding the test for recapture of grid control. This test may be the reapplication of anode voltage. A picture is presented according to which any sudden change of grid potential sets up an unstable charge distribution in the plasma and sheaths within the tube. This unstable configuration goes over into a quasi-stationary one in times determined by diffusion considerations. Evidence for this picture is presented.

INTRODUCTION

IN Part I¹ of this series, the effect of grid resistance on the Recovery Time (T_R) of thyratrons was considered.† It was shown that grid resistance affected T_R only insofar as it caused a delay in return of grid potential to its bias value. The results there presented indicated that T_R does not appear to depend upon the grid potential during the afterglow period. Further experiments indicate that this is not quite so. Sudden changes in grid potential shortly before testing for recovery do affect observed T_R values. It is the purpose of this paper to describe and interpret these experiments. These tests were all carried out on standard commercial thyratrons except where otherwise indicated.

EXPERIMENTAL SETUP

In these tests it was desired first to fire the tube for some definite length of time. Then, during the rest period following the interruption

* Decimal Classification: R337.12.

¹ L. Malter and E. O. Johnson, "Studies of Thyatron Behavior, Part I—The Effect of Grid Resistance on the Recovery Time of Thyratrons", *RCA Review*, pp. 165-177 of this issue.

† For reasons explained in Part I the term "Recovery Time" is used to designate the quantity more commonly referred to as "Deionization Time."

of the discharge, it was desired to place pulses of variable length, amplitude, and time position on the control grid in order to vary the "history" of the grid potential during its rest period.

The means for applying pulses to the plate as described in Part I¹ proved suitable. In order to secure unambiguous results, a grid drive circuit was required which possessed low output impedance and which was capable of delivering long pulses. The circuit of Figure 1* was employed for the desired purpose. The multivibrator system in which the variable-length, variable-position pulses are generated, being fairly conventional, is not shown in detail. The signal at point A serves to

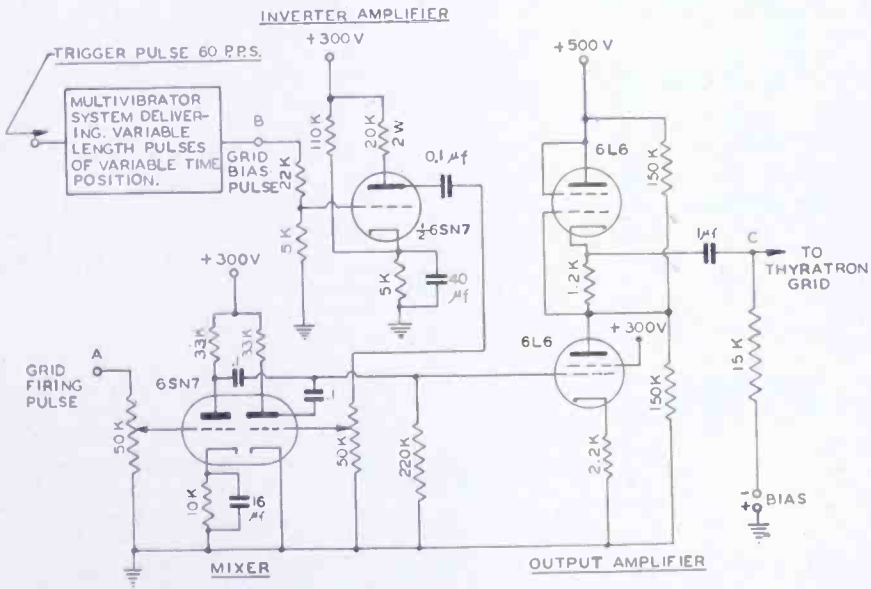


Fig. 1—Grid-pulse and bias drive circuit.

supply the initial grid firing pulse (positive at point C). The signal at point B serves to supply the delayed grid bias (negative at point C). The output impedance of the circuit as shown is of the order of 1000 ohms which is so low that there were no disturbing effects therefrom.

Test Number 1

A commercial 2050 thyatron was employed in this test.

The test procedure can best be explained by the pulse chronology shown in Figure 2.

For a fixed value of τ the length of τ_g (the grid pulse overlap time), was varied between 0 and τ and the values of the grid pulse bias voltage e_g needed to just prevent the tube from refiring were measured. When $\tau_g = \tau$ microseconds, the direct-current grid bias conditions are simulated. Thus, a continuous transition from the pulse-bias case

* The form of the output stage employed was suggested by H. B. DeVore of these Laboratories.

to the direct-current case can now be made and one would expect to find where the deviation between the direct-current and pulse cases occurs, if any. Some of the experimental results are plotted in Figure 3.

It is seen that if the pulse bias is applied considerably in advance of the plate test pulse (τ_p large), the values of direct-current bias and pulse bias required to just prevent refiring are the same within the limits of measurement. From this one may conclude that the deionization is essentially independent of the previous history of grid potential and that the value of T_R depends essentially on the instantaneous value of grid potential. The reason for the deviation from these conclusions for low values of τ_p will be discussed later in this paper. It may

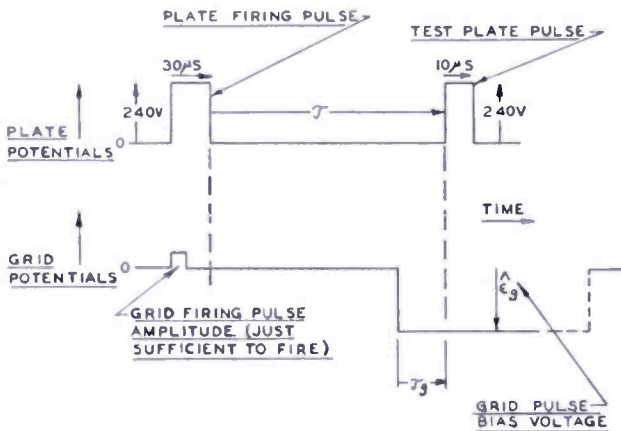


Fig. 2 — Grid and plate potential time courses.

be briefly stated at this point, however, that following any abrupt change in grid potential, the plasma-sheath conditions in the tube will not attain a state of quasi-equilibrium for some time, and that during this time the fields in the neighborhood of the grid opening will be such that a greater negative grid potential is required to hold off refiring. Thus, the divergence between direct-current and pulse study results, for low values of τ_p , may be considered as being due to a non-steady state in the tube, which does not in a fundamental fashion affect our conclusions regarding effect of grid potential on rate of deionization* or on T_R .

Test Number 2

Another test which reinforces the preceding results is illustrated chronologically in Figure 4. The magnitudes of \hat{e}_g and τ are fixed as shown in the same figure. τ_p was varied from zero out to where \hat{e}_g overlapped the plate test pulse. The corresponding values of direct-

* As in Part I, "Deionization" means the decrease of ion and electron density in a plasma following the interruption of a discharge.

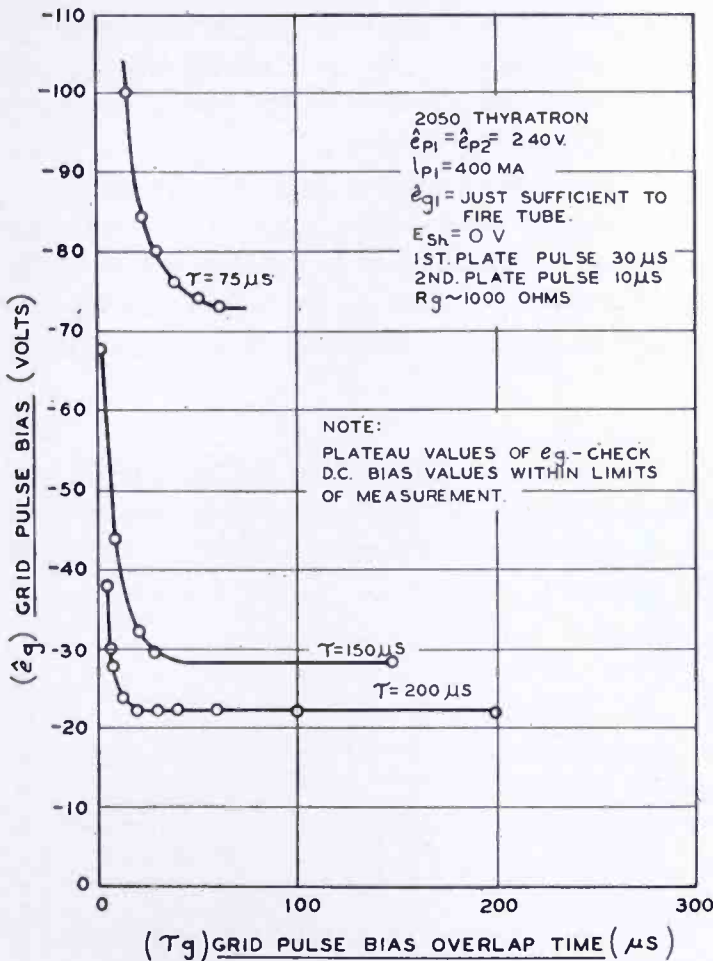


Fig. 3 — Grid-pulse bias required to prevent refiring as function of overlap time with plate repulse (see Figure 3).

current bias (E_g) required to just prevent refiring were measured and are plotted in Figure 5. It is observed that if the grid pulse is terminated earlier than 30 microseconds before the application of the test plate pulse, the direct-current bias value (E_g) required to just prevent refiring remains fixed at -60 volts. As the test plate pulse is approached more closely, the value of E_g decreases, and when the grid pulse overlaps the plate pulse, E_g decreases to -9 volts. Since

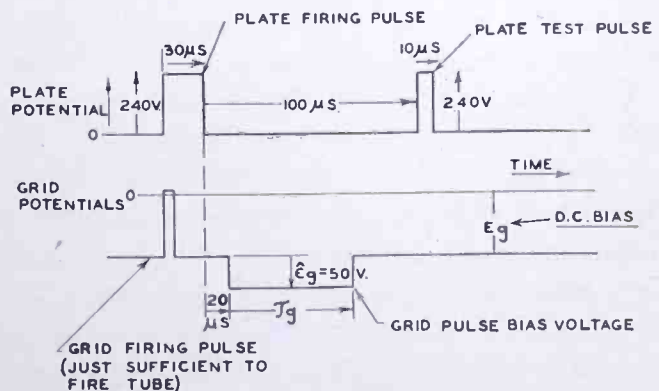


Fig. 4 — Grid and plate potential time courses.

$\hat{e}_g = -50$ volts, it is seen that the sum of the direct-current bias (-9 volts) and the pulse bias (-50 volts) is now very closely equal to the initial value of the direct-current bias (-60 volts) when the bias pulse overlaps the plate pulse. This is as it should be.

These results yield the same conclusions as those of test number 1. The behavior when the terminal edge of the grid pulse closely approaches the leading edge of the plate pulse is again ascribed to the existence of a transitory non-steady state in the tube following any sudden potential change on an electrode. This will be discussed below.

Test Number 3

Another variation involves fixing the width of the grid pulse bias and varying its position in the rest interval between the interruption of the discharge and the application of the plate test pulse. The pulse chronology is shown in Figure 6.

The results are as follows:

Table I

τ_g (microseconds)	E_g (volts)
0	60
40	60
50	58
60	56
70	52
76	48

In this table E_g is the direct-current bias just sufficient to prevent refiring. These results further confirm those of tests numbers 1 and 2.

Test Number 4

In this test (carried out in a 2050 structure with argon at 150 microns) the procedure was as follows: A variable direct-current bias was applied to the grid. Forty microseconds after the interruption of the discharge, a 57-volt negative pulse 10 microseconds long was impressed on the grid in addition to the direct-current bias. The plate test pulse position was increased steadily from zero time and the following results were observed. The tube fired until the test pulse was moved out to about 40 microseconds. At that point (denoted in the table below by T_{R1}) the tube failed to refire (due to the sudden increase in bias). When the plate test pulse passed out beyond 50

microseconds (the point where the grid bias returns to its direct-current value) the tube refired and stayed fired until some later time designated as T_{R2} . The approximate grid potential course is shown in Figure 7.

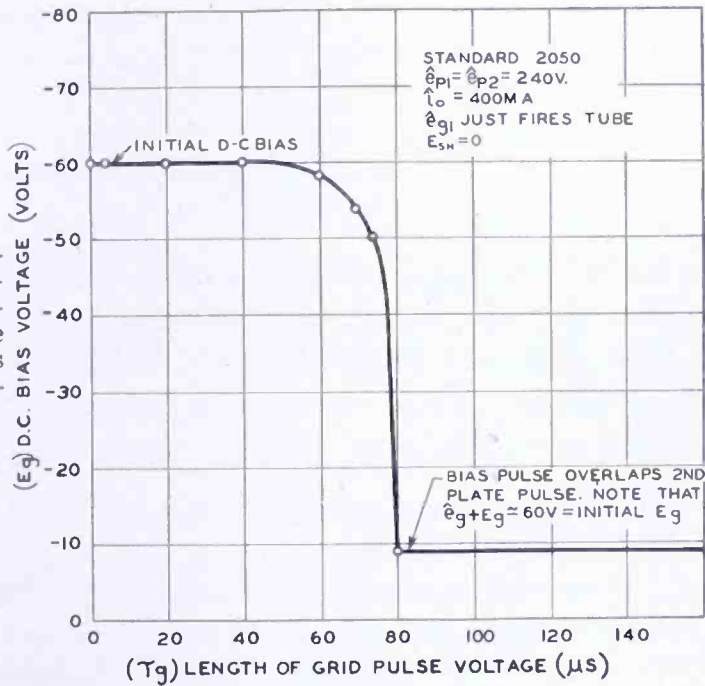


Fig. 5 — Direct-current grid bias required to prevent refiring for variable length grid bias pulse during after-glow.

The data obtained in these tests are presented in Table II.

Table II

(1) Direct-Current Bias (Volts) E_g	(2) Grid Pulse (Volts)	(3) First Recovery (micro-seconds) T_{R1}	(4) Refiring (micro-seconds) T_F	(5) Second Recovery (micro-seconds) T_{R2}	(6) Direct-Current Case E_g	(7) T_R
-5	-57	42	48	137	-5	138
-10	-57	42	49	125	-10	125
-20	-57	40	49	82	-20	81
-30	-57	42	50	67	-30	68

It is seen that by applying a larger bias for a short length of time during the decay period, the tube can be made to recover temporarily. Following this pulse, the bias returns to its direct-current value, the tube can refire, and the measured value of T_R (column 5 of Table II) is the same as though the pulse bias had not been applied and only the

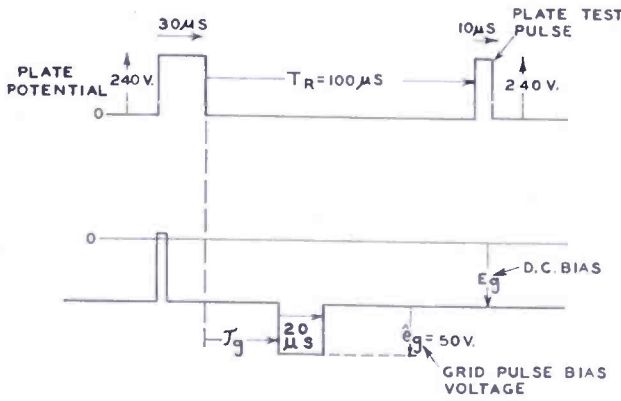


Fig. 6 — Grid and plate potential time courses.

direct-current bias is present (column 7 of Table II). This indicates that the rate of deionization is not a function of the grid potential and that T_R is not influenced by changes in grid potential which precede the plate repulse by some time. Similar tests on commercial tubes yield the same results and conclusions.

DISCUSSION OF RESULTS OF TESTS 1-4

In tests 1-4, just described, it is observed that T_R depends only on the instantaneous value of grid potential provided the grid potential does not experience an abrupt change shortly before the application of the plate test pulse. At first glance this appears to be in conflict with the results and conclusions of Part I¹ wherein it was stated that: 1. the positive-ion grid current and rate of deionization are essentially independent of grid voltage and resistance; and 2. T_R depends largely upon the instantaneous value of grid potential and not upon its prior history. These apparent conflicts need resolving.

The matter can be cleared up by means of the concepts embodied in Figure 8. This figure is a duplicate of Figure 1 of Part I. It represents the approximate potential distribution across a section of a typical thyratron during the afterglow, with the anode potential re-

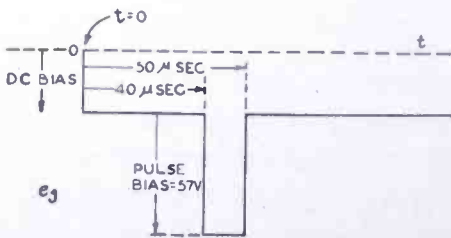


Fig. 7—Grid potential time course.

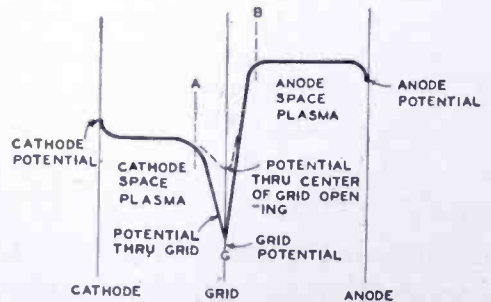


Fig. 8 — Potential distribution along thyratron section following reapplication of anode potential during afterglow. Grid sheath has filled grid opening.

applied. Whether or not the tube refires depends closely on whether or not a thyatron with cathode at A, anode at B, and grid at G, and with the potentials as shown in Figure 8, will fire. Suppose that the thyatron has been in its "rest state" for a time t_1 following the interruption of a discharge and that during this rest period the cathode and anode have been at zero potential and the grid has been at some fixed negative potential e_{g1} . Suppose further that sufficient time has elapsed so that the grid sheath has filled the grid opening thus isolating the plasma on anode and cathode sides of the grid. Then, as was explained in Part I, the cathode-grid plasma will be slightly below cathode potential (i.e. zero) and the grid-anode plasma will be slightly above anode potential. Then at time t_1 , the potential distribution through the tube may be as represented by Figure 9.

The possibility for recovery of grid control now exists. Now let the negative grid potential be instantaneously increased from e_{g1} to e_{g2} at time t_1 . The potential distribution through the center of the grid opening will momentarily assume a form resembling that shown in Figure 10.

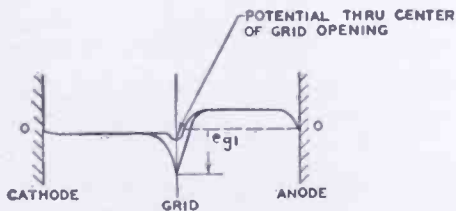


Fig. 9 — Potential distribution along thyatron section during afterglow following closure of grid opening by sheath.

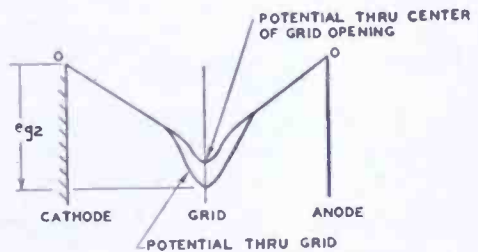


Fig. 10 — Instantaneous potential along thyatron section during afterglow following closure of grid opening by sheath and application of negative grid pulse.

The potential configuration shown in Figure 10 is an extremely unstable one. In it, fields exist in the plasmas. Under the influence of these fields some electrons will be driven out of the plasmas as a consequence of their high mobility, thus very quickly restoring the plasmas to their normally field-free state. The resulting potential distribution through the center of the grid opening is then as shown in Figure 11.

The transition between the states of Figure 10 and Figure 11 occurs in a small fraction of a microsecond for the tubes studied. Since the rise times of the pulses employed are also of this order, it may safely be stated that the conditions represented by Figure 10 do not exist for any practical purpose, but that the tube goes from the state of Figure 9 to that of Figure 11 during the pulse rise.

The potential distribution of Figure 11 is also an unstable one.

The sheath region between A and B is one in which the charge distribution does not correspond to that given by the Langmuir-Child space-charge equation

$$j = k \frac{V^{3/2}}{d^2}, \quad (1)$$

where j is the diffusion current density of positive ions out of the plasma into the sheath.

In using Equation (1), it is assumed that mean-free paths are large compared with sheath thickness. This condition is definitely satisfied in the tubes studied. The sheath system now "attempts" to satisfy (1). In doing so, ions are drawn out of the sheath to the grid; the times

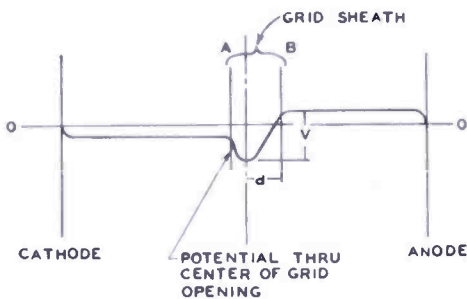


Fig. 11—Same as Figure 10 but slightly later following redistribution of sheath and plasma electrons.

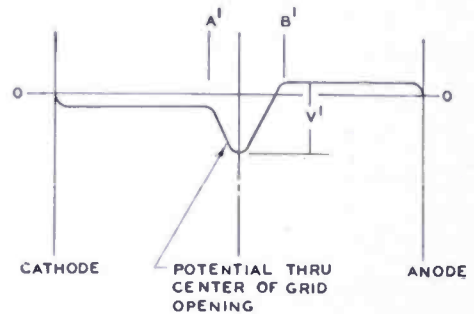


Fig. 12—Same as Figure 11 but slightly later following redistribution of grid sheath ions.

involved are of the order of tenths of a microsecond. As ions leave the sheath, the field from the grid penetrates into the plasma in order that Poisson's equation

$$\nabla E = \frac{\rho}{\epsilon} \quad (2)$$

be satisfied. This requires that the sheath edge A of Figure 11 move slightly to the left and the edge B slightly to the right. This "exposes" the region of the grid opening to the influence of a high positive charge density and thus prevents the potential at the center of the grid opening from dropping very far. The new potential distribution through the center of the grid opening may be represented as in Figure 12.

The change from the state of Figure 9 to 10 to 11 to 12 occupies a time of the order of a microsecond in the tubes studied. It may thus be considered as being the potential configuration at the end of the rise of the negative grid pulse.

The system still tries to satisfy Equation (1). However, at the same time the density distribution in the plasma also seeks an equilib-

rium state, or rather a state of quasi-equilibrium in which the fundamental diffusion equilibrium equation

$$\nabla^2 n + \frac{n}{\Lambda_1^2} = 0 \text{ (see Reference 2)} \quad (3)$$

is also satisfied (n is the charged particle density in the plasma, and Λ_1 is the lowest characteristic diffusion length, determined by the tube geometry).

A measure of the time it takes the system to achieve diffusion equilibrium is given by a quantity τ_1 , where

$$\tau_1 = \frac{\Lambda_1^2}{D_a} \quad (4)$$

where D_a is the ambipolar diffusion coefficient.

Thus the return of the entire plasma-sheath system to equilibrium is determined almost entirely by the rate at which the plasma density assumes its steady state under diffusion action primarily. One may conclude, finally, that the system will assume a state of quasi-equilibrium in a time of the order of τ_1 . Independent determinations of τ_1 in this laboratory by measuring the rate of decay of plasma density yield values which are of the order of the time observed for steady-state conditions to be attained following sudden changes in grid potential (see tests 1-3, above).

Further evidence for the view that it is diffusion which determines the rate of return of a disturbed system to a state of quasi-equilibrium is given by some measurements in a 2050 structure filled with argon at 150 microns rather than with xenon at 185 microns. If mobility considerations were dominant, little change in the rate of return to equilibrium should have been expected. Actually the rate of return in the argon tube was much more rapid than in the xenon tube and just about what would be expected from the relative diffusion rates of the two types of ions.

A picture has now been presented which appears to account well for the existence and duration of the non-steady state following sudden changes in grid potential. It remains to be shown why a steady bias is more effective than a pulse bias applied just before the plate repulse in holding off refring.

² M. A. Biondi and S. C. Brown, "Measurements of Ambipolar Diffusion in Helium", *Phys. Rev.*, Vol. 75, No. 11. p. 1700, June 1, 1949.

In Figure 12 (an unstable potential distribution which occurs within a microsecond or so following a sudden change in grid potential) the average positive ion density in the sheath (i.e., between A and B) is greater than that which would be present if the grid potential had had the value e_{g2} for some time before t_1 . Since the average positive-ion density in the latter case is less than in the former, the potential in the grid opening will also be lower in the latter case. It may be represented by Figure 13. (For comparison, in Figure 13 is shown the unstable potential distribution present shortly after the sudden application of e_{g2} to the grid. This is patterned after Figure 12.) It is seen that in going from the upper (unstable) state of Figure 13 to the lower state (of quasi-equilibrium) not only does the effective potential at the center of the grid opening decrease, but the sheath thickness increases. Both of these effects serve to make the direct-current bias more effective than pulse bias (applied shortly before anode repulse) in preventing refiring.

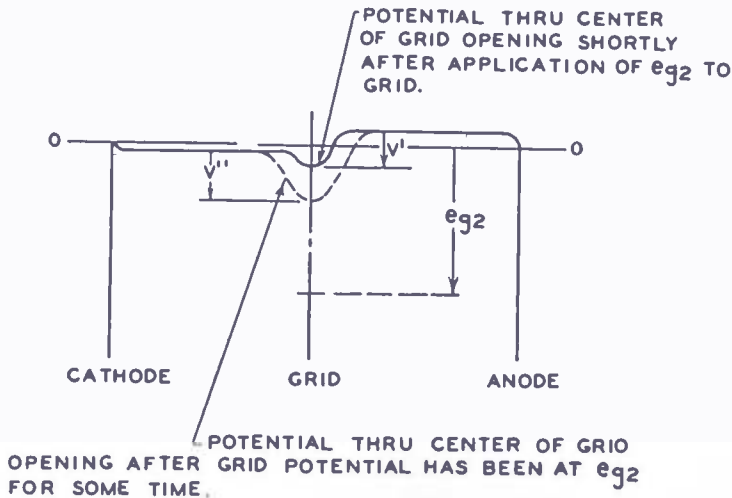


Fig. 13 — Same as Figure 12 but considerably later following establishment of diffusion equilibrium.

The upper state of Figure 13 is unstable, and since it tends towards the lower state, it is seen why the observed phenomena are as they are, i.e., why direct-current bias appears to be more effective than pulse bias (applied just before plate repulse) in preventing refiring and why the grid pulse approaches the direct-current bias in effectiveness, the greater the time interval between the application of the grid pulse and the plate repulse.

These considerations explain the results of test number 1 above. The results of tests numbers 2 and 3 may be similarly explained and will not be presented here.

The above analysis is largely qualitative. The picture presented does, however, describe the observed phenomena.

The reason for the more rapid apparent return to equilibrium for the case $\tau = 200$ microseconds than for the shorter T_R cases in Figure 3 merits discussion. It appears to lie in the fact that for the short T_R cases, the sheaths are much thinner and consequently the system is much more sensitive to small deviations from the state of quasi-equilibrium. Thus deviations from quasi-equilibrium which are undetectable in the case $T_R = 200$ microseconds, where the sheaths are relatively thick, can make themselves felt in the 75-microsecond case, where the sheath is much thinner.

CONCLUSIONS

The conclusions can now be formulated as follows: *Recovery time is a function of the instantaneous effective grid potential and not of the previous history of the grid potential.* By effective grid potential is meant the potential at the center of the grid opening. Since, as can be seen from Figure 13, the pulse and equilibrium states differ not only in effective grid potential, but in the magnitude and extent of the field, and since these quantities, too, determine the refiring possibilities, the preceding italicized statement cannot be a completely accurate formulation of the system behavior. However, certainly in a qualitative sense and, very likely, quite closely in a quantitative sense, it does describe the observations.

A form of the conclusion with which there can be little argument is the following: *Recovery Time is a function of the instantaneous grid potential and not of the previous history of the grid potential provided that the grid potential did not experience an abrupt change shortly before the application of the plate repulse.*

ACKNOWLEDGMENT

The authors are indebted to H. H. Wittenberg of the RCA Victor Division, Lancaster, Pa., for stimulating and cogent questions regarding many aspects of this work. Some of his unpublished work suggested the need for a portion of the experiments described in this paper.

A NEW ULTRA-HIGH-FREQUENCY TELEVISION TRANSMITTER*

BY

L. S. LAPPIN AND J. R. BENNETT

Engineering Products Department, RCA Victor Division,
Camden, N. J.

Summary—A description is given of a new television transmitter which operates in the proposed ultra-high-frequency band at a frequency of 529-535 megacycles with a power output at the peak of the synchronizing pulses of 1000 watts. Several novel circuits have been developed, including multi-tube cavities operating as tripler and power amplifier stages. The transmitter conforms to all the standards pertaining to transmitters operating in the very-high-frequency band and is comparable in performance to present day very-high-frequency transmitters.

INTRODUCTION

THE increasing need for additional television channels placed greater emphasis on the utilization of the ultra-high-frequency channels which have been proposed by the Federal Communications Commission. Practical employment of these frequencies was hampered by the lack of operational experience which could only be obtained by scheduled operation at power levels capable of delivering a useful signal in an urban area. While propagation tests and demonstrations were conducted during the Summer of 1948, it became obvious that further tests under practical operating conditions would be required to demonstrate the suitability and possible limitation of television broadcasting in these channels. It was decided that an output power of the order of one kilowatt would be satisfactory for this purpose.

In November 1948, the development of such a television transmitter was undertaken. The frequency was to be 529-535 megacycles, the power output was to be of the order of one kilowatt using currently available tubes, and the design was to be such that the transmitter could be used in commercial operation and would conform with present very-high-frequency (VHF) television standards. Thirteen months later, on December 29, 1949, the completed transmitter, designated TTU-1A, went on the air at Bridgeport, Connecticut.

* Decimal Classification: R583.4 × R310.

The first consideration in the development of this transmitter was to find a type of tube suitable for the job. In the interest of expediting the design it was decided to employ multiple operation of readily available tubes. Two tubes which offered possibilities were the 4X150A and the 5588. To make comparison tests, single tube cavities were built, and the characteristics of each tube were measured at 530 megacycles. The final decision was in favor of the 4X150A for two reasons. First, the 4X150A, a tetrode, would have a higher stage gain and be easier to modulate than the 5588 triode. Second, the 4X150A was much more stable than the 5588 which would definitely require neutralization. Even though it might become necessary to neutralize the 4X150A, neutralization of a tetrode would be much simpler and much less critical in practical operation.

The second consideration was to determine the type of radio-frequency circuits to be used. The most straightforward way would be to use several single tube cavities and combine their outputs by suitable passive networks. Another possibility would be to arrange the tubes around a circle in a single cavity and drive them in parallel. A test cavity was built to see if the proper mode could be set up in such a cavity. The encouraging results obtained led to the decision to use this type of circuit.

A tentative radio-frequency tube lineup was decided upon, and from these basic decisions, the TTU-1A transmitter was developed.

DESCRIPTION

The TTU-1A transmitter is housed in six cabinets fastened together to form a single assembly as shown in Figures 1 and 2. On the left is the aural section and on the right is the visual section.

The TTU-1A is built around the RCA TT-500B Television Transmitter, a commercial transmitter operating on channels 7 to 13 with a peak visual power output rating of 500 watts and an aural power output rating of 250 watts. The TT-500B serves as a driver for the ultra-high-frequency stages and the video modulator as shown in block diagrams Figures 3 and 4. The visual radio-frequency chain comprises a crystal oscillator and four multiplier stages followed by an amplifier all of which are part of the TT-500B transmitter. These in turn drive an eight-tube tripler consisting of eight type 4X150A tubes in parallel in a single cavity. The power amplifier consists of eight type 4X150A

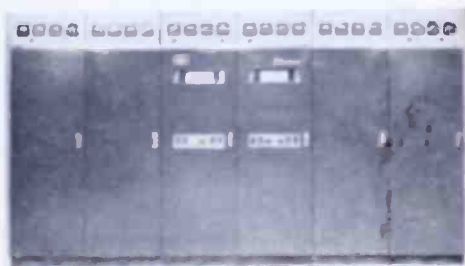


Fig. 1—Front view—doors closed.

tubes in a similar cavity. The output of the power amplifier is fed to the antenna through a reflectometer which measures the incident and reflected waves on the transmission line and thus indicates the standing wave ratio. The reflectometer is calibrated in peak output power so that the output of the transmitter may be continuously metered.

The video modulator chain consists of three low-power video amplifiers, including a clamp circuit, all located in the TT-500B transmitter and direct coupled to the modulator through a regulated "bucking bias" power supply to provide the necessary bias to the modulator. The modulator consists of eight type 6L6 tubes fed in parallel and connected as cathode followers with the output of each tube directly coupled to the grid of a single power amplifier tube. A video monitor amplifier is supplied to provide the necessary phase reversal for viewing on a monitor tube.

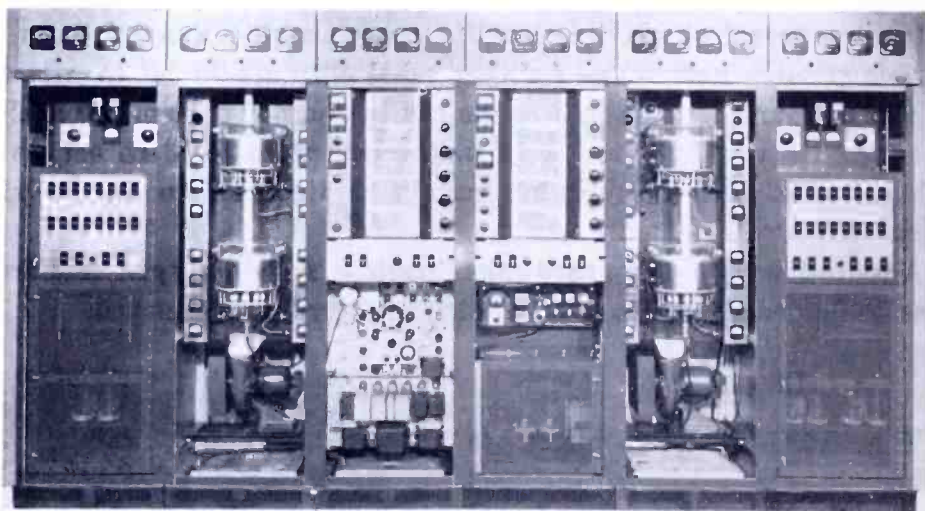


Fig. 2—Front view—doors removed.

The aural radio-frequency chain comprises the frequency-modulation exciter, to be described later, followed by two multiplier stages and an amplifier, all located in the TT-500B transmitter. The output of the TT-500B, which is at one third carrier frequency is followed by an eight-tube tripler cavity and an eight-tube power amplifier cavity identical to those used in the visual transmitter.

The tripler and power amplifier cavities are designed as plug-in units so that in the event of the failure of any component other than a tube, the faulty cavity may be removed and replaced by a spare cavity.

The control circuits are conventional except that indicators are provided to assist in the rapid location of a faulty tube in the cluster. Individual circuit breakers are connected in the cathode circuit of each tripler and power amplifier tube so that, in the event of an over-current

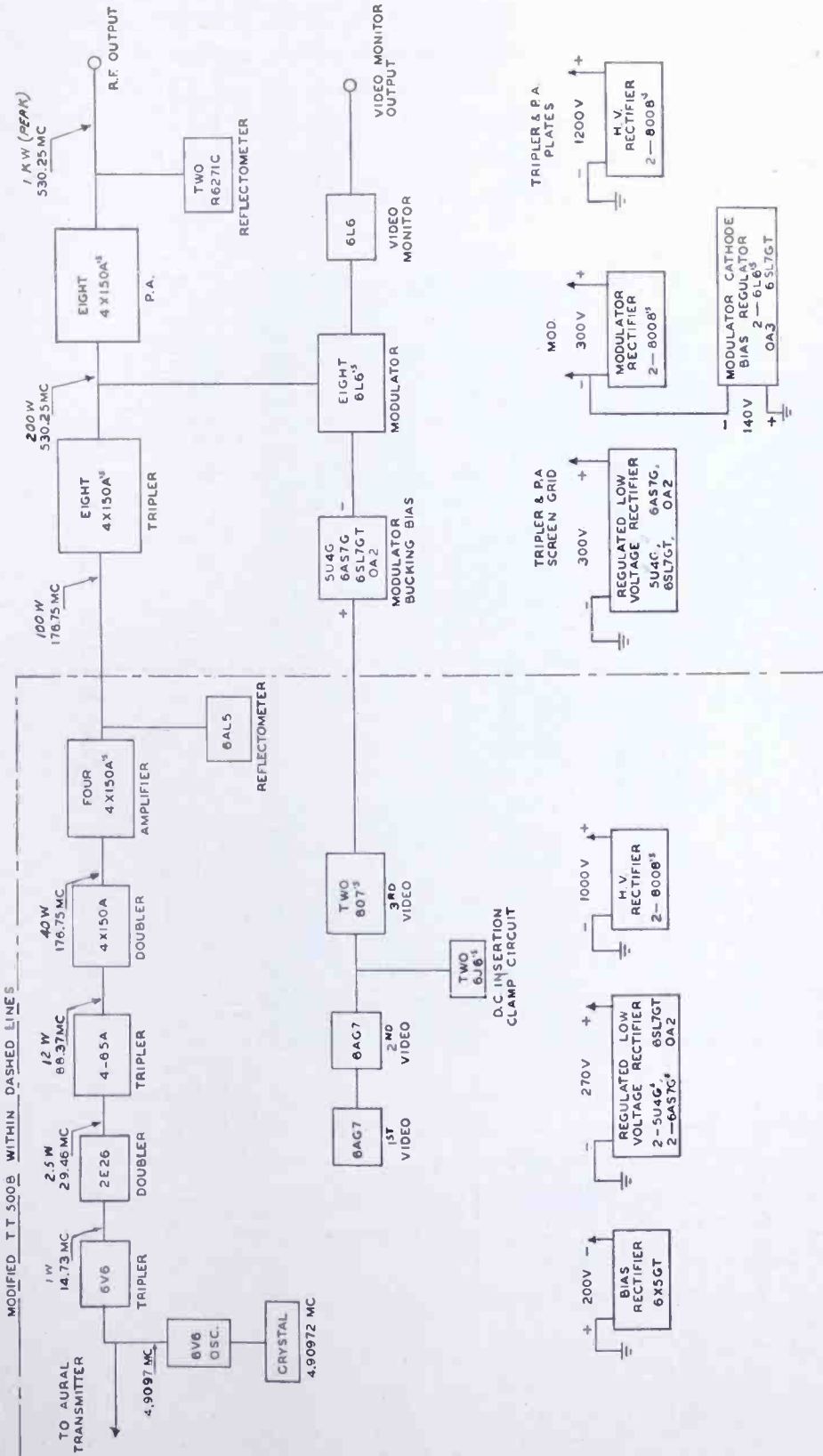


Fig. 3—Block diagram of visual transmitter.

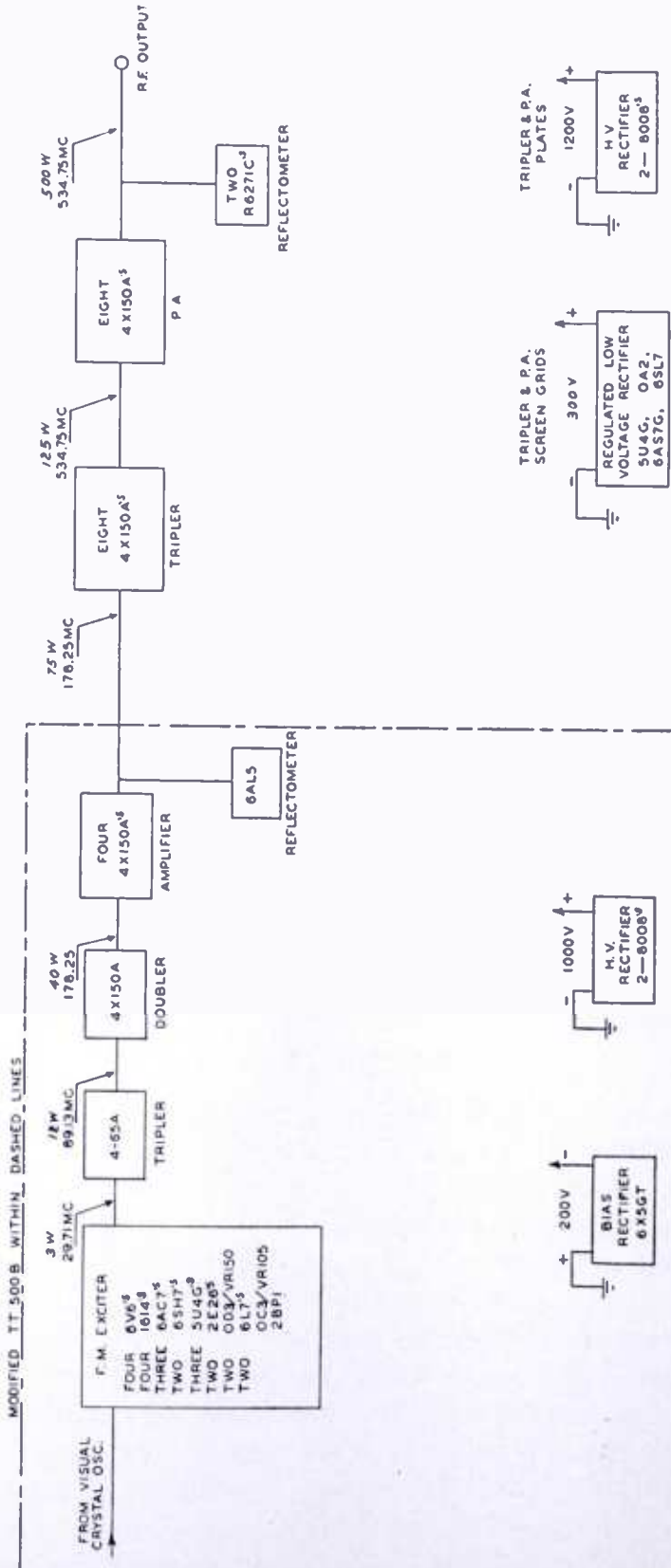


Fig. 4—Block diagram of aural transmitter.

in any tube, the associated circuit breaker trips instantly, providing the desired indication and at the same time removing the plate voltage from all tubes. Indicator lamps are also provided so that there is an overload indication even when the doors are closed.

A separate meter is provided to measure the cathode current of each tripler and power amplifier tube to facilitate the tuning of the cavities.

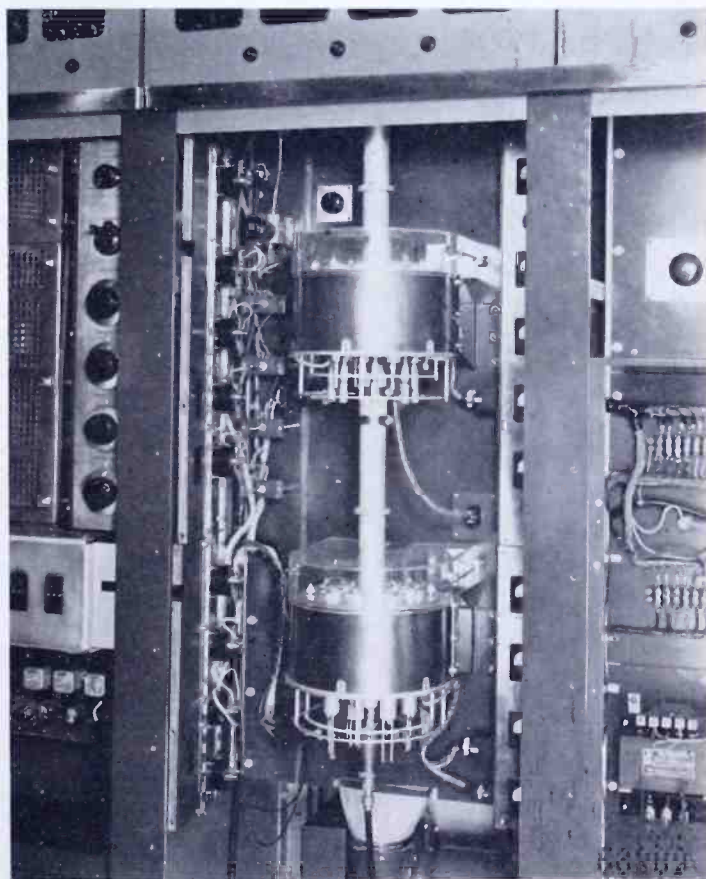


Fig. 5—Tripler and power amplifier stages.

The power supply circuits are conventional except that all circuits in the visual transmitter which are critical to voltage variations are supplied by regulated power supplies. These circuits include all video amplifier stages as well as the screen grids of the intermediate power amplifier, tripler, and power amplifier tubes.

RADIO-FREQUENCY CAVITY DESCRIPTION

The high-frequency tripler and power amplifier are operated as grounded cathode-grounded screen amplifiers. Each uses eight 4X150A tubes mounted in a single cavity. Figure 8, a cross-sectional view of the cavities and the coupling between them, shows that the power

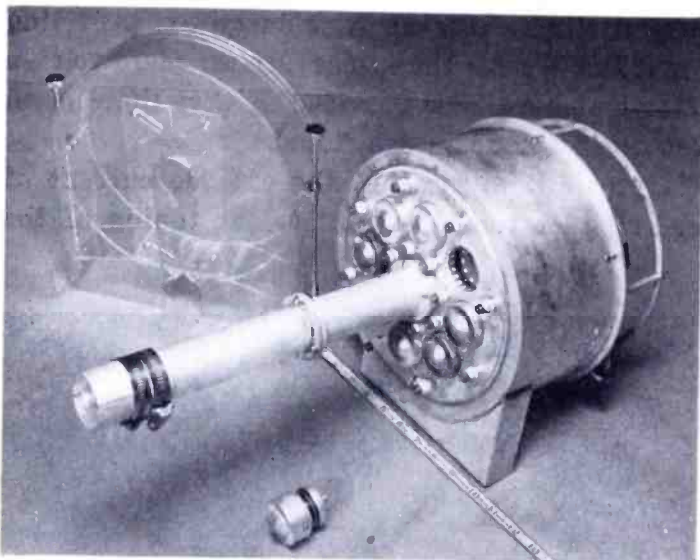


Fig. 6—Power amplifier cavity.

amplifier and tripler cavities are identical except for the grid circuits. Each cavity consists of three concentric cylinders shorted at one end and capped by three flat circular plates, referred to as the anode, screen, and grid plates. These plates provide a base on which the tubes and sockets are mounted.

A sheet of silvered mica placed over the "anode-plate" of the cavity forms the plate blocking capacitor. A thin phosphor-bronze sheet which is cut and formed to provide spring contact fingers for the anodes of all the tubes is laid over the mica and a metal plate provides rigidity to the assembly. The entire assembly is fastened together by means of insulated studs.

The screen grid of each tube is terminated in a ring at the base of the tube. These rings are connected through the screen contact fingers to a flat circular plate. A sheet of mica between this plate and the "screen plate" of the cavity forms the screen by-pass capacitor.

The center conductor of the output transformer is connected to the screen grid. That part of the conductor inside the cavity is an induct-

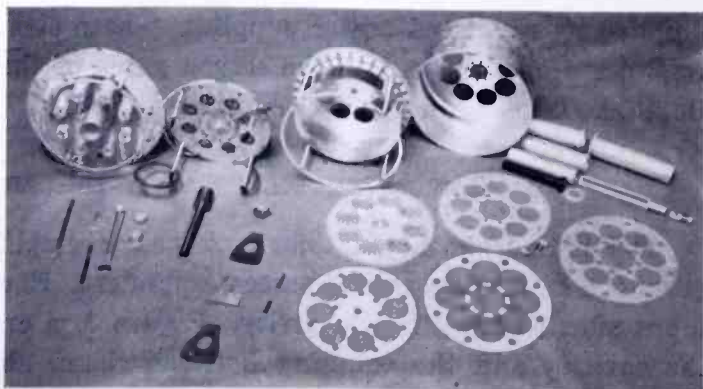
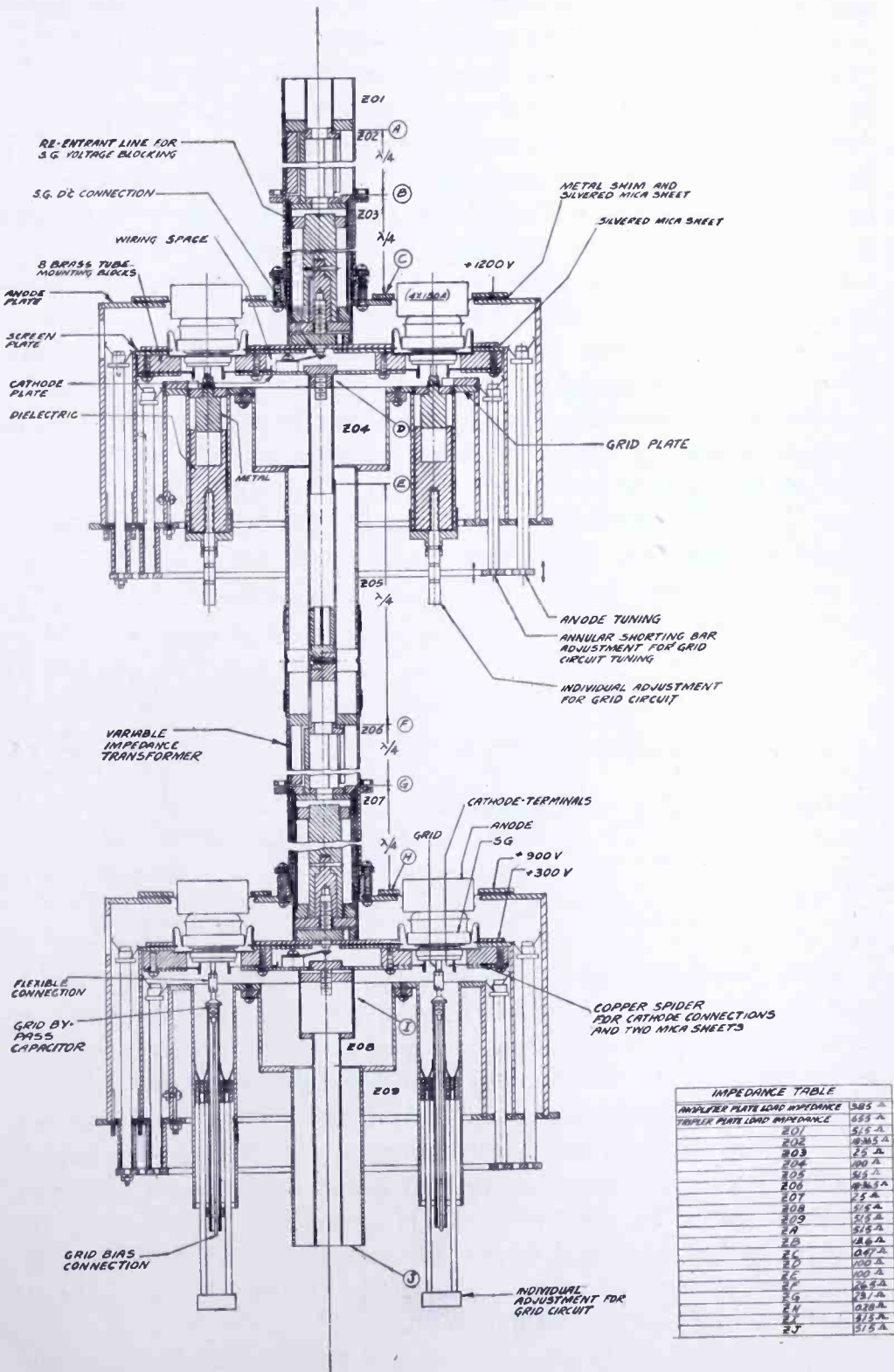


Fig. 7—Disassembled cavity.



IMPEDANCE TABLE	
ANALYER PLATE LOAD IMPEDANCE	585 Ω
TRAPLER PLATE LOAD IMPEDANCE	515 Ω
Z01	48.5 Ω
Z02	25 Ω
Z03	100 Ω
Z04	85 Ω
Z05	48.5 Ω
Z06	25 Ω
Z07	515 Ω
Z08	25 Ω
Z09	100 Ω
A	18 Ω
B	18 Ω
C	207 Ω
D	100 Ω
E	100 Ω
F	26 Ω
G	28 Ω
H	28 Ω
I	515 Ω
J	515 Ω

Fig. 8—Cavity cross section diagram.

ance which is a part of the resonant circuit of the cavity. If the cavity were to be cut into eight pie sections, each tube would be in the center of a half-wave resonant line foreshortened by the tube capacity. The equivalent electric circuit is shown in Figure 9. The circuit has been designed so that when it is resonated at 530 megacycles, approximately half the tube displacement current will flow out toward the shorting bar, and half will flow in toward the transformer. This tends to keep the current distribution uniform in the tube seals. The output impedance of the power amplifier is about $\frac{1}{2}$ ohm at full power output, while the impedance in the tripler is about $\frac{1}{4}$ ohm.

The cathode of each tube is individually by-passed to a "cathode plate" which is connected electrically to the "screen plate." Thus the direct-current component of the cathode current of each tube may be metered separately. There is no radio-frequency field in the space between the "screen plate" and the "cathode plate"; therefore this space is used for the direct-current and 60-cycle leads to the filament, screen, and cathode. These leads are brought out from the cavity through four copper tubes which are mounted along the inside of the "screen cylinder."

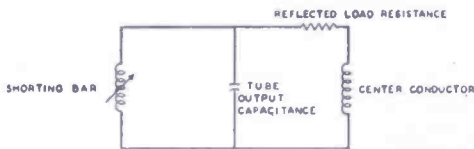


Fig. 9—Equivalent plate circuit of a single tube.

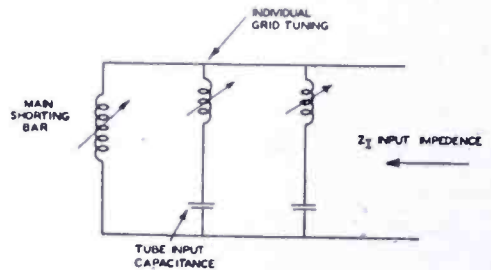


Fig. 10—Equivalent circuit of tripler grid cavity.

In the tripler, the grid of each tube is connected to a feed-through type by-pass capacitor which is screwed into the center conductor of each tuning stub. The outer conductor of each tuning stub is soldered to the "grid plate" of the cavity. The equivalent electrical circuit is as shown in Figure 10 where only two of the eight grids are shown. By adjusting the main shorting bar and the individual tuning adjustments, the grid cavity can be resonated and the drive on each tube can be balanced. By differentially tuning the main shorting bar and all eight of the individual tuning adjustments, the input impedance, Z_I , may be varied for proper matching. The tripler has been designed to match a 51.5-ohm coaxial line.

The design of the power amplifier grid tank is different from that in the tripler because at 530 megacycles, the reactance of the cathode and grid leads is approximately equal to the input capacitive reactance.

In order to resonate the power amplifier grids with the main shorting bar, an equivalent capacitance is inserted in series with the grid. This is done by the individual open circuited tuning stubs the capacitance of which is made adjustable by means of a movable dielectric sleeve. The equivalent circuit for the grid tank is shown in Figure 11.

The input impedance to the grids can be adjusted by differentially adjusting the main shorting bar and individual tuning adjustments as described for the tripler, but the power amplifier grid circuit is designed to have an input impedance of 100 ohms.

The power amplifier grid bias connection is not shown in Figure 8. The requirements of such a circuit are that it prevent all radiation outside the cavity, and present a high impedance to ground for the video frequencies. Eight quarter-wave chokes do this quite effectively. Since the radio-frequency impedance is low at the grid terminal of the socket, the center conductor of each choke is connected at this point. The choke is mounted in an insulating block adjacent to the individual grid tuning stub and the outer conductor of the choke is connected to the modulator output.

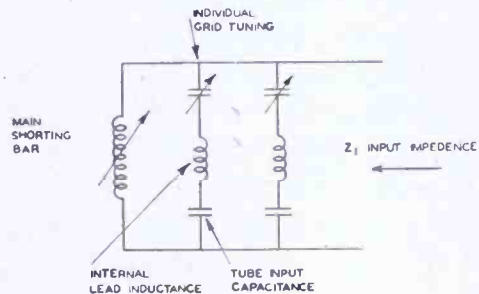


Fig. 11—Equivalent circuit of power amplifier grid cavity.

Both the anodes and grids of the 4X150A tubes require forced air cooling to prevent overheating of the seals. To accomplish this, air is forced through a screened slot in the side of the cavity in the anode tank. Inside the cavity, the air splits into two paths. Part of the air is forced out of the cavity through the anode radiators, and the rest is forced down across the grid seals of the tubes and out the grid cavity. To increase the air flow across the grid seals, three short bakelite pins are cemented into the tube socket. These raise the tube slightly above the socket and allow the air to pass across the base of the tube and through the center hole in the socket into the grid cavity. A plastic shield fastened over the top of the cavity creates a back pressure which further increases the flow of air across the grid seals and in addition provides a safety cover for the anodes of the tubes which would otherwise be exposed.

OUTPUT COUPLING TRANSFORMERS

The output coupling of the power amplifier cavity consists of a two-section impedance matching transformer. Each section is a quarter wavelength long, and together they transform the 51.5-ohm

line impedance down to $\frac{1}{2}$ ohm at the output of the power amplifier cavity. Since the inner conductor of the first section is at the same direct-current potential as the screen of the tubes, a re-entrant quarter wave section blocks the direct-current screen voltage but provides a low impedance radio-frequency path between the inner conductors of the first and second sections of the output coupling transformer.

Transforming from 51.5 to 0.5 ohms would ideally require two sections of surge impedance, 1.59 and 16.2 ohms respectively for maximum broadbanding, but if a $1\frac{5}{8}$ -inch line is used as the outer conductor a section of 1.59-ohm surge impedance is mechanically impractical especially since a potential of about 300 volts exists between the outer and inner conductor. As a compromise, a surge impedance of 2.5 ohms was chosen for the first section. This fixes the surge impedance of the next section at 25 ohms, but in order to vary the loading on the power amplifier, this section was made variable. A two-to-one change in surge impedance of this section results in a four-to-one change in power amplifier output impedance, which was considered adequate. The surge impedance of the second transformer section should therefore be adjustable between 18 ohms and 36 ohms.

A cross section of a tentative design was laid out to scale and a flux plot was made to determine the capacitance per unit length. A flux plot gives a fairly accurate determination of the capacity if it is done carefully. To make one, the electric and magnetic lines are sketched free-hand following a knowledge that:

1. The electric lines terminate perpendicular to the conductor.
2. Electric and magnetic lines are mutually perpendicular.

If the electric and magnetic lines are drawn to approximate squares, then:

$$C = \frac{\text{Number of "squares" along magnetic lines}}{\text{Number of "squares" along electric lines}} \times 8.854 \text{ micromicrofarads per meter.}$$

A cross-sectional view of the final design is shown in Figure 12. The outer conductor consists of three square rods soldered to the inside of the $1\frac{5}{8}$ -inch tube and the inner conductor consists of three half-round rods supported by a plate at each end as shown. To change the surge impedance, the outer conductor is rotated with respect to the inner conductor. A slotted flange at one end limits the travel from maximum to minimum surge impedance. From the flux plot, $Z_{0 \text{ max.}}$ and $Z_{0 \text{ min.}}$ were found to be 38.7 ohms and 18.1 ohms respectively. After the transformer was built, the surge impedance was measured

on a slotted line. The realized values of $Z_{0 \max}$ and $Z_{0 \min}$ were 37.3 and 20.2 ohms respectively.

Although the output impedance of the tripler cavity is $\frac{1}{4}$ ohm, it is desirable to use the same type of output coupling. If this is done, the variable section of the output coupling must be terminated in 25 ohms. Since the input impedance to the power amplifier grid cavity is 100 ohms, a quarter-wave section of 51.5-ohm line will provide the proper match. The cavities are mounted far enough apart to do this, and a short section of 100 ohm line completes the connection.

MODULATOR

The modulator design is based on the TT-500B modulator which is designed to operate from a standard RMA composite video signal. The TT-500B modulator (two type 807 tubes in parallel) is capable of fully grid modulating four 4X150A tubes with a bandwidth of about 5 megacycles. Since the TTU-1A transmitter requires that the eight 4X150A tubes be similarly modulated, it is clear that sufficient voltage can be obtained for modulation, but at a reduced bandwidth due to the additional grid capacity of the extra tubes. In order to reduce the capacity that the 807 tubes must work into, they are followed by a cathode follower which in turn delivers its output to the grids of the power amplifier tubes. Several advantages are gained by the use of the cathode follower. The input capacitance of the cathode follower is considerably reduced because of degeneration provided by the cathode resistor and the linearity is very much improved. In addition, with a given capacitance load and bandwidth, it is possible to use a larger load resistor, which results in less modulator plate current.

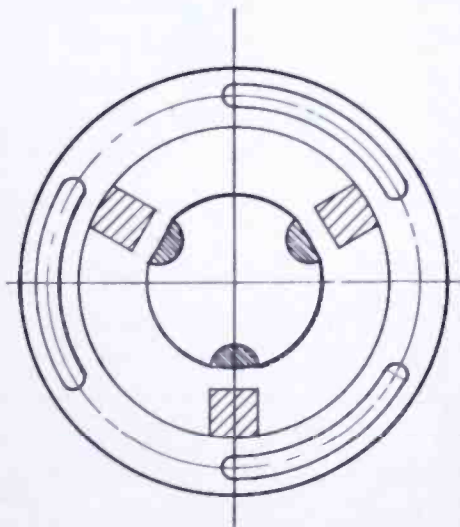


Fig. 12—Cross section of variable impedance transformer.

The choice of a modulator tube was the next problem. It was decided to use eight modulator tubes with the grids connected in parallel for video signals, rather than one larger tube for several reasons. First, by providing a separate bias control for each modulator tube and direct coupling each modulator tube to a single power amplifier tube it becomes quite simple to compensate for any unbalance in static plate currents. Secondly, an unreasonably large tube operating

at a fairly high plate voltage would be needed to deliver the required 71 volts peak to peak to the 300-micromicrofarad load presented by the grids of the eight power amplifier tubes. The one objection to the use of a multiplicity of modulator tubes was the high input capacitance which made the design of the input circuit more difficult. The number of components in the input circuit becomes quite large when the direct-current grid potentials must be separately adjustable as noted above. Thus, it becomes essential that the components be as small as possible and the location of all grid circuit components becomes very critical.

A simplified schematic diagram of the modulator is shown in Figure 13. The video output tubes of the TT-500B transmitter are direct coupled to eight 6L6 tubes with grids connected in parallel for video frequencies and each tube is direct coupled to a single power amplifier tube.

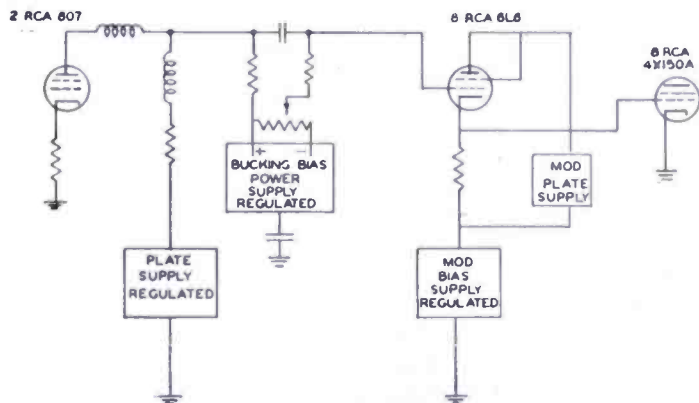


Fig. 13 — Simplified schematic diagram of modulator.

A "bucking bias" power supply was connected between the plates of the 807 tubes and the grids of the 6L6 tubes in order to overcome the positive voltage at the plates of the 807 tubes. Since the power supply has a considerable capacity to ground and is at video potential above ground it was necessary to isolate the supply by means of high resistance in both positive and negative leads. This was possible since the modulator tubes do not draw grid current. In order that the shunt impedance presented by these resistors and the power supply capacitance be held constant over the video frequency range, the power supply capacity was increased to make the RC constant of the shunt network equal to 0.025 second. Thus, for all frequencies above approximately 40 cycles there is a loss of about 2 per cent compared to the direct-current response.

A video amplifier is provided for monitoring the modulator output. The input to the monitor amplifier is obtained from the grids of the power amplifier tubes by means of eight voltage dividers. These are

connected together at the low-potential end which is connected to the grid of the amplifier. Thus, the video input is the average of the signals applied to the eight power amplifier tubes. The resistors used for the voltage dividers are of the deposited carbon type which have good high frequency characteristics and a shunt capacitance of only 0.8 micromicrofarads. This value of capacitance is almost sufficient for high frequency compensation of the divider. However, a capacitance of 1.5 micromicrofarads across only one of the resistors results in nearly complete compensation up to about 5 megacycles. By proper choice of resistance values, the voltage divider also serves as a meter multiplier, so that the average grid voltage of the eight power amplifier tubes may be read on a single meter.

In modulating the power amplifier it was found that the response of the modulated wave had a deep valley at approximately 3.5 to 4 megacycles, although the video voltage applied to the grids of the power amplifier was flat to 5 megacycles. This was traced to resonance in the cathode circuits of the power amplifier between the cathode bypass capacitors and the cathode lead inductance. These leads are of necessity quite long because the cavities are plug-in. The inductance was reduced as much as possible by shortening the lead length and shielding the leads and in addition each cathode circuit was critically damped by means of a blocking capacitor and damping resistor connected to ground. This eliminated all traces of cathode resonance.

SOUND EXCITER

The frequency-modulation sound exciter is designed to accept the standard RMA audio input signal of 10 dbm* \pm 2 dbm at 600 ohms and deliver to the multiplier stages of the transmitter a frequency modulated signal at 1/18 the output frequency of the transmitter and at a power level of about three watts. The exciter is similar to the standard frequency-modulation exciter¹ developed for the RCA FM broadcast transmitters except that the center frequency is stabilized so that the output frequency of the aural transmitter is maintained 4.5 megacycles higher than that of the visual transmitter within \pm 450 cycles. This relative stability is considerably in excess of that which is required for the satisfactory operation of receivers of the inter-carrier-sound type. The tolerance proposed by several RMA technical committees is \pm 5 kilocycles.

Figure 14 shows a block diagram of the frequency control system.

* Decibels referred to a zero level of 1 milliwatt in 600 ohms.

¹ N. J. Oman, "A New Exciter Unit for Frequency Modulated Transmitters", *RCA Review*, Vol. 7, No. 1, pp. 118-130, March, 1946.

The visual and aural transmitters are driven by a crystal oscillator operating at 4.9097 megacycles and a master oscillator operating at 4.9514 megacycles respectively. The master oscillator is frequency modulated by a reactance tube modulator.

The frequency of the master oscillator is accurately maintained at $1/108$ of the transmitter output frequency by means of a motor controlled capacitor connected in the oscillator tank circuit. The motor is controlled by a frequency detector which compares two frequencies derived respectively from a crystal oscillator and from the difference frequency between the visual and aural oscillators. Thus, any error in the master oscillator frequency causes a correcting force to be applied to the tuning capacitor.

One of the reference frequencies operating the frequency detector is obtained directly from an auxiliary crystal oscillator operating at a frequency of 104.165 kilocycles through a frequency divider with a division ratio of five to one to produce the reference frequency of approximately 20.8 kilocycles.

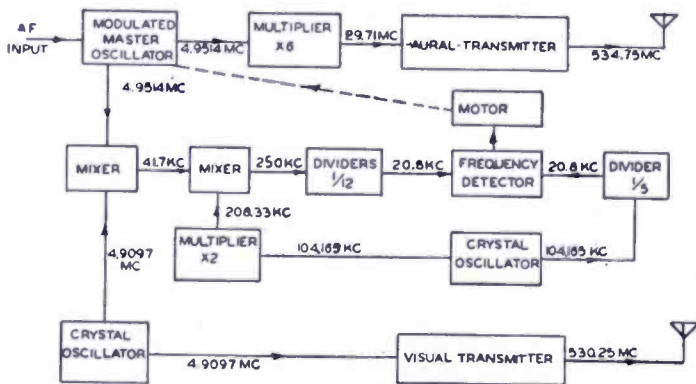


Fig. 14 — Block diagram of frequency control system.

The other reference frequency is obtained by combining the outputs of the visual and aural oscillators in a mixer to produce a frequency of approximately 41.7 megacycles which is the difference between the oscillator frequencies. This frequency is mixed again with the second harmonic of the auxiliary crystal oscillator to obtain a new frequency of 250 kilocycles, which after being divided by 12 becomes the second reference frequency of 20.8 kilocycles. Thus any deviation of the master oscillator frequency from 4.9514 megacycles causes a change in the second reference frequency which in turn causes the motor to rotate and correct the oscillator frequency. In this manner, the frequency stability of the visual transmitter is determined only by the visual crystal oscillator. The center frequency of the aural transmitter is stabilized with reference to the visual output frequency so that the frequency difference is maintained within the specified limits.

TANK CIRCUIT

During the initial operating tests of the cavity, a power output of 475 watts was obtained with a power input of 2000 watts. The difference between output and input power represents loss due to plate dissipation in the tubes and also radio-frequency losses in the tank circuit. The tank circuit losses were found in the following manner.

The unloaded Q of the cavity was measured to be 94 and an output capacity reactance of 8 ohms was calculated for the eight tubes in parallel. Substituting these values in the formula

$$P_d = \left[\frac{E_{\text{max}}^2}{2X_o} \right] \left[\frac{1}{Q_d} \right], \quad (1)$$

and assuming a radio-frequency output voltage of 900 volts peak, which is consistent with the plate voltage applied, the power dissipated in tank circuit losses is shown to be 540 watts.

It is interesting to note that the loaded Q of the cavity can also be calculated. Restating (1) and substituting $P = 475 + 540 = 1015$ watts gives

$$Q_o = \frac{E_{\text{max}}^2}{2X_o P} = 49.7, \quad (2)$$

where Q_o is the loaded Q of the cavity.

The above calculations are not strictly accurate because they neglect the energy stored in the electric field of the cavity itself, but they do give a fair enough approximation to indicate an excessive amount of circuit loss and in addition point to a possible method of obtaining a quantitative breakdown of the various losses in the cavity.

Since the Q of any electrical circuit is the ratio of the stored energy to the energy dissipated in the circuit, the quantity $1/Q$ is proportional to the power loss in that circuit. Thus, to find the loss factor, $1/Q$, of any component, the Q of the cavity can be measured with the component in and out. As long as the stored energy in the circuit has not been changed, the loss factor for the particular component will be the difference between the two $1/Q$ factors. It was decided to break down the circuit losses by successive Q measurements to determine which parts of the cavity contributed the most loss.

Originally, it was supposed that the low current densities resulting from the size of the cavity would allow the top plates to be fitted to the cylinders by a press fit. These seams were soldered and a considerable improvement was measured.

Various other possible losses were measured in order to isolate each loss as much as possible. For example, the loss in the shorting bar was measured by opening half the finger contacts and measuring the increase in loss. This increase is equal to the loss in the shorting bar. In this manner, many of the losses in the cavity were measured.

A summary of these results is given in Table I. The values represent the average of several readings, and are probably accurate to within 10 or 15 per cent.

Table I

Loss	Loss Factor — (1/Q)	
Total		87.5×10^{-4}
Plate—cylinder seams	30.5×10^{-4}	
Plate mica by-pass	24.4×10^{-4}	
Screen mica by-pass	6.4×10^{-4}	
Tubes	11.7×10^{-4}	
Transformer section	3.3×10^{-4}	
Main plate shorting bar	6.5×10^{-4}	82.8×10^{-4}
Unaccounted for		4.7×10^{-4}

It should be noted that the unaccounted loss contains the accumulated error of all readings and is approximately 5 per cent of the total loss.

Both the plate and screen micas were silvered, and the direct-current screen terminal was changed from the tube sockets to the center point of the screen finger plate (see Figure 8). Table I shows that these improvements together with the improvement made by soldering the seams should have increased the Q to 380 if all losses in the plate and screen by-pass capacitors had been eliminated. When the unloaded Q was again measured, it was found to be 350. With these changes a power output of 1050 watts was measured.

There are two other items of importance in connection with the design of the radio-frequency cavities. The first is the spurious responses in the plate cavity. When the cavity is operated in the desired mode, the electric field is constant around the cavity. Since the cross section of the cavity represents an electrical half-wave circuit, it acts like a wave guide at cut-off, and there can be no mode propagated around the cavity at the fundamental frequency. A few megacycles above the resonant frequency however, such modes can be propagated and a great many spurious resonances can occur above the fundamental resonance because of the multiple reflections of the curved walls of the cavity.

The frequencies of these spurious resonances are far enough away from the fundamental frequency so that they are not excited by either the carrier or the radio-frequency modulation components.

One other item of interest is the method of neutralizing the tubes. Although the 4X150A proved very stable as far as oscillation was concerned, it was found necessary to neutralize the amplifier in order to reduce the "feed through" power and improve the modulation characteristic at the cut-off end. Since the screen by-pass capacitance was fixed, it was decided to neutralize by means of a Bridged-T circuit. The neutralizing voltage is provided by the inductance of the screen contact fingers. A single-tube cavity was set up and several different types of screen fingers were measured for minimum feed-through.

EIGHT-TUBE CAVITY PERFORMANCE

The following discussion of the performance of the eight-tube cavity is divided into two parts. First, a comparison of tube performance at 530 megacycles and at low frequencies, and second a comparison of the performance of an eight-tube cavity versus the performance of a single-tube cavity.

There are four principal differences between the tube performance at 530 megacycles and the calculated performance which is based on low frequency operation. These are:

1. Increased driving power,
2. Lower apparent plate efficiency,
3. Increased radio-frequency grid voltage required for a given value of plate current,
4. Back heating of the cathode.

The first two effects were determined to be almost entirely due to circuit losses. If all the known circuit losses are taken into account by the method previously described, the measured radio-frequency power is 90 per cent of the calculated value. The remaining 10 per cent is due to transit time effects and to variation in tube characteristics.

The increased radio-frequency grid voltage and cathode back heating are probably both due to transit time effects at ultra-high frequencies. Measurements showed that the grid drive was about 50 per cent more than the calculated value for any specified plate current. The back heating was easily compensated for by reducing the filament voltage from 6.0 to 5.2 volts.

An accurate comparison between the operation of an eight-tube

cavity and a single-tube cavity requires the operation of eight tubes, one at a time, in a single-tube cavity and comparing this operation with the operation of the same eight tubes in an eight-tube cavity. Although this was not done, the performance of a single-tube cavity had been observed on numerous occasions, and enough data was available to compare the two types of operation under equivalent conditions. For example, a 4X150A in a single-tube cavity developed 150 watts power output at 240 milliamperes plate current, and under the same conditions each 4X150A developed an average of 137 watts or 92 per cent of the single-tube output in the eight-tube cavity. The unloaded Q of the single-tube and eight-tube cavities were found to be 488 and 350 respectively. Loaded Q of a single-tube cavity was not measured, but assuming it to be the same as the value measured for the eight-tube cavity ($Q = 58$) it can be shown that the circuit efficiencies of the eight-tube and single-tube cavities are 83.5 and 88 per cent respectively. From this one would expect the output of the eight-tube cavity to be 95 per cent of the output of the single-tube cavity, a discrepancy of 3 per cent from the measured value.

The conclusion is that when cavity losses are taken into account the operation is essentially the same in either a single-tube or an eight-tube cavity.

PERFORMANCE

The TTU-1A transmitter is designed to meet the proposed standards for commercial ultra-high-frequency television transmission. The performance limits for VHF transmitters as stated in RMA standards and in the FCC "Standards of Good Engineering Practice Concerning Television Broadcast Stations," have been met wherever they apply. In addition the relative stability of the carrier separation has been greatly improved over that required by current or proposed standards.

The visual transmitter is conservatively rated at a peak output power of one kilowatt when transmitting a black picture. Under these conditions the output tubes are operating considerably below the maximum allowable plate dissipation. The regulation of the output is such that the peak output varies less than 5 per cent from an all black picture to an all white picture.

The output of the transmitter contains both sidebands; however, the lower sideband is removed by means of a vestigial sideband filter externally connected. The radiated signal has the standard RMA vestigial sideband characteristic.

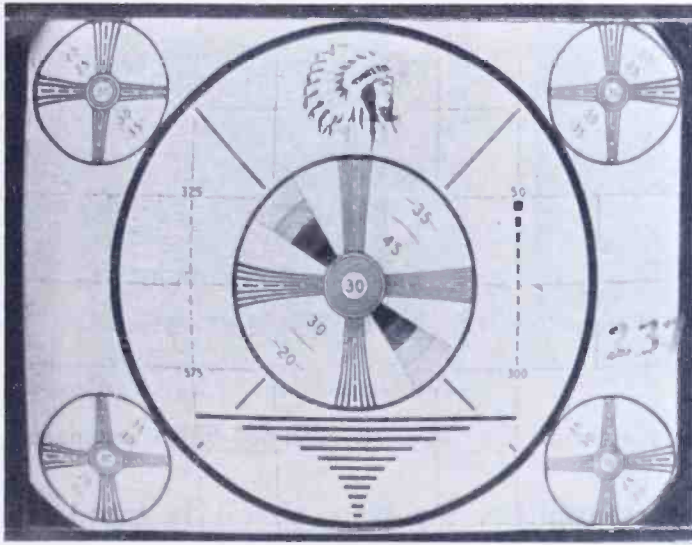


Fig. 15—Picture at input of transmitter.

The aural transmitter is rated at a power output of 500 watts. It is frequency modulated and is capable of more than ± 50 kilocycles swing with less than 5 per cent distortion from 30 cycles to 15 kilocycles; ± 25 kilocycles swing represents 100 per cent modulation. The distortion at 100 per cent modulation is less than the limits stated in RMA Standard TR104-A.

The carrier frequency of the visual transmitter is held constant to within 0.002 per cent of the assigned value. The frequency difference between the aural and visual carrier frequencies is constant to within ± 450 cycles which compares very favorably with the stated requirement of ± 5 kilocycles.

The bandwidth of the plate circuit of the power amplifier is sufficiently broad so that the picture quality is not affected by plate circuit

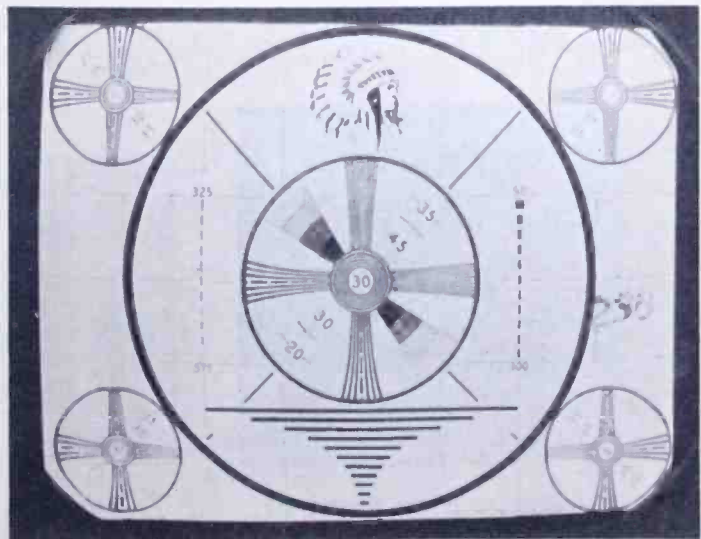


Fig. 16—Picture at output of transmitter.

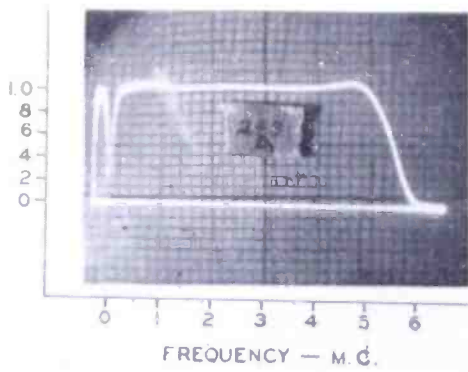


Fig. 17—Modulator video response.

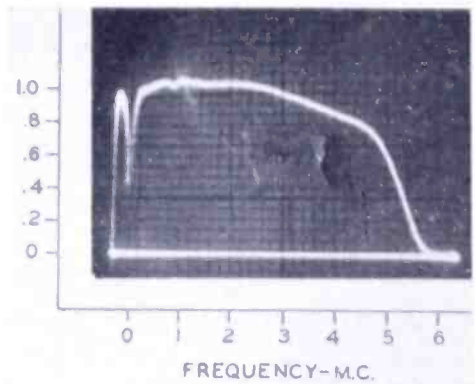


Fig. 18—Overall video response.

tuning. In tuning the transmitter, the plate circuit is tuned for maximum output. Optimum broadbanding of the grid circuit is readily obtained by slightly detuning on the high frequency side of resonance.

The performance of the visual transmitter is shown by Figures 15 to 20. Figures 15 and 16 show the input and output signal respectively when the standard test pattern is transmitted and viewed on a commercial master monitor.

Inspection of Figure 16 shows a vertical resolution of about 460 lines. Figure 17 shows the video response of the modulator measured at the grids of the power amplifier tubes. The response is flat to approximately 5 megacycles. Figure 18 shows the overall frequency response of the transmitter when operating into a dummy load and Figure 19 shows the response to a square wave pulse with a rise time of 0.07 microsecond. It indicates an increase in rise time to 0.11 microsecond. Figure 20 shows the overall modulation characteristic and indicates a feed-through power of only 0.3 watt. A maximum power of 1460 watts is indicated.

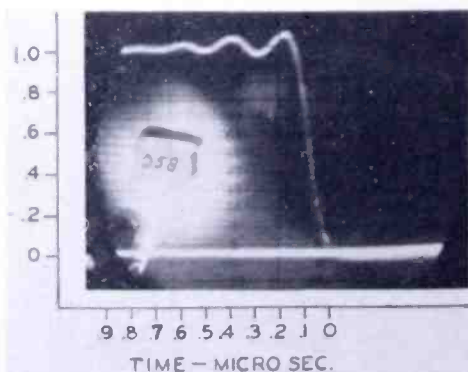


Fig. 19—Square wave response.

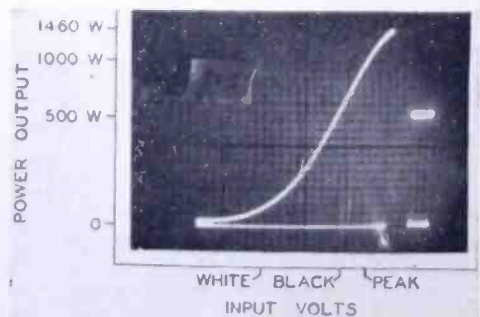


Fig. 20—Modulation characteristics.

CONCLUSION

The TTU-1A transmitter is capable of radiating a signal in accordance with the current FCC "Standards of Good Engineering Practice Concerning Television Broadcast Stations," and the RMA "Electrical Performance Standards for VHF Television Transmitters."

The quality of the transmitted picture is equal to that transmitted by commercial transmitters currently in operation on the VHF channels. In construction and design this transmitter is entirely suited for commercial operation from both the operational and performance standpoints.

ULTRA-HIGH-FREQUENCY ANTENNA AND SYSTEM FOR TELEVISION TRANSMISSION*

BY

O. O. FIET†

Engineering Products Department, RCA Victor Division,
Camden, N. J.

Summary—An omni-directional, horizontally polarized ultra-high-frequency antenna with a power gain of 17.3 is described. Some of the performance characteristics and development problems are given. A vestigial sideband filter and notch diplexer constructed of concentric transmission line is described. Measured performance characteristics and design considerations are also given. The concentric transmission line used to feed the transmitter output to the antenna is described briefly. A broad frequency characteristic is obtained by use of compensated undercut insulators supporting the inner conductor. Waveguide, elbows, and transitions to concentric line have been developed for operation in the 500 to 750 megacycle band. Considerations which make waveguide attractive for ultra-high-frequency television service and measured characteristics of the components developed are presented. The antenna system was developed for the operation at ultra-high-frequency experimental television station KC2XAK at Bridgeport, Connecticut. The antenna system involves the antenna, transmission line or waveguide, a notch diplexer and vestigial sideband filter.

ANTENNA

AN EFFECTIVE RADIATED power of 10 to 20 kilowatts was desired for the experimental ultra-high-frequency (UHF) television broadcast station at Bridgeport, Connecticut.¹ A study of the problems involved indicated the antenna should have as much gain as practical, consistent with stability of radiated signal. Deflection of the antenna and supporting tower by high winds causes the vertical pattern of the antenna to tilt from the horizontal. This may cause the received signal to decrease to an unacceptable value in some receiver locations during high winds. Previous experience and study of the vertical pattern accompanying a given gain indicated a gain of 20 to 25 would give acceptable coverage. Experience obtained

* Decimal Classification: R326.81×R117.2.

† The material in this paper for which the author is directly responsible, together with certain other material, forms the basis of a Doctor's thesis in Electrical Engineering to be presented to the faculty of the Graduate School of the University of Pennsylvania.

¹ R. F. Guy, J. L. Seibert and F. W. Smith, "Experimental Ultra-High-Frequency Television Station in the Bridgeport, Connecticut Area," *RCA Review*, Vol. XI, No. 1, pp. 55-67, March, 1950.

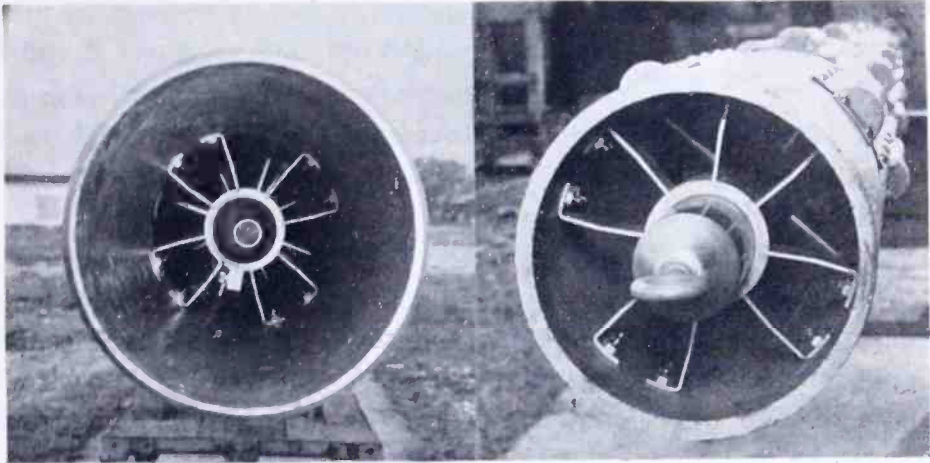


Fig. 1—End views of the antenna.

with the antenna herein described, which has a power gain of 17.3, will determine the practicability of higher power gains.

Very-high-frequency television transmitting antennas utilize a branching-type feeder system to each radiating element to obtain the desired bandwidth and pattern characteristics. An extension of this practice to UHF high-gain antennas would result in a very complicated feeder system due to the large number of radiating elements involved. In the case of the antenna constructed for Bridgeport, the radiating system would have required 88 branch lines; this clearly was not desirable and a feed system of greater simplicity was developed.

The antenna consists of a $3\frac{1}{8}$ -inch outside diameter copper tube mounted coaxially inside a $10\frac{3}{4}$ -inch outside diameter, $\frac{1}{2}$ -inch wall steel tube (Figure 1). The steel



Fig. 2—Antenna installed in the normal vertical position in a rotating socket for measuring horizontal patterns.



Fig. 3—Antenna mounted on horses horizontally over space cloth to absorb ground reflections.

tube is in two lengths, each approximately 20 feet long joined by means of flanges at the radiation center of the antenna (Figures 2 and 3).

Each layer of the radiating system consists of four half-wave slots equally spaced around the circumference of the steel tube. There are twenty-two such layers of half-wave slots, making eighty-eight individual slots in the steel tube.

The antenna is divided into two electrically identical groups of half-wave slots, the slots being spaced approximately a half wave length between ends or approximately a full wave length between centers. The upper and lower groups of slots consist of eleven layers each with a space of 1.66 wave lengths between the ends of the two groups. Each successive layer of slots is rotated 45 degrees to suppress transmission of the $TE_{1,1}$ and other noncylindrical modes within the steel cylinder. The modes which do not have cylindrical symmetry would cause unequal excitation of individual slots in a layer resulting in a non-circular horizontal pattern. Horizontal patterns deviating considerably from circular were observed during development work and the staggering of the layers was found to eliminate such variations from circular. It was interesting to observe, when only one layer was driven, that the pattern was closely circular, checking theoretical calculations.²

The 3 $\frac{1}{8}$ -inch copper tube installed within the antenna tube acts as a transmission line to distribute the transmitter output to the various layers of slots. The slots are driven by radial probes fastened within the antenna tube on one edge opposite the center of each slot. The current passing through the probe capacity also passes through the driving point impedance of each radiating slot. A set of radial probes is used between each layer to obtain an impedance bandwidth at the input of each succeeding layer of the antenna which is approximately equal to the bandwidth of the end layers.³ A similar antenna may be constructed without the tuning probes between layers. However, it is observed that the system input bandwidth becomes progressively narrower as the number of layers, and consequently the gain, is increased.

The 3 $\frac{1}{8}$ -inch diameter copper tube within the antenna has an inner conductor within the lower half which serves as a transmission line to carry the transmitter output to the center of the antenna feed system. The center feed avoids any tilt or other dissymmetry in the vertical pattern with changes in frequency which would be character-

² G. Sinclair, "Patterns of Slotted Cylinder Antennas," *Proc. I.R.E.*, Vol. 36, No. 12, p. 1487, December, 1948.

³ H. J. Riblet, "Microwave Omni-directional Antennas," *Proc. I.R.E.*, Vol. 35, No. 5, p. 477, May, 1947.

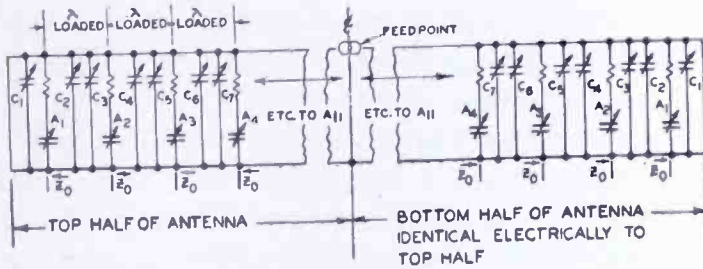


Fig. 4—Diagram of electrical distribution system.

istic of an end fed broadside array. The feed point may be shifted from the center of the array if desired to produce a phase difference of the currents in the upper and lower half of the antenna. Any such phase difference between currents in the two halves of the antenna is accompanied by a corresponding tilt in the vertical pattern. This adjustable tilt in vertical pattern may be used to advantage in any particular installation to adjust for particular terrain conditions or cover densely populated valleys, etc.

Figure 4 is a line diagram illustrating the electrical operation of the feed system used in the antenna. The tuning and feed probe settings for successive layers are different. The probe settings required for matched impedances in the corresponding layers of the top and bottom half of the antenna were usually different due to small mechanical variations in the antenna structure.

A study of the characteristics of the antenna was made using a microwave model at approximately 5000 megacycles (Figure 5). A matched load was inserted in the end of the microwave antenna tube. The relative magnitude and phase of the voltage across the load was measured by conventional methods. Phase and magnitude measurements made with one layer of the antenna matched by means of the tuning probes for various settings of the slot probes gave a curve of additional phase retardation versus relative power absorbed by the radiating layer. This curve was used to determine the proper spacing between layers to compensate for the additional phase shift introduced by the tuning probes. The proper amount of power absorbed by each layer of slots relative to the power transmitted to the subsequent layers is determined as follows for the eleven layers in the top and bottom halves of the antenna.

The end layers, top and bottom extremity of the complete 22-layer antenna, have no succeeding layers to which power must be trans-

Fig. 5—One-tenth scale microwave model of one-half of the antenna (top or bottom half).



mitted. Consequently, they must absorb all of the power which is contained in the incident wave. This is accomplished by adjusting the four slot feed probes and the shorting plug at the end of the antenna until this layer matches the characteristic impedance of the concentric line within the antenna, which is approximately 68 ohms. The second layer from each end must absorb $\frac{1}{2}$ of the power and transmit $\frac{1}{2}$ of the power to the end layers. A combination of feed probe and tuning probe settings is then found which will give this power distribution; i.e., reduce the voltage on the matched load in the end of the antenna to .707 of the value obtained when no tuning or feed probes are inserted. The tuning probes must be adjusted for an impedance match each time the feed probe setting is changed. The setting of the feed probe for the third layer transmits $\frac{2}{3}$ of the incident power and absorbs $\frac{1}{3}$, the fourth layer absorbs $\frac{1}{4}$ and transmits $\frac{3}{4}$ of the power etc. to the 11th layer which absorbs $\frac{1}{11}$ of the power and transmits $\frac{10}{11}$. The settings of the feed and tuning probes and the spacing between each layer of slots determined by this experiment were made and the vertical pattern and gain of the model were measured. The measured vertical pattern closely resembled the expected pattern for 11 layers in phase with equal currents. The power gain measured by substitution of a standard horn reference for the microwave model was 11.4. This checked the gain obtained by integration of Poynting's vector obtained from the measured vertical pattern.

The spacing of successive layers of the full scale UHF antenna was obtained by scaling the dimensions of the microwave model.

The tuning probe locations and settings could not be successfully scaled from the model, and it was necessary to repeat the work of adjusting the tuning probes individually for each layer. The probes were adjusted to obtain an impedance match leaving the slot feed probes set at the dimension determined by scaling the model. Since the magnitude and phase of the currents in each layer of the full scale antenna were not checked, some degradation of vertical pattern and gain of the full size UHF antenna resulted. The gain of the full size antenna was 17.3 instead of 23 or 24 which would have been obtained if the individual layers were directly adjusted for equal phase and currents. The variation of results between the model and full size antenna is attributed to mechanical variations between the model and the full size antenna. It has been found quite difficult to duplicate, electrically and mechanically, all of the practical requirements of the full scale antenna in a one-tenth scale model.

Each layer of the full scale antenna was adjusted to obtain an impedance match at 531 megacycles. Difficulty in adjustment of the

entire antenna by adjusting each successive layer from each end simultaneously led to the discovery that the tuning probe settings for corresponding layers from each end were not the same if the input impedance was matched. The proper reference conditions on the slotted measuring line for each half of the antenna were obtained by shorting out one-half of the antenna a wave length from the feed point and substituting a matched load in the unshorted half of the antenna after all feed probes and tuning screws had been removed. The matched load was constructed of four radial fins of phenolic laminate about 10 feet long mounted on a sleeve which would permit the fins to slide freely on the $3\frac{1}{8}$ -inch diameter inner conductor of the antenna and just clear the inside of the outer steel tube. The fins were covered on both sides with 377 ohms per square space cloth and had a linear taper on the input end about three wave lengths long. When the load was adjusted for a match, the input impedance to the antenna feeder system did not change when the load was moved on the $3\frac{1}{8}$ -inch inner conductor. After the reference conditions were obtained with the matched load, it was possible to tune each half of the antenna either by using the matched load in one half and tuning the other half or shorting out the one half with the shorting disk installed at a point located an integral number of half waves from the feed point.

Experiments with the microwave model and a large sheet of metal to simulate a perfect conducting earth indicated an error in free space impedance measurements of about ± 6 per cent would occur if the UHF antenna were mounted horizontally 6 feet above the earth's surface. This was considered undesirable, and experiments using the microwave model with space cloth having the impedance of free space (377 ohms per square) and a metal ground sheet with space cloth equivalent to a full size sheet of space cloth (9×40 feet) placed under the antenna $\frac{1}{4}$ wavelength above the ground plane indicated that impedance measurements could be made with the horizontal antenna above the ground if the 9×40 foot space cloth absorber were placed $\frac{1}{4}$ wave above the ground. The full size space cloth absorber was constructed on a group of wooden frames with space cloth on the top and wire screen on the bottom to assure terminating the wave in a good conductor placed at the earth's surface. The setup of the antenna for impedance tests over the space cloth absorbers is shown in Figure 3. Later impedance measurements on the horizontal antenna 6 feet over plain earth without the ground reflection absorbing sheets indicated the ground may not affect the impedance as much as expected (see Figure 6).

Calculations of reflection coefficient of the earth's surface for

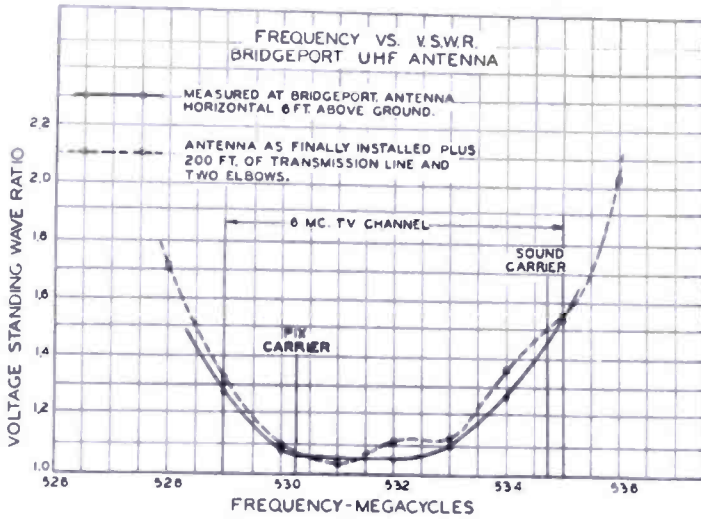


Fig. 6—Standing-wave-ratio characteristic of the antenna.

normal incidence using a dielectric constant of 16 for earth gives a reflection coefficient of -0.6 compared to the assumed perfectly conducting earth reflection coefficient of -1 . If this were the case, one might expect the error in impedance measurements, due to the ground 6 feet distant, to be in the order of ± 3.6 per cent. Observations have indicated that it is probably less than this.

Vertical patterns were measured by horizontally rotating the antenna while mounted on a vertical spindle under the center of radiation as shown in Figure 7. A receiver was set up at a distance sufficiently great from the transmitting antenna that the transmission path length difference to the receiving antenna from the ends and from the center of the transmitting antenna was less than one-tenth wave length. The observer at the receiver setup was in constant communication with the engineer at the transmitting antenna (see right inset, Figure 7). An accurate compass dial and vernier were installed on the transmit-

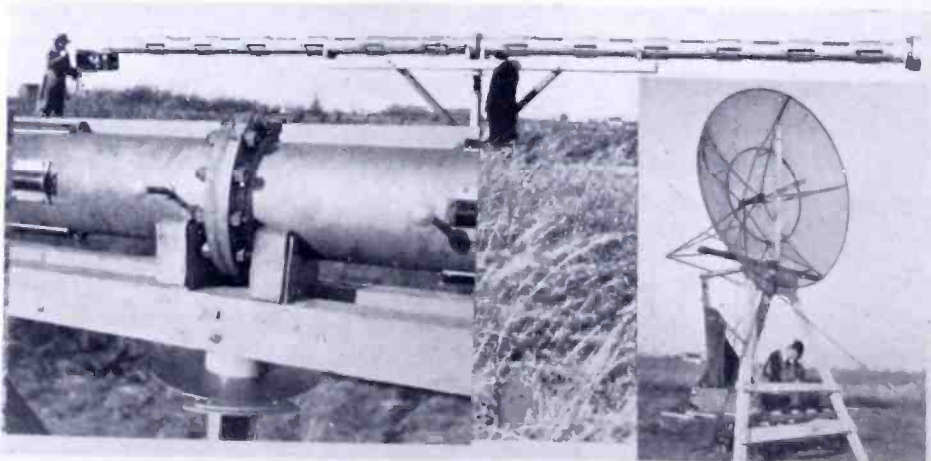
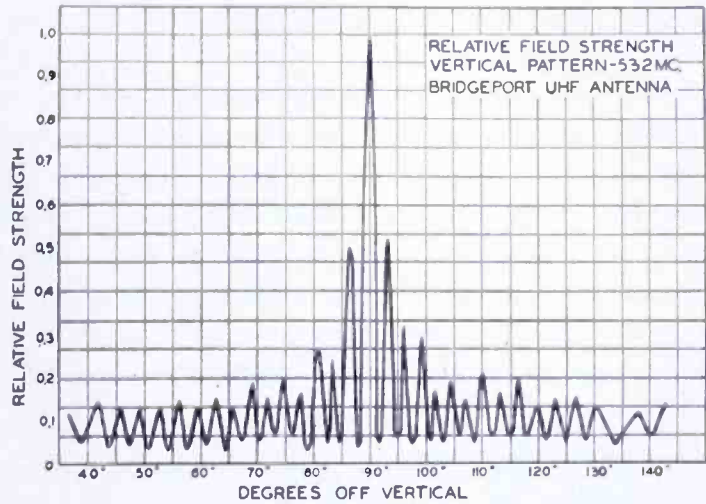


Fig. 7—Vertical pattern test setup for the antenna.

Fig. 8—Vertical pattern measured for the antenna.



ting antenna spinner to indicate the azimuth with better than .1 degree accuracy, as the transmitting antenna was rotated by hand and the signal recorded point by point. The vertical pattern was measured at 529, 532 and 535 megacycles and found to remain about as shown in Figure 8. Poynting's vector integrations using the measured vertical patterns, give the gain frequency characteristic shown in Figure 9. The vertical pattern calculated from the eleven section microwave model pattern measurements is shown in Figure 10. The greater side lobe levels of the full scale antenna and the deviation of the null angles compared to those obtained with the microwave model are largely due to variations of the amplitude and phase of the currents in the various layers of the full size UHF antenna. The side lobe level of the full size antenna may be reduced to compare with the microwave model if the current magnitude and phase of each layer are correctly adjusted.

Calculations were made to determine what transmitter power would give an adequate received signal for the vertical pattern measuring set-

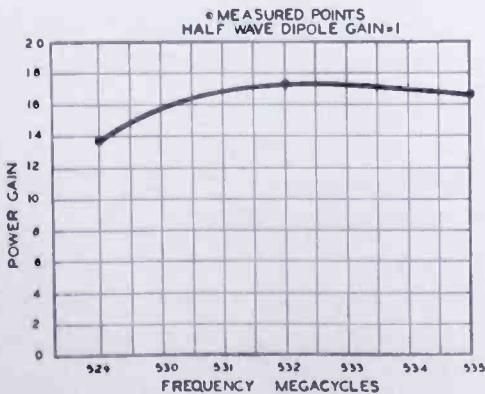


Fig. 9—Power gain versus frequency.

up used (Figure 7). Based on the premise that the ground reflection coefficient near grazing incidence was -1 , these calculations indicated that a transmitter power in the order of 100 watts would be required. Experiments with the actual test setup and location indicated adequate received signal could be obtained with about 2 milliwatts transmitter power. This suggests the ground reflection coefficient including the effects of brush, grass

and irregular terrain is nearly zero or is actually positive (see terrain of Figure 7).

The horizontal pattern was measured in the setup shown in Figure 2. The antenna was mounted vertically in a socket and could be readily rotated. The receiver and antenna were mounted at a distance, opposite the radiation center of the transmitting antenna. The measured horizontal pattern varied less than ± 1 per cent from circular, which is in close agreement with the pattern calculated for staggered slots.²

TRANSMISSION LINE

The commercial very-high-frequency, air dielectric, concentric transmission line has a uniform tubular inner conductor with supporting ceramic disc insulators clamped to it at one-foot intervals. This type of line is satisfactory for very-high-frequency service where the characteristic impedance is practically constant. However, the uncom-

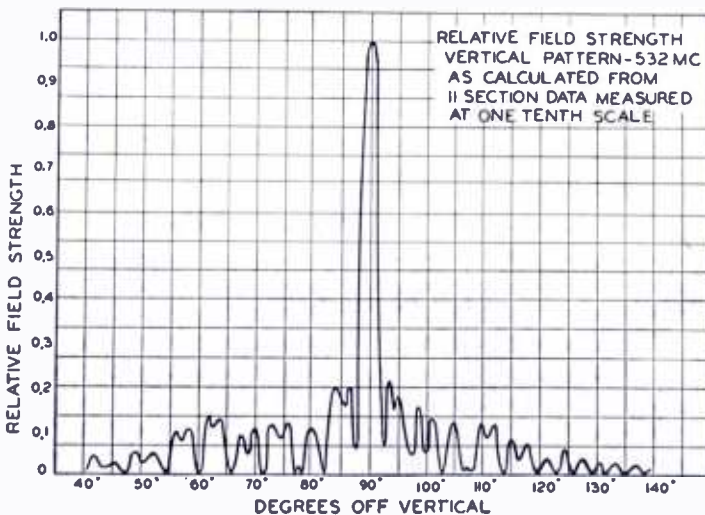


Fig. 10—Vertical pattern for full antenna calculated from measurements on the microwave model.

pensated beads at periodic intervals make the line have characteristics similar to a low pass filter with attenuating bands in the UHF region. The characteristic impedance fluctuates rapidly with frequency and is reactive over much of the UHF band. A line of this type is clearly not suitable for the stringent standing wave requirements of television transmitting antenna systems in the UHF band where a nearly constant resistance load must be used.

There appear to be many approaches to the UHF insulator support problems^{4, 5} for concentric line. The method developed by D. W. Peter-

⁴ R. W. Cornes, "A Coaxial Line Support for 0-4000 Mc," *Proc. I.R.E.*, Vol. 37, No. 1, p. 94, January, 1949.

⁵ D. W. Peterson, "Notes on A Coaxial Line Bead," *Proc. I.R.E.*, Vol. 37, No. 11, p. 1294, November, 1949.

son was used in the Bridgeport installation because satisfactory line of this type was available. The transmission line in the installation changed the standing wave characteristic of the antenna very little, as indicated by measurements, taken with the antenna mounted on the tower, through 200 feet of transmission line (Figure 6).

The insulator supports on the transmission line used at Bridgeport were mounted in undercut spaces on the inner conductor. Small series inductances were cut in the faces of the undercut to compensate for the step capacity^{6, 7} as shown in Figure 11. The standing wave characteristic of a sample of the transmission line used is shown in Figure 12. The line was terminated in a resistance of 52 ohms and measured on a 52-ohm measuring line.

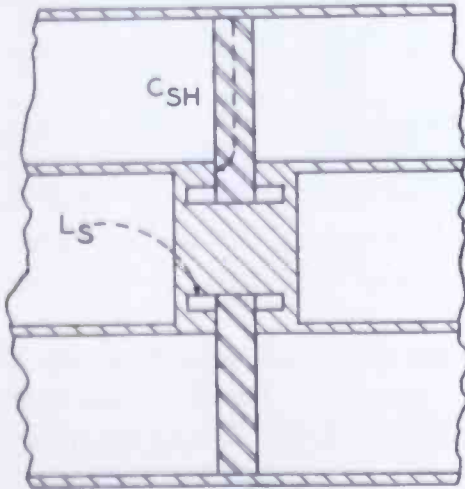


Fig. 11—Section of compensated undercut insulator for 3 1/8-inch diameter coaxial line.

The standing wave characteristic of a sample of the transmission line used is shown in Figure 12. The line was terminated in a resistance of 52 ohms and measured on a 52-ohm measuring line.

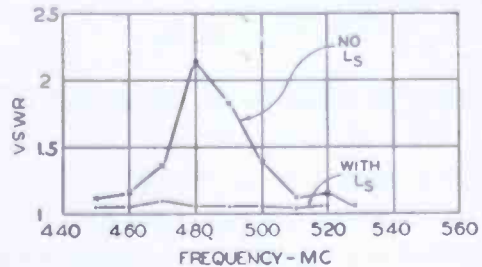


Fig. 12—Standing wave ratio of sample run of UHF transmission line.

WAVE GUIDE

The simplicity and relatively low loss of wave guide led to its consideration for experimental line to transmit power from the transmitter to the antenna. Various wave-guide components were developed for this purpose including transitions for terminating the wave guide in coaxial lines and E and H plane bends (Figures 13, 14, 15 and 16). The problems of using wave guide near the lower end of the UHF band are new, and considerable development work and experimentation is required before it can be utilized commercially.

The wave guide investigated is rectangular having inside dimensions $7\frac{1}{2} \times 15$ inches. It is fabricated from sheet metal. Hot dipped galvanized steel, aluminum or copper clad steel are suitable materials.

A comparison of the loss of wave guide and common size concentric

⁶ HANDBOOK OF DESIGN DATA, Brooklyn Polytechnic Institute, Report No. R-158-47.

⁷ J. R. Whinnery, H. W. Jamieson and T. E. Robbins, "Coaxial Line Discontinuities," *Proc. I.R.E.*, Vol. 32, No. 11, p. 695, November, 1944.

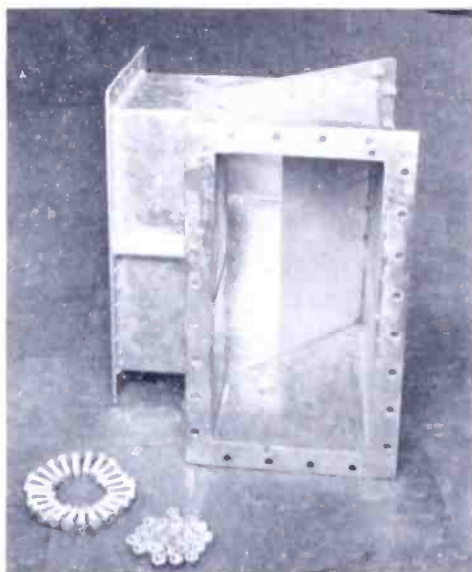


Fig. 13—E plane bend for $7\frac{1}{2} \times 15$ -inch wave guide.

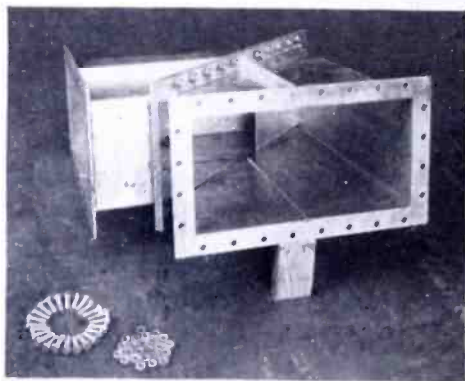


Fig. 14—H plane bend for $7\frac{1}{2} \times 15$ -inch wave guide.

shown in Figures 18, 19, 20 and 21.

The wave guide and components developed correspond closely to those employed in current microwave practices. However, the large size created new electrical and mechanical problems. It was convenient to do much of the development work on the wave guide and components using $\frac{1}{2}$ and $\frac{1}{10}$ scale models at higher frequencies. No difficulties similar to those observed in scaling the antenna were experienced, since the wave guide was so simple that all important features could be accurately scaled.

transmission lines is given in Figure 17. The standing wave frequency characteristics of some of the wave-guide components developed for experimental work are

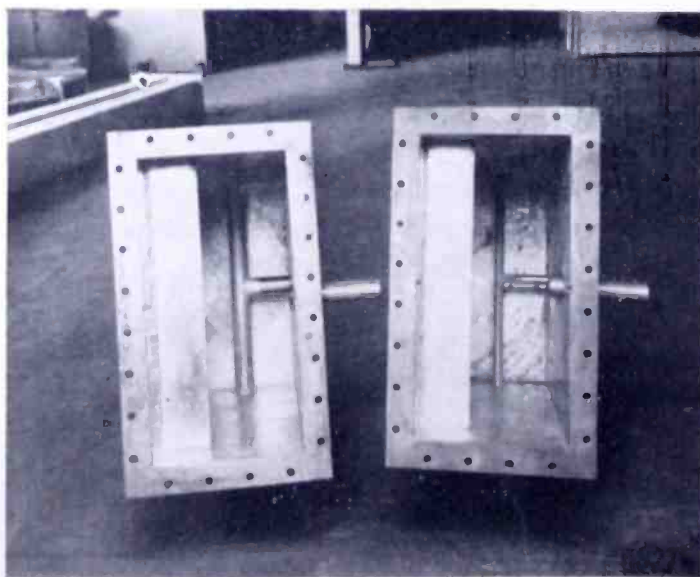


Fig. 15—Transitions from $7\frac{1}{2} \times 15$ -inch wave guide to coaxial line.



Fig. 16—Straight wave-guide section $7\frac{1}{2} \times 15$ inches.

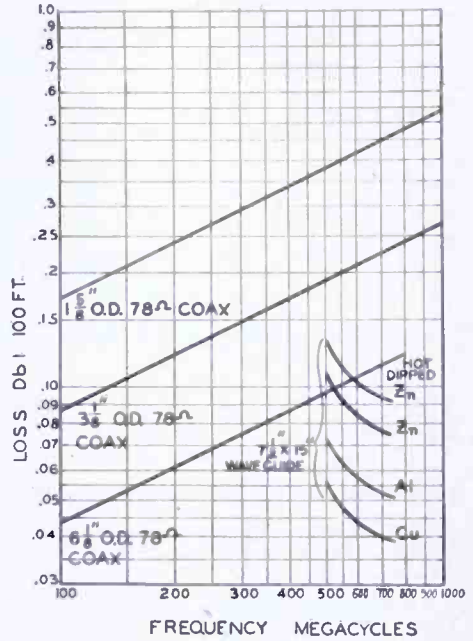


Fig. 17—Curve showing loss of various $7\frac{1}{2} \times 15$ -inch wave guides and standard size coaxial lines.

VESTIGIAL SIDEBAND FILTER

A high-level vestigial sideband filter for use on the output of the transmitter was developed. The filter used was designed to present a constant input resistance for picture carrier and both sidebands, although only the upper sideband and a portion of the lower sideband is transmitted. The transmission characteristic of the sideband filter installed at Bridgeport is shown in Figure 22.

The sideband filter was constructed of coaxial transmission line (Figure 23). A line diagram of the circuit arrangement used is shown in Figure 24. Some of the resonant

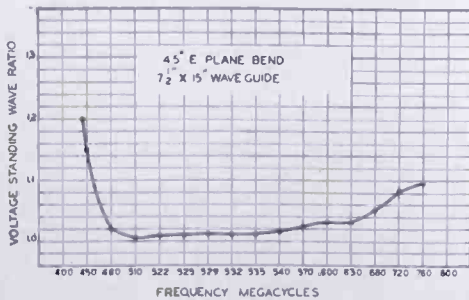


Fig. 18—45-degree E plane bend standing-wave ratio versus frequency.

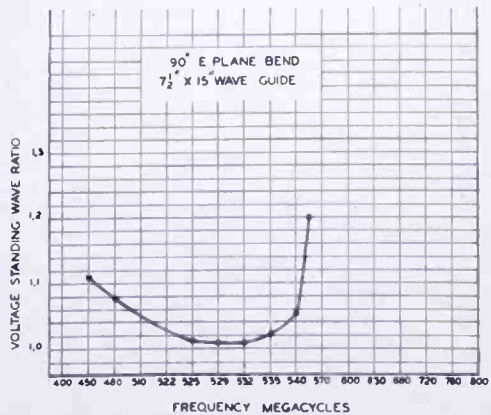


Fig. 19—90-degree E plane bend standing-wave ratio versus frequency.

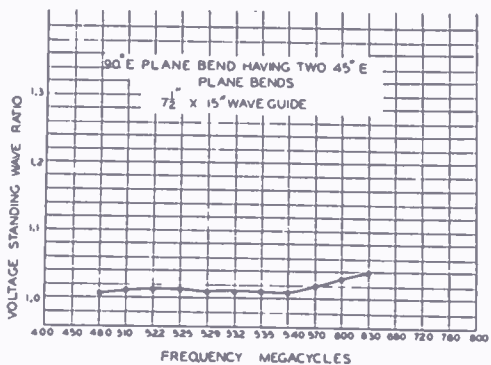


Fig. 20—90-degree E plane bend consisting of two 45-degree bends—standing-wave ratio versus frequency.

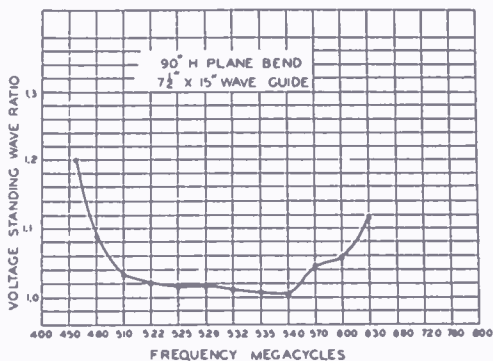


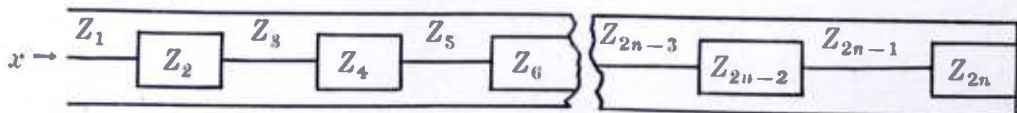
Fig. 21—90-degree H plane bend standing-wave ratio versus frequency.

circuit elements are constructed of stepped quarter-wave sections to obtain a high reactance slope without using long transmission lines. The reactance slope obtained with a stepped open-end transmission line is:



$$\frac{dx}{df} = \frac{\pi Z_1}{2f_0} \left\{ 1 + \frac{Z_1}{Z_2} \left[1 + \frac{Z_3}{Z_2} \left(1 + \frac{Z_3}{Z_4} \left\{ 1 + \frac{Z_5}{Z_4} \left[\dots \left(1 + \frac{Z_{2n+1}}{Z_{2n}} \right) \right] \right\} \right) \right] \right\} \cdot (1)$$

The equation for the reactance slope of a stepped shorted-end transmission line is obtained by letting Z_{2n+1} equal zero in Equation (1):



$$\frac{dx}{df} = \frac{\pi Z_1}{2f_0} \left\{ 1 + \frac{Z_1}{Z_2} \left[1 + \frac{Z_3}{Z_2} \left(1 + \frac{Z_3}{Z_4} \left\{ 1 + \frac{Z_5}{Z_4} \left[\dots \left(1 + \frac{Z_{2n-1}}{Z_{2n}} \right) \right] \right\} \right) \right] \right\} \cdot (2)$$

All steps in impedance are a quarter-wave long at the resonant frequency.

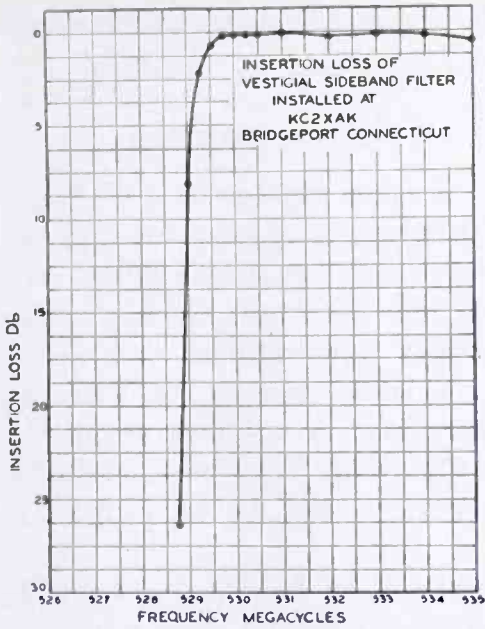


Fig. 22—Sideband filter insertion loss versus frequency.

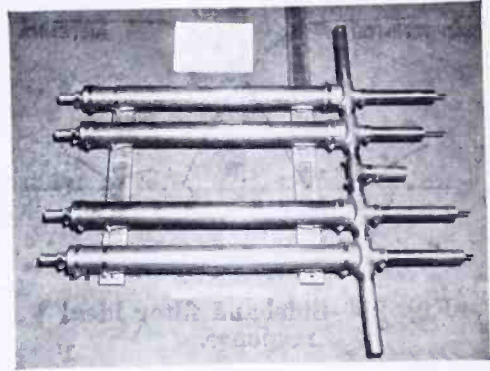
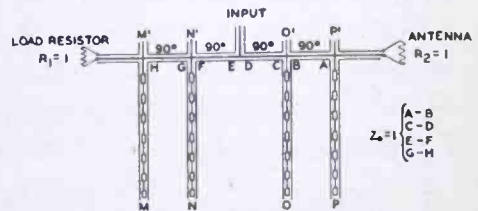


Fig. 23—Sideband filter photograph.

The sideband filter is designed to have five points of input impedance match. One is at the crossover frequency, where the output to the antenna is reduced 3 decibels. This is obtained by making the input impedance of the low pass and high pass portion of the sideband filter complementary. The normalized conductance of the input to the low pass and high pass sections are equal to $+ \frac{1}{2}$ at the crossover frequencies. The normalized susceptances are equal and opposite in sign, thus making the input admittance to the filter system a normalized conductance of one with zero susceptance at crossover. The rejector circuits in the high pass portion of the filter are parallel resonated at one frequency $f_0 + \Delta_2$ in the pass band. The impedance is matched at a frequency very close to this parallel resonant frequency. The rejector circuits in the low pass portion of the filter are similarly parallel resonated at a frequency $f_0 - \Delta_2$ in the reject band resulting in a similar matched impedance point in the reject band. The reject circuits in the high pass and low pass portions of the filter are tuned to different frequencies. Proper selection of the reactance slopes and reject frequencies causes one rejector circuit to compensate for the mismatch introduced by the other to obtain an additional matched impedance point in the pass and reject band. The ideal transmission characteristic of

The sideband filter is designed to have five points of input impedance match. One is at the crossover frequency, where the output to the antenna is reduced 3 decibels. This is obtained by making the input



REACTANCE SLOPES USED - N & O 159 OHMS/MC
M & P 7 OHMS/MC

LINE	SHORT CIRCUIT FREQ.
M	$f_0 + \Delta_1$
N	$f_0 + \Delta_2$
O	$f_0 - \Delta_2$
P	$f_0 - \Delta_1$

AT $f_0 - \Delta_2$ PARALLEL RESONATE M' WITH M AND N' WITH N
AT $f_0 + \Delta_2$ PARALLEL RESONATE O' WITH O AND P' WITH P.

Fig. 24—Sideband filter line diagram.

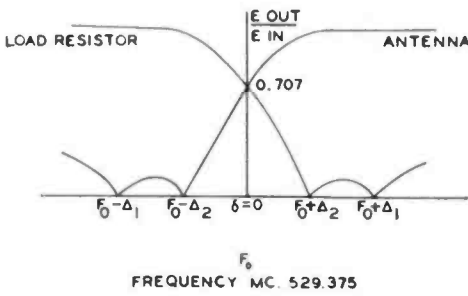


Fig. 25—Sideband filter ideal response.

the vestigial sideband filter is shown in Figure 25.

NOTCH DIPLEXER

A notch diplexer is a filter circuit which is required to feed the sound and picture transmitter output into the single antenna transmission line without interaction

between the transmitter outputs. A coaxial line circuit was developed for the Bridgeport installation (Figure 26). A line diagram of the circuit arrangement used is shown in Figure 27. The circuit used does not differ greatly from the notch diplexers used for very-high-frequency television.

The operation of the notch diplexer is as follows, referring to Figure 27: The lines of length $11\lambda/4$ are tuned for a short circuit at picture frequency on junctions *D* and *E*. The short circuit at picture

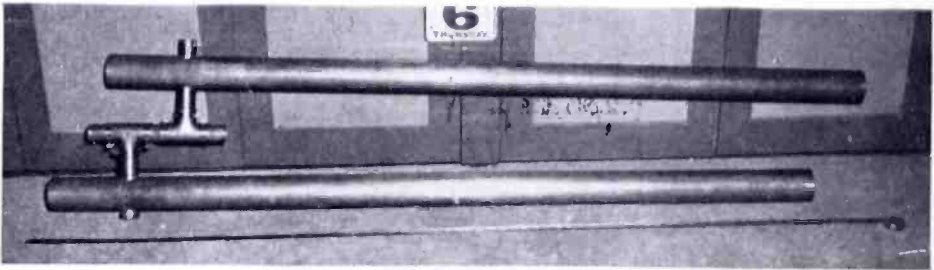


Fig. 26—Notch diplexer photograph.

frequency for junction *D* is transformed to an open circuit at junction *F* by a quarter-wave line *DF*. The open circuit at junction *F* permits the picture transmitter output to go to the antenna. The line *CA* is selected a quarter-wave at picture carrier and therefore does not shunt junction *C* at picture carrier. The length between junction *F* and *C* is selected to obtain a good impedance match for picture fre-

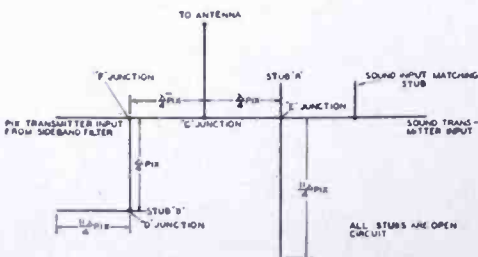


Fig. 27—Notch diplexer line diagram.

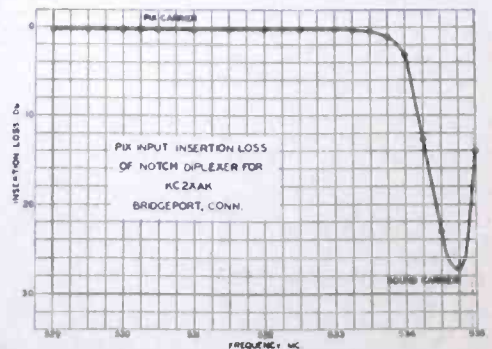


Fig. 28—Notch diplexer insertion loss.

quencies just below the sound notch thus obtaining a sound notch with steep skirts and a sharp shoulder. Stubs *A* and *B* are adjusted so that when each $11\lambda/4$ circuit is attached at junction *D*, maximum rejection of sound frequency on the picture input exists. This adjustment does not correspond to minimum standing wave ratio on the sound input and an additional stub is used on the sound input line to obtain a matched input at sound carrier frequency. The standing wave ratio and transmission characteristics obtained on the picture input for the coaxial line diplexer installed at Bridgeport, Connecticut are shown in Figures 28 and 29.

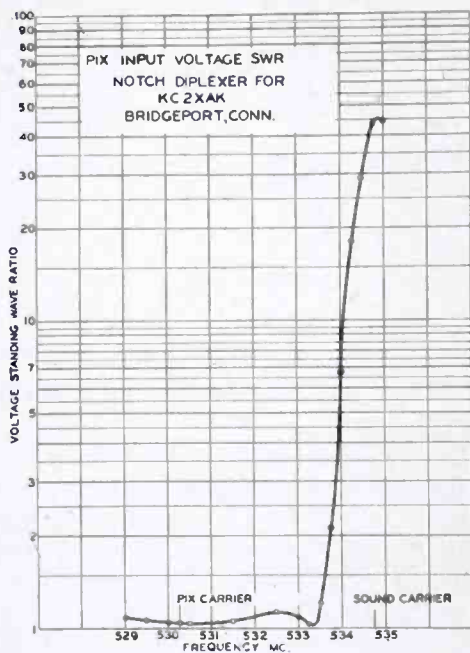


Fig. 29—Notch diplexer standing-wave ratio versus frequency.

CONCLUSION

The various components of the UHF television antenna system have been constructed and tested. The practicability of UHF television transmitting antenna equipment has been demonstrated by the experimental test results obtained and will be confirmed by operational experience with the experimental UHF Television Station KC2XAK in Bridgeport, Connecticut. Adequate power gain can be realized in a practical structure to permit adequate service with low power transmitters. The antenna development indicated no fundamental obstacles in the design of a practical commercial antenna for ultra-high-frequency television. The antenna described is a prototype of the improved type TFU-20A commercial ultra-high-frequency transmitting antenna.

ACKNOWLEDGMENT

The developments described were the contributions of many engineers of the RCA Victor Division, RCA Laboratories Division and the National Broadcasting Company, Inc.

GENERAL DESCRIPTION OF RECEIVERS FOR THE DOT-SEQUENTIAL COLOR TELEVISION SYSTEM WHICH EMPLOY DIRECT-VIEW TRI-COLOR KINESCOPIES*

A Progress Report

BY

RCA LABORATORIES DIVISION AND RCA VICTOR DIVISION,
Princeton, N. J., Harrison, N. J. and Lancaster, Pa.

Summary—Color television receivers are described which incorporate two forms of the first tri-color kinescopes to be successfully demonstrated. Each of the two forms employs the same type of direct-view color screen. In one of these forms three electron guns are used, the electron beams of which pass through the same tube neck and the same deflection yoke to strike the color screen. In the other form a single electron gun is used, again with a single deflection yoke. Both are fabricated in 16-inch metal cones and produce pictures approximately 9 inches by 12 inches.

The direct-view color screen is composed of an orderly array of small, closely spaced, aluminized phosphor dots arranged in triangular groups, each group comprising a green-emitting dot, a red-emitting dot and a blue-emitting dot. In the first laboratory sample tubes used in receivers, there are 351,000 such dots, 117,000 of each color; the objective is to double these numbers in later models. The screen is viewed in the same manner as a conventional black-and-white kinescope.

THREE-GUN TRI-COLOR KINESCOPE

THE manner in which the color screen produces a color picture is best understood by considering first the operation of the three-gun tri-color kinescope. An apertured mask is interposed between the three guns and the dot-phosphor screen in such a manner that the electrons from any one gun can strike only a single color phosphor no matter which part of the raster is being scanned. The mask is comprised of a sheet of metal spaced from the phosphor screen and containing 117,000 holes, or one hole for each of the tri-color-dot groups. This hole is so registered with its associated dot group that the difference in the angle of approach of the three oncoming beams determines which color is excited. Thus, three color signals applied to the three guns produce independent pictures in the three primary colors, the pictures appearing to the eye to be superimposed because of the close spacing of the very small phosphor dots.

Insofar as the color aspects are concerned, this three-gun tri-color kinescope may be utilized in a receiver in much the same manner as

* Decimal Classification: R583.5.

three single-color kinescopes, except, of course, that no optical superposing or registration means need be provided and deflection power need be provided for only one deflection yoke.

The research-type receiver which employs the three-gun tri-color kinescope and high-level sampling,¹ utilizes 46 tubes and consists essentially of a 27-tube black-and-white television receiver to which have been added 19 tubes for color synchronization, sampling, additional power supplies, etc.

SINGLE-GUN TRI-COLOR KINESCOPE

The operation of the single-gun tri-color kinescope is analogous to the operation of the three-gun tri-color kinescope in that the beam from the single gun is magnetically rotated so that, in effect, it occupies, in time sequence, the three positions of the three guns in the three-gun kinescope. Thus, when the beam is in a position corresponding to the green gun of the three-gun kinescope it excites only the green phosphor dots and is at this particular time modulated only by the green component of the video signal. A short time later the beam has been rotated to a position corresponding to the red gun of the three-gun kinescope and is modulated by the red component of the video signal to excite red phosphor dots. A third position similarly produces the blue picture. Sampling is automatically provided by rotating the beam synchronously at sampling frequency.

The research-type receiver employing the single-gun tri-color kinescope utilizes 37 tubes and consists essentially of a 27-tube black-and-white television receiver to which have been added 10 tubes for color synchronization, beam rotation, additional power supplies, etc.

RECEIVER FOR THE THREE-GUN TRI-COLOR KINESCOPE

A block diagram of the principles of the circuit arrangement employed in the receiver utilizing the three-gun tri-color kinescope is shown in Figure 1. Video signal from a conventional black-and-white television receiver is applied simultaneously to the three, internally-connected, control grids of the three-gun kinescope. Another signal, derived from the video amplifier, is used to actuate an automatic color phasing and sampling synchronization circuit² which produces a local 3.58-megacycle sampling wave. The latter is applied through an ampli-

¹ "A Simplified Receiver for the RCA Color Television System," Bulletin, RCA Laboratories Division, February, 1950.

² "Recent Developments in Color Synchronization in the RCA Color Television System", Bulletin, RCA Laboratories Division, February, 1950.

fier tube and appropriate delay lines to three gating tubes which supply three sampling pulses, differing in phase by 120 degrees at 3.58 megacycles, to the three cathodes of the kinescope. Thus, each gun is turned on in time sequence corresponding to the original sampling process at the transmitter and the beam current from each gun excites only one of the three phosphor colors.

The tuning adjustment in the plate circuit of the 3.58-megacycle sampling-signal amplifier permits fine adjustment of the overall color phasing. However, proper color phasing is essentially determined by the permanently installed delay lines which are initially cut to proper length.

The front-panel operating controls are the same for color as for black-and-white operation. Individual service adjustment controls are provided in the cathode circuits of the three guns in order to permit initial equalization of the control characteristics of the three guns.

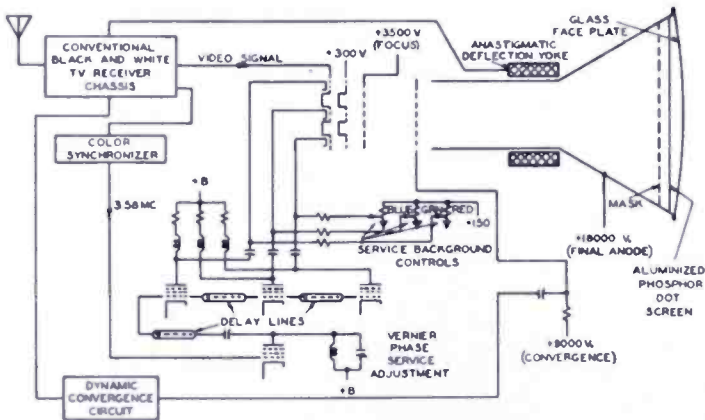


Fig. 1 — Block diagram of receiver circuit principles for the three-gun tri-color kinescope.

The deflection circuitry is of the conventional type. Minor changes in deflection-tube types have been made to supply additional deflection power occasioned by the increased kinescope second-anode potential (18 kilovolts). The deflection yoke is of the anastigmatic type and has an internal diameter of two inches to accommodate the converged beams from the three guns.

The registration in this three-gun tube is built in by the proper registration of the masking apertures with their corresponding groups of phosphor dots. Means are also provided to converge the three beams to the same point on the phosphor screen during scanning. This is done for the undeflected beams by a convergence electrode, operated at 9000 volts, and, when necessary, by small correcting magnets set up initially as a permanent service adjustment when the tube is installed. Because of the essentially flat face of the phosphor screen, simple geometrical considerations show that slightly less convergence is desirable as the

beam is deflected from center. This dynamic convergence is accomplished by deriving a voltage from vertical and horizontal deflection circuits of the receiver and applying it to the convergence electrode through a capacitor.

A radio-frequency type anode voltage supply provides a potential of 18 kilovolts for the kinescope final anode, 9 kilovolts for the electrostatic converging electrode and approximately 3.5 kilovolts for the parallel-connected first anodes which produce initial electron-beam focus. A small auxiliary power unit provides heater and +B power for the other added circuits.

RECEIVER FOR THE SINGLE-GUN TRI-COLOR KINESCOPE

A block diagram of the principles of the circuit arrangement employed in the receiver utilizing the single-gun tri-color kinescope is shown in Figure 2. Video signal from the output of the video amplifier

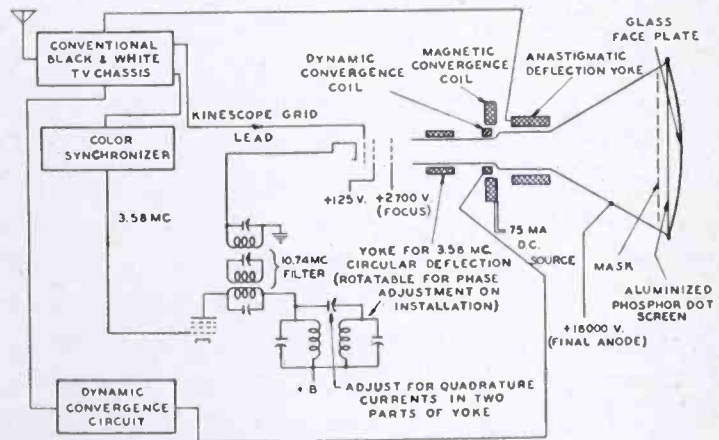


Fig. 2 — Block diagram of receiver circuit principles for the single-gun tri-color kinescope.

of a conventional black-and-white television receiver is applied to the control grid of the single-gun kinescope in the conventional manner. Here again, as in the previous receiver, another signal from the video amplifier actuates an automatic color phasing and sampling synchronization circuit² which produces a local 3.58-megacycle signal which is locked in step with the transmitter sampler. Circular deflection of the beam, which produces sampling automatically, is provided by a small deflection yoke having two sets of coils which are fed with quadrature currents at sampling frequency to produce a rotating field. Service adjustment of color phasing is provided by mechanical positioning of this yoke. The amplitude of the circular deflection is adjusted to produce the proper convergence angle as required by the mask and phosphor-dot screen. The duration of the sampling period is controlled by

a signal having a frequency three times the sampling frequency which is injected into the kinescope cathode circuit. The amplitude and phase of this 10.74-megacycle signal are determined by the alignment of a filter circuit which utilizes the third harmonic of the circular-deflection driver tube.

As in the receiver for the three-gun tube, the front panel controls of the single-gun set are the same as those used in a conventional black-and-white receiver. Because a single gun is used in this kinescope, color balance may be achieved by proper deposition of the phosphor dots.

The deflection circuitry and deflection yoke are the same as those employed in the three-gun receiver described in the preceding section.

The kinescope gun which is employed is the same as that used in the commercial type 5TP4 kinescope. Potentials of 18 kilovolts for the final anode and 2.7 kilovolts for the electrostatic focus electrode are derived from the kick-back voltage on the horizontal-deflection output transformer just as in conventional black-and-white receivers. A small auxiliary power unit provides heater and +B power for the other added circuits.

Convergence of the circularly deflected beam is produced by a magnetic lens in this single-gun kinescope instead of the electrostatic method employed in the three-gun version. A coil similar to the focus coil normally employed in conventional black-and-white receivers is used for this purpose. The dynamic convergence variation is likewise applied magnetically in this tube and is introduced by means of a smaller auxiliary coil located near the main convergence coil. As in the previous receiver, the dynamic convergence waveforms are derived from the deflection circuits.

PROGRAM CONTROL CONSOLE FOR INTERNATIONAL PROGRAM SERVICE*

BY

S. H. SIMPSON, JR., R. E. HAMMOND AND M. P. REHM

Operations Department, RCA Communications, Inc.,
New York, N. Y.

Summary—Interest in international shortwave programs, which began with experiments in 1927, grew rapidly, and in 1931 RCA Communications, Inc. established a separate department for handling international addressed program transmissions. In 1932 the service was offered on a regular commercial basis. This service is entirely different from the regular transoceanic telephone service, and an explanation is given to show how a typical addressed program transmission is handled. While the equipment required in the control room for coordinating and switching the program signals is somewhat similar to standard broadcast apparatus, the requirements are sufficiently different to necessitate special treatment. The control console and auxiliary equipment installed at New York and San Francisco was designed and built to provide a modern and efficient means of better serving the broadcast organizations which use the international program service. The program selector switches, amplifiers, monitoring facilities, microphone control circuits, jack arrangement, and other features of the installations are described in detail along with the reasons for some of the special requirements.

INTRODUCTION

THE program control console and auxiliary equipment described herein was designed and built to satisfy the particular requirements of RCA Communications, Inc. program transmission service. Two identical sets of equipment were constructed: one for use in the Central Radio Office at New York where circuits with Europe, Africa, the Caribbean, and South America terminate; the other for use in the Central Office at San Francisco, which is the terminus for communicating with Alaska, Australia, China, Hawaii, Japan, the Philippines, and other points in the Pacific and the Far East.

While the principles and technique utilized in handling the program transmission circuits are somewhat similar to standard broadcast practice, there is sufficient difference to necessitate the use of specially designed equipment for this unique service. In order to better understand these requirements, it will perhaps be helpful to first know something of the history and development of the RCA program transmission service and just how the service operates.

* Decimal Classification: R400.

HISTORICAL DEVELOPMENT

The first experiments toward establishing a regular program service from Europe were conducted in 1925 and 1926 at the Belfast, Maine receiving station of the Radio Corporation of America. Here a special experimental station was erected for receiving the 1600-meter signal from the British station 5XX and the received signal was relayed over an 80-meter circuit to the RCA Research Laboratory then located in Van Cortlandt Park in New York City. From there the signal was sent over a telephone line to the original WJZ broadcasting station located on the roof of Aeolian Hall, where it was broadcast to the audience in this country.

In 1927 the British transmitter G5SW at Chelmsford, England went into operation on a frequency of 11,750 kilocycles. One of the earliest receptions from this station was a New Year's program consisting mostly of the chimes of Big Ben which was received in Van Cortlandt Park and rebroadcast over WJZ. Judged by present day standards, the results were quite poor but they held a promise and a challenge for the future.

Consistent monitoring of this British pioneer shortwave station, G5SW, and of a Hollandish station, PCJJ, on 9,590 kilocycles indicated that shortwave program transmission and reception was promising and merited further investigation and development.

Such a program of development was set up in June 1928 and several RCA groups instituted a cooperative program of intense research having as its objective the development of a system which would successfully receive European shortwave broadcast programs for re-broadcasting in this country over stations of the National Broadcasting Company. An isolated spot on the property of the RCA receiving station near Riverhead, Long Island was chosen for this work and a small experimental station with suitable antennas was erected. Special program line facilities between this building and the National Broadcasting Company headquarters, then 711 Fifth Avenue, were soon made available.

The RCA diversity receiving system had already been put into commercial service for the reception of shortwave telegraph signals and its many advantages and excellent performance in telegraph service made it a logical basis and starting point for the development work on a program receiving system. Numerous schemes were tried for combining the outputs from the separate receivers each operating from its own antenna and after many hours of listening and comparing an arrangement was worked out which proved quite satisfactory.

It soon became apparent in the course of this work that there were

more problems than merely the development of antenna systems and receiving equipment. Broadcasts would be scheduled and when the appointed hour for the program arrived the signal might be excellent, fair, or absolutely useless. This state of affairs did not fit into the normal operation of the National Broadcasting Company and a method of correlating propagation data to enable prediction of conditions was inaugurated which would enable the broadcasting company to schedule their foreign program with reasonable assurance of success.

This early work was a forerunner of the more elaborate studies now being carried on by several organizations throughout the world in an attempt to obtain better utilization of the shortwave frequencies by having a better knowledge of their characteristics.

As this development program progressed from 1929 through 1931, blind reception of broadcast programs became less and less satisfactory. Many foreign broadcasting stations did not adhere to strict time schedules and there was serious difficulty from the viewpoint of American broadcasting companies in bringing the foreign program through at the proper time. Other problems such as the improper choice of frequency, occasional interference from adjacent radio channels, and technical difficulties such as low modulation made it desirable to have a contact with the foreign point in order to coordinate the timing and to supervise the operations. This requirement led to the development of portable modulators for use with the Rocky Point telegraph transmitters of RCA which would permit these facilities to be used as a voice control circuit so that a contact could be maintained with the foreign station prior to and throughout the entire program transmission. Such technical control on one-way programs established the first international program service on a point-to-point basis as differentiated from blind reception of foreign shortwave broadcast signals.

Early in 1931 RCA Communications established its International Program Transmission Service as a separate department and a public service, offering its facilities to all the broadcasters as a means of exchanging programs between the United States and other countries. In 1932 a special program control room was built in the Central Radio Office at New York so that better coordination could be maintained between the studios of the broadcasting companies and the foreign program points.

OPERATION OF PROGRAM TRANSMISSION SERVICE

Perhaps the best way to describe the manner in which the International Program Transmission Service operates is to explain the arrangements and the technique for handling a typical program. Sup-

pose that a broadcasting company wants a program from their commentator in Paris. When the time and date for the program have been established, the broadcasting company's newsroom will ask their traffic department to arrange the necessary facilities and at the same time they will advise their commentator in Paris of the program time and details. The traffic department will then order the overseas facilities from the international communication company and will make the necessary scheduling for their master control to pick up the program from the New York terminal of the international company.

Upon receipt of the order, the international company decides what frequencies will be the most suitable and a message is sent to the international communications company in France ordering the facilities for the scheduled time. Upon receipt of this order, the French company will contact the broadcaster's correspondent in Paris to double-check the arrangements and make sure that a suitable studio is reserved for the program.

On the day of the program, fifteen or twenty minutes prior to the actual program time the communications company in New York will go on the air with its contact-control transmitter directed toward France, and their receiving station will tune in the French transmitter on the scheduled frequency. As soon as contact is established and there is assurance that the circuit is working in the best possible manner, the technical operator will ask for a trial speech from the commentator in the Paris studio, which will then be fed through to the broadcast studio in New York as a final test.

A few minutes prior to program time, the New York technical operator will connect the newsroom through to the studio in Paris so that the director of the program in New York may talk with the Paris commentator and make last minute arrangements. When everything is arranged, the commentator will stand by for his cue. When the announcer in New York says, "We take you now to Paris", the announcer's voice is fed out over the New York contact-control transmitter, is picked up by the Paris receiving station, and fed into the studio where the commentator is waiting. This is the cue to start and the commentator begins his speech as soon as he hears it. Throughout the program the technicians at both ends of the circuit maintain a constant vigil to insure that the circuit performance is good. When the program is finished, the control is turned back to the international company's technical operator by the broadcaster's newsroom and the technicians close down the circuit.

From this description of how the International Program Transmission Service functions, it should be clear that the service is entirely

different from a telephone service. Whereas in the telephone service the facilities are utilized for the most part for private conversation between two individuals, the facilities in the International Program Transmission Service, except for testing immediately prior to and following the program, are utilized for carrying a program which must be broadcast over a radio station at one or both ends of the circuit.

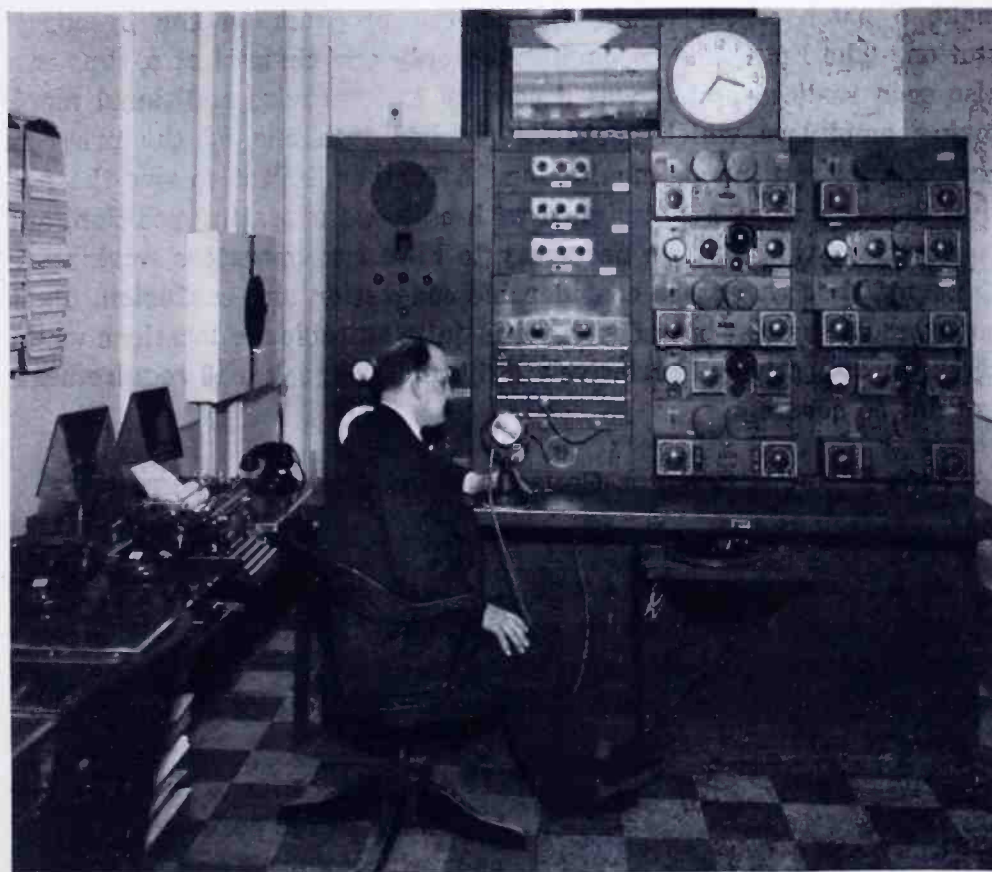


Fig. 1—An early type of program control board installed in Central Radio Office, New York, in 1936.

EARLY EQUIPMENT AND TECHNIQUES

The equipment which was installed in the central office at New York in 1936 for handling Program Transmission Service is shown in Figure 1. Essentially this equipment consisted of high quality line amplifiers; monitoring facilities which permitted listening to any incoming or outgoing circuit; talk-back microphone and control; a jack field for terminating landlines, cross-connecting circuits, and for substitution of equipment in case of failure; and auxiliary equipment such as coils and line equalizers, a beat-frequency oscillator for use in checking

landlines, an all-wave receiver for monitoring purposes, and a 78 revolution-per-minute turntable with pickup.

While the equipment served its purpose well during the early days of Program Transmission Service, experience soon indicated that this system was somewhat limited as to the number of programs which could be handled simultaneously in an efficient manner. The method of interconnecting channels by the use of patch cords on the jack field (Figure 2) held the possibility that the technician might incorrectly make a patch which would disrupt the program on the broadcast station. The limitation to monitoring only one channel at a time was also soon realized and it was necessary to improvise additional monitoring amplifiers which could be patched into one of the program channels for continuous monitoring. A further limitation was the fact that the equipment was designed with only one operating position, and on occasions when it was necessary to have two operators working at the same time there was considerable congestion and confusion. Such a system as has just been described is quite suitable for locations where the program activity is relatively light and the peak load requirements are not so severe.

NEW PROGRAM CONTROL CONSOLE EQUIPMENT AND TECHNIQUES

Objectives in the New Design

As a result of experience with this early equipment, it was decided to design a new system which would provide, insofar as possible, fool-proof and convenient operation by either one or two technicians, and which at the same time would provide greater capacity for peak-period operation.



Fig. 2 — Early program control board showing jack field in use for program switching.

A consideration of these requirements led to the decision to remove as much equipment as possible from the operating position and to provide the technician with only the necessary controls for switching, monitoring, and supervising the circuits. Toward this end it was decided to utilize a console similar in style to those used in broadcast stations and to place all the auxiliary equipment in racks conveniently adjacent to the console. The console as it was finally built is shown in Figure 3.

To overcome the inconvenience of using patch cords on the jack field for switching the circuits and to eliminate the necessity for expensive and difficult to maintain relays and push buttons, a special rotary selector switch was designed to provide for direct switching of incoming signal. Throughout the design an attempt was made to locate all controls and indicators in a position associated with the function which they performed, as, for example, the gain control on each channel which is located on the switch panel immediately below the VU meter* that indicates the level of the outgoing signal. The VU meter itself is



Fig. 3—Program control console installed at Central Radio Office, New York, in 1949.

located directly beneath the rotary selector switch which feeds the line amplifier whose output level is indicated by the VU meter.

In order to eliminate any confusion in handling the microphone circuits, a new arrangement was worked out whereby the technician merely inserts a plug into a jack on the switch panel handling the outgoing channel on which he wishes to talk. An additional feature is the use of a small twist switch in conjunction with the microphone key to permit the transmission of either program modulation, steady tone of one thousand cycles for use in setting up, or a keyed tone for sending telegraph identification.

Facilities are also provided for telephone communication over a private line system which connects directly with the master control in

* Volume level indicator.

the broadcast studios and with the regular RCA Communications, Inc. inside dial and P.B.X. system.*

In the new design, accessibility was considered as being important in order to facilitate maintenance. Rather than attempt to mount amplifiers and other equipment in the console itself, it was decided to put this auxiliary equipment in racks adjacent to the console which would simplify the design of the console and result in a much better arrangement for both servicing and operating. For further ease in maintenance, all amplifiers are plug-in types which can be readily removed for service work. All equipment mounted either in the console or in the auxiliary racks is terminated on terminal blocks at the bottom

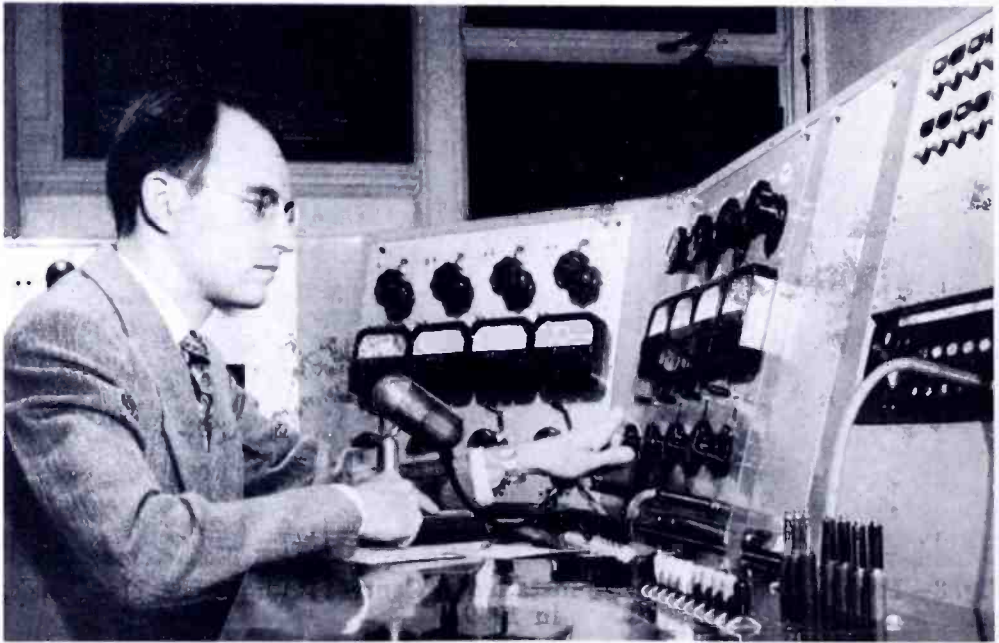


Fig. 4—Close up of console operating position showing the details of the switching control panels.

of the respective racks rather than directly connected to other equipment. This arrangement permits interchangeability if necessary by merely altering the cross-connections between the terminal blocks. For the same reason, all jacks in the jack fields are terminated on blocks located in the bottom of the racks so that any circuit can be easily connected to a jack without disturbing the wiring at the back of the jack strips.

It was also felt highly desirable to keep the appearance of the console itself as neat and attractive as possible, and for this reason, particular attention was given to the shape factor, the color scheme, and the system of labels and notations used throughout.

* Private Branch Exchange.

Description of Program Selector and Control Panels

As shown in Figures 3 and 4, there are four program selector and control panels; each panel comprising the necessary rotary switches, volume indicator meters, and gain controls for controlling four outgoing program channels. The program selector switches designed and built especially for this purpose by the Daven Company are shown in detail in Figure 5.

Each selector switch has three pies or banks of contacts, two of which handle the audio circuit and the third for controlling the lights which indicate that a selector switch is connected to an incoming line. To guard against accidental dislodging of the selector switch and to insure that the operator does not rotate the switch inadvertently, it is necessary to press the switch knob and engage a pin before the switching action can be initiated. This operation at the same time opens a Form B switch mounted on the rear of the selector switch that opens the input to the line amplifier so that while the selector switch is in rotation there will be no signal on the outgoing line. This switch is shown in Figure 11 between the program selector switch and the bridging transformer and attenuator.

The selector switch is constructed with twenty-five points, the first point being normally the "off" position and the other twenty-four carrying the incoming circuits to be selected. As an integral part of the switch mechanism there is a dial which rotates with the switch arm, and the numbers engraved on this dial appear illuminated through the bullseye located directly above the switch. This number indicates to which of the twenty-four available incoming lines the switch is connected. At the same time, whenever one of the selector switches is connected to an incoming line, an illuminated number in the group of twenty-four signal lamps located in the center of the console just above the telephone switchboard lights up to show that a selector switch has been connected to a particular incoming line. This arrangement serves as an indication of the lines which are in use and the lines which are still available for assignment of other incoming signals.

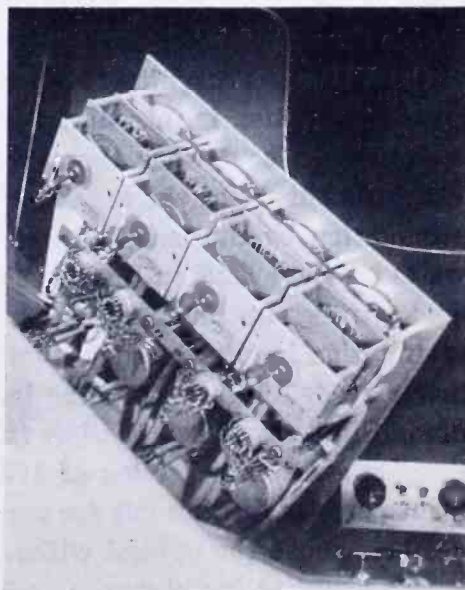


Fig. 5 — View from above switch panel showing how the panel hinges open for maintenance and the construction of the rotary selector switches.

The circuit through the rotor of the selector switch passes through the Form B contacts mounted on the rear of the switch which serve to open the circuit when the switch knob is depressed, and connect to the input of a bridging transformer mounted in the console immediately below the switch panels. This transformer which has an input of 20,000 ohms and an output of 250 ohms provides about 16 decibels isolation so that, in the case of multiple feeds, when more than one selector switch is connected to the same incoming line, the effect on the level of the outgoing signals is negligible. This provision is necessary since it is often desirable to connect and disconnect outgoing channels while a program is actually under way without disturbing the level of the other channels.

In order to provide a gain control for regulating the level of the signal feeding into each line amplifier, a 60-decibel attenuator graduated in steps of 2 decibels is mounted on the switch panel immediately below the VU meter. This attenuator is connected between the output of the bridging transformer and the input of the line amplifier. Connected between the output of the attenuator and the input to the line amplifier there is a pair of Western Electric type 218-A jacks insulated from ground. These jacks which are located at the bottom of each switch panel are used for inserting the local microphone control plug.

Each channel is provided with a Weston type 862 illuminated VU meter which carries an upper scale graduated in percentage and a lower scale in decibels. Immediately below each VU meter there is a double throw locking key-switch which varies the amount of attenuation in the VU meter circuit. With the switch in the normal position, sufficient attenuation is introduced in the meter circuit to make the meter read 100 per cent when the output of the line amplifier is +14 dbm*. With the output of the amplifier at this level and due to the 6 decibel attenuation by the isolation pad, the level will be +8 dbm or 6 milliwatts on the outgoing line which is the normal level for feeding high quality program lines. When the key is pushed to the left, additional attenuation is introduced so that when the gain is raised until the VU meter reads 100 per cent, the level on the outgoing line becomes +10 dbm. Similarly, when the key is thrown to the right, the level on the line for a meter deflection of 100 per cent is +12 dbm. This arrangement permits feeding out for special requirements a level either 2 or 4 decibels above the normal without the VU meter reading off scale.

To simplify maintenance and permit ready access for cleaning and servicing, each control panel is hinged at the bottom and swings open as shown in Figure 5 to give access to the switch mechanism.

* Decibels referred to a zero level of 1 milliwatt in 600 ohms.

The four channels located in the control panel at the extreme right end of the console are specially wired for handling radiophoto signals. Each of the channels on this panel is provided with two amplifiers so that the rotor feeds into two amplifiers instead of one. With this arrangement a radiophoto signal can be fed to a customer through the regular line amplifier in the normal manner and a duplicate of the signal can be fed through the other amplifier to either a recording storage device or to a radiophoto machine for recording the picture photographically. Except for this, all of the sixteen channels of the console are identical.

Description of Amplifiers

In choosing the amplifiers for use in the system it was desirable to keep the types to a minimum and to utilize a plug-in feature for simplified maintenance. Since some of the signals coming into the console arrive over long and heavily equalized lines, some of the incoming signals arrive at a level as low as -28 dbm. In order to bring this level up to $+8$ dbm and to make up for the 16-decibel loss in the bridging transformer and the 6-decibel loss in the isolation pad ahead of the outgoing line, it is necessary to have an amplifier with a minimum gain of 58 decibels.

The amplifier chosen for this service was the RCA type BA-3-A, later superseded by the type BA-13-A having essentially the same characteristics. These types provide 65 decibels gain and sufficient fidelity to meet the requirements for use as a line amplifier and are also suitable for the monitoring amplifier systems and as the microphone amplifiers.

The only requirement in the system which the BA-3-A does not fulfill is for a high gain amplifier with low noise level to use as a noise measuring and line checking amplifier. For this purpose the type BA-4-A with a gain of 100 decibels was selected.

This choice of amplifiers results in a minimum of tube types and almost complete standardization of one type of interchangeable amplifier throughout the console system.



Fig. 6 — Type BA-3-A plug-in amplifier.

Figure 6 shows the general construction and plug-in feature of the type BA-3-A amplifier. The dimensions of the chassis which are $8\frac{1}{2}$ by 13 inches permit mounting two of the amplifiers on one shelf resulting in a compact assembly.

Since these amplifiers are built with an input impedance of 600 ohms, it was necessary to use external bridging transformers in the program channels to provide the required isolation. However, this is no disadvantage since the microphone and monitor amplifiers do not require a bridging input and by using the BA-3-A amplifiers with internal wiring for 600-ohm input, all amplifiers throughout the system with the exception of the line measuring amplifier are interchangeable.

Description of Monitoring Facilities

As mentioned earlier, one of the disadvantages in the early program control equipment was the limitation in monitoring facilities. To overcome this limitation by providing for increased monitoring, each operating position in the new console is equipped with two independent monitoring systems; one for monitoring incoming signals, and the other for monitoring outgoing signals. In each system key-switches are provided, as shown in Figure 7, to select any of the twenty-four available signals and thus one incoming and one outgoing signal can be monitored simultaneously at each of the two operating positions.

Because the circuits to be monitored are all terminated in the equipment racks, and the monitor key-switches located in the console itself, the question arose as to whether to extend the audio circuits to the console or whether to provide a remote control system for monitoring. In spite of the extra equipment required for a remote control system it was felt advisable to install such a system, and step-type rotary switches were finally employed for the purpose. This arrangement has the added advantage that additional monitoring systems can be set up at any location by installing additional step-type switches in the console racks with direct-current control wires from the remote location.



Fig. 7—Console operating position showing the monitor key-switches and microphone controls.

The audio signals from the jack field are wired to the step-type switches, shown in Figure 8, located immediately below the jacks. A direct-current circuit is connected between the monitor keys located on the console and the driving mechanism which rotates the step switches. This arrangement provides within itself an interlock feature so that only one audio channel at a time can be connected to the monitoring amplifier. Some difficulty was encountered with clicks in the monitoring loud speaker caused by sparking of the stepper mechanism but this was overcome by using a condenser-resistor suppressor circuit and a delay relay which shorts the input to the monitor amplifier during the operation of the switch to insure against the annoyance of clicks in the monitor system.

A simple method of providing isolation and at the same time some measure of protection against faults which might develop in the audio lines running to the stepping switches is the insertion at the jacks of a 10,000-ohm carbon resistor in each leg of the monitoring circuit. This method is used instead of providing an external bridging transformer for each monitoring amplifier.

Located within convenient reach of the operator is a control panel upon which is mounted a gain control for each of the monitoring amplifiers and a switch which cuts off the loud speaker. This switch is utilized if it is desired to listen only with headphones which can be plugged in either at the jacks in the apron of the console immediately in front of the operator or for supervisory purposes on the monitor control panel.

In addition to these facilities for monitoring the incoming and outgoing lines, a panel mounted radio receiver is located in the left end of the console for use in observing standard broadcast stations and for obtaining cues when a separate cue line is unavailable.

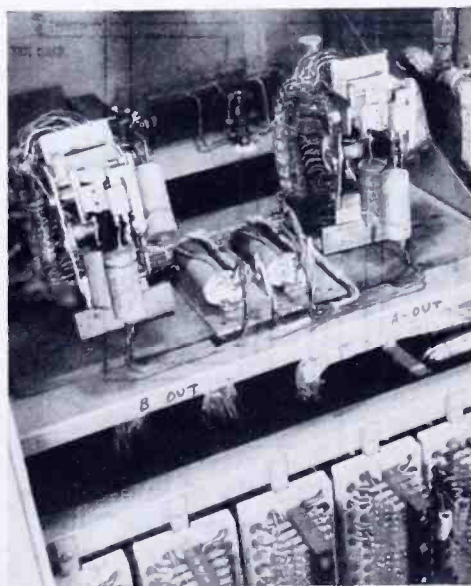


Fig. 8—Step-type rotary switches used in monitoring circuits. Below are shown the terminal blocks which are located at the bottom of the racks for making interconnections between the racks.

Description of Microphone Switching System

The microphone control and switching arrangement has been de-

signed to make its operation as foolproof as possible by reducing to a minimum the operations required to switch the microphone into an outgoing channel.

Schematic diagram Figure 9 shows the microphone key-switch and plug arrangement which has proved to be a very satisfactory method of inserting the local microphone into an outgoing channel to enable the technician to talk over the circuit. To insure patching the microphone into the correct channel, the jacks are mounted at the bottom of each switch panel channel so that the physical association of the jack with the channel is a safeguard against plugging into the wrong circuit.

Two microphone keys and associated Western Electric Type 137 plugs are provided at each of the two operating positions on the console so that the technician may talk on either one or two circuits alternately

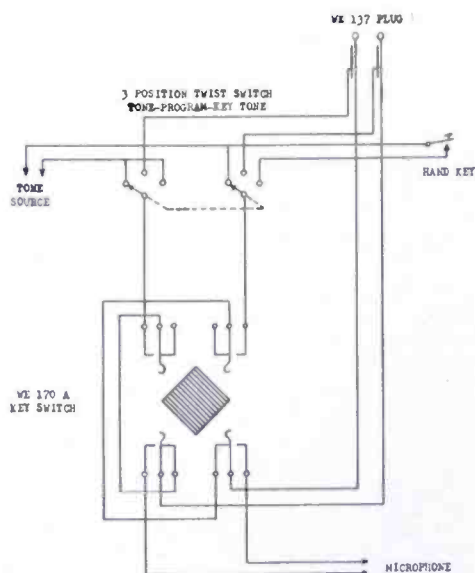


Fig. 9 — Schematic of microphone key-switch and plug circuit.

or simultaneously by merely operating the microphone keys once the plugs have been inserted in the jacks on the switch-panels. To guard against the microphone being left in the circuit with the microphone alive, the microphone keys are non-locking and must be held back while the microphone is being used. The three position twist switch shown in the schematic provides a selection of either 1000 cycles steady tone for use in setting up the transmitter, the program modulation which is passing through the channel into which the microphone plug is inserted, or a keyed tone which is used for telegraphy.

One of the problems which arose while working out the details of the microphone system was that of matching the microphone level to the level of any of the outgoing channels on which it was desired to talk. Principally to eliminate this problem it was decided to run all the line amplifiers at full gain and to control the signal level into the line amplifiers by means of the attenuators mounted on the switch panels. With this arrangement and by locating the microphone jack between the output of the attenuator and the input of the amplifier, the microphone always plugs into the amplifier operating at full gain regardless of the channel into which it is plugged. Although with the line ampli-

fiers operating in this manner there is more chance of picking up cross talk and other interference, the use of separately shielded cables in all rack and console wiring is evidently a satisfactory solution for experience has indicated no difficulty from this source. This arrangement also obviates the necessity for using a microphone amplifier if the microphone has an output of at least -50 dbm. Since it is preferable to have the microphone relatively insensitive to room noise, the technician must "close talk" into the microphone and it is easy to keep the microphone amplifier output at the proper level by speaking closer to or further from the microphone.

Description of Jack Field

All of the equipment located in the five racks as well as the input and output of the switch panels located in the console and other auxiliary equipment in the console is terminated on jacks mounted in the jack field located in racks three, four, and five as shown in Figure 10. While this arrangement increases somewhat the amount of wiring in the installation, it is entirely justified by the flexibility which it provides and by the relative ease in locating faults in any of the equipment.

Double rows of Western Electric type 217-A jacks are utilized for all circuits so that each input or output is provided with "cutoff" and a "multiple" or "monitor" position. Each rack provides space for twelve circuits arranged in vertical rows. The twenty-four incoming lines which ultimately terminate on the twenty-four taps of the rotary selector switches are arranged horizontally across the top of the jack field in the racks at the extreme right.

As shown in Figure 11, each circuit is normalled through from top to bottom so that it passes through the jacks labeled "line in", "equalizer/coil in", "equalizer/coil out", and terminates in the jack marked "switch tap in". The circuits coming from the rotors of the sixteen program selector switches are likewise arranged in vertical rows and normalled through the jacks "switch arm out", "amplifier in", "amplifier out", "pad in", "pad out", and "line out".

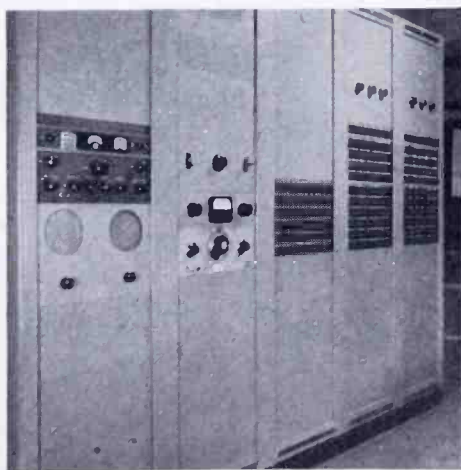


Fig. 10 — The five racks of associated auxiliary equipment showing the jack fields in the three racks on the right.

The jack field in the middle rack is smaller than the other two and accommodates all the miscellaneous circuits such as the microphones, monitor amplifiers, line checking amplifier, local loops within the building, and the output of the monitor receiver located in the rack.

In all of the racks each jack is terminated on a terminal block located in the base of the rack which facilitates making connections

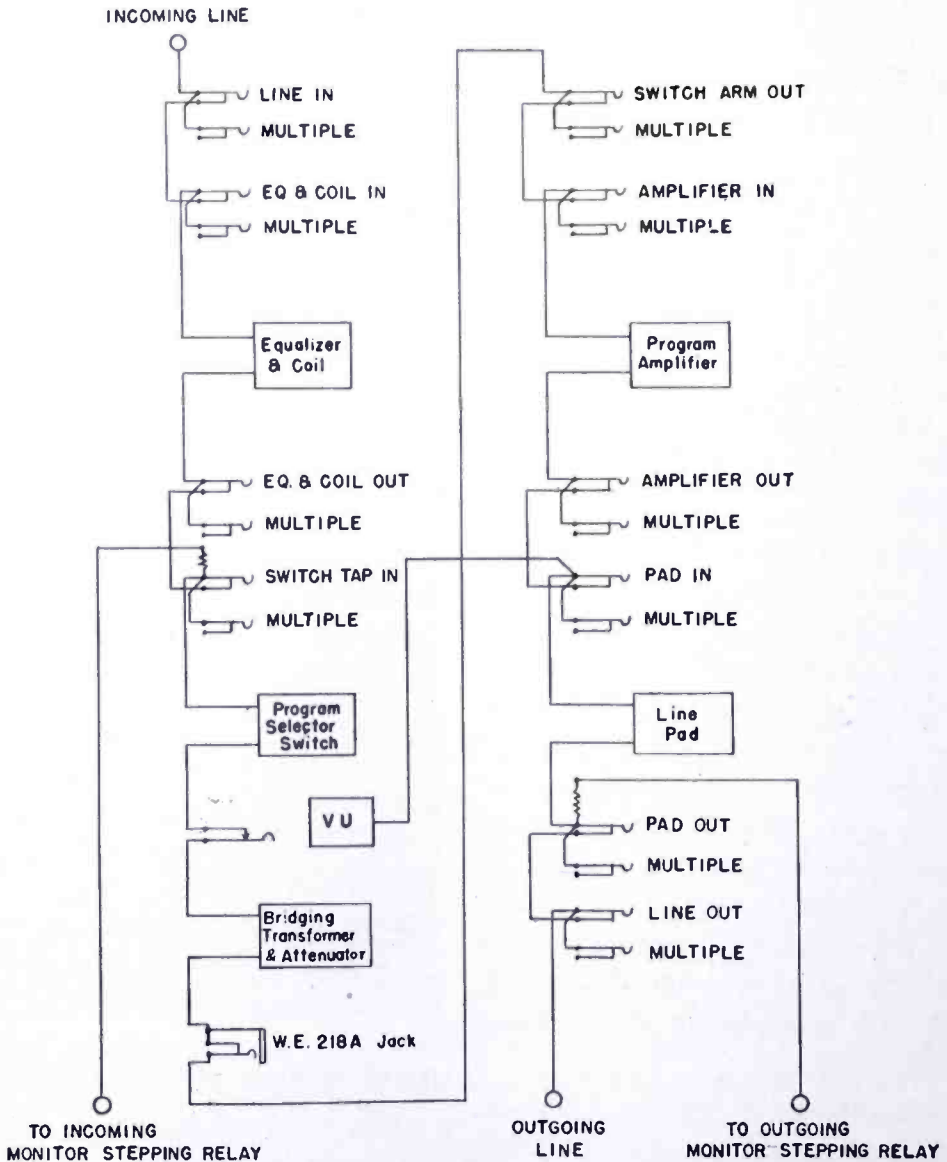


Fig. 11—Schematic of typical channel through console equipment showing interconnection at selector switch of incoming and outgoing circuits.

and permits changes if it is found necessary to rearrange the jack assignments at any time.

Console Design and Details

Considerable thought was given to the size of the console and

toward obtaining proportions which would provide facilities for simultaneous operation by two technicians, and yet not be too big to be convenient for one man operation. The final design as shown in Figure 3 resulted in two similar end sections with a common center section providing the two-position telephone facilities that are shared by the two technicians. For normal operation, one technician has ready access to two control panels, each controlling four channels so that a total of eight channels can be conveniently operated from each position. However, since each of the channels is normally assigned to a regular customer, it may be necessary to temporarily shift the position of the customer assignments on the various control panels in order to keep the ones in use within convenient reach when operating with only one technician. This shift is accomplished very easily by patching at the jack panel.

To arrive at the optimum dimensions for the console, a paper layout of the operating shelf and the sloping switch panels was built to full scale to make sure that all controls would be easily accessible and located for the most comfortable handling. The final design resulted in a console having an overall length of 11 feet 6 inches, operating shelf 31 inches above the floor, and a maximum height of 4 feet which permits the technician to look across the top of the console. The opening between the ends of the operating shelf is 7 feet which is sufficient to permit two technicians to work at the operating positions without crowding.

A small scale wooden model of the entire console was built in order to adjust the various dimensions for the most pleasing appearance. The panels within the console were kept to a width of 19 inches in order to be standard with regular rack mounting panels. The slope of the panels follows the usual practice with an angle of 17 degrees from the vertical in order to give the best vision and appearance.

Equipment Racks

All of the major equipment, with the exception of the switch panels, is mounted in the five cabinet racks shown in Figure 10 which, although separated from the console itself, are still close enough to be within convenient reach of the technician at the console.

Each cabinet rack accommodates standard 19-inch panels and the equipment in the racks which is not designed for panel mounting is mounted on horizontal shelves.

As shown in Figure 10, an RCA Model AR-88 receiver and a panel containing two loud speakers with associated volume controls are mounted in the rack at the extreme left. In the next rack to the right

are mounted the line measuring equipment with associated VU meter and below it an audio oscillator. The rack in the center and the two racks toward the right contain the jack fields and the controls for the six variable line equalizers. Mounted behind the blank panels in the racks are 28 type BA-3A or BA-13A amplifiers; 1 type BA-4A amplifier; the stepping relays for the monitoring systems; and the coils, equalizers, and pads associated with the incoming and outgoing lines. The amplifiers are distributed among the several racks and their separate power feeds provide safety in case of power failure in one rack.

In the bottom of each cabinet rack are mounted honeycomb terminal blocks where all of the equipment in the rack is terminated. The interconnections between the racks and the console itself are made on these terminal blocks. With this arrangement each of the racks becomes an independent unit when the cross connections are removed and, if it is necessary to move the equipment to a new location or to make any rearrangement, it is not necessary to disturb the wiring to the equipment within each rack.

Auxiliary Apparatus

In addition to the major pieces of equipment already described in detail, there is other apparatus such as the private line switchboard, line pads, coils, equalizers, audio frequency oscillator, line measuring equipment, and an electric clock setting device, all of which contribute toward convenient and efficient operation and therefore worthy of brief description.

The private line telephone switchboard can be seen in Figure 3 in the lower portion of the center panel of the console. This switchboard accommodates ten private lines which connect with the broadcast companies who are the principal customers. Calls coming into the console from these customers operate a relay which sets off a buzzer and lights an indicator lamp above the customer's jack. Plugging into the customer's jack to answer the call puts out the lamp and turns off the buzzer. Two sets of handsets are provided which plug into jacks mounted in the front apron of the operating table, each set convenient to the technician's operating position. Each of the handsets terminates on four of the eight cord circuits shown in the operating table just below the switchboard. These parallel cord circuits permit each of the technicians to set up conference circuits between himself and as many as four private lines. Each cord circuit is connected with a two-position key-switch which in one position is used for

ringing and in the other position for isolating its associated cord from the conference arrangement if it is desirable to talk with only one of the customers during a conference set-up. Each bank of cords is also provided with a rering feature so that if a cord is left plugged into a customer's line thus disabling the buzzer and light signals, the customer's ring will cause a red light to flash intermittently until the rering key is actuated by the technician at the board. This rering feature is quite useful when a customer's circuit is either inadvertently or intentionally left plugged up and it becomes necessary for the customer to rering in order to attract the technician's attention. The dial instrument mounted at the center of the operating table apron is associated with a six position key box which is part of the house dial system and which gives the technician access to extensions from the P.B.X. board.

The fixed pads which connect between the output of the program line amplifiers and the outgoing lines themselves are of the balanced H type with input and output impedances of 600 ohms. The insertion loss of these pads is 6 decibels which is sufficient isolation to prevent the terminal equipment from altering the characteristics of the line to any extent and to give a measure of protection to the equipment in case of certain line troubles.

All incoming program lines are terminated in 1:1 coils having an impedance of 600 ohms with a 600-ohm shunt resistor across the secondary and a line equalizer across the primary or line side of the coil. For use on lines which remain connected permanently, 18 RCA type 56-C line equalizers are available; and for temporary lines, 6 type 56-E variable equalizers with the control knob mounted on the front panel are provided.

The audio-frequency oscillator furnishes audio frequencies between 20 and 20,000 cycles at fairly constant output level for use in transmitting tones of various frequencies over lines being equalized for running frequency characteristics on transmitters.

For use in measuring levels on the incoming program lines, a type BA-4-A amplifier with 100 decibels gain is provided which, along with one 40-decibel variable H pad and two 40-decibel fixed H pads, can be used to measure levels ranging from -120 up to about $+20$ dbm. In checking the noise level on incoming lines the sending station feeds normal level 1000-cycle tone over the line which is passed through the three H pads and the BA-4-A amplifier to which is connected a VU meter. Attenuation is slowly removed by adjusting the variable pad and closing the shorting switches on the fixed pads until the VU meter indicates 100 per cent deflection. This establishes an arbitrary refer-

ence level. The tone is then removed at the sending station and the attenuation further decreased in the H pads until the VU meter again indicates 100 per cent. The difference in decibel attenuation between the two settings of the pads is the difference in decibels between the line noise and the normal tone. This is a quick yet sufficiently accurate method of checking the noise level on incoming lines.

Since a program may frequently be fed to a customer in another state or in a foreign country making it necessary to adjust the operator's clock in New York to match the customer's timing, it is desirable to have a convenient method of setting the New York operator's clock. For this purpose a rather simple device has been installed which comprises an oscillator operating at about 120 cycles and feeding into a voltage amplifier which has sufficient output power to drive the clock for a short period. The clock, which normally operates from the 60-cycle mains, can be stopped and set by momentarily depressing a push button which opens the main power source. It can be speeded up and set by pushing another button which substitutes the 120-cycle source for the regular 60-cycle supply, consequently driving the clock at twice its normal speed. This method of adjusting the operator's clock from the push buttons at the technician's position has been found to be very convenient.

Inter-connects and Use of Wiring Sheets

In wiring the equipment in the racks and in the console itself, and in making the inter-connections between the racks and console, shielded cable was used throughout in order to reduce the danger of picking up cross talk and other forms of interference. To further reduce the probability of trouble from this source, all cables carrying low levels such as incoming lines, microphone outputs, and input circuits to line amplifiers were kept separated from cables carrying relatively high levels such as amplifier outputs.

Since practically all the circuits in the installation are direct connections between the terminals of the various pieces of equipment, and since many of the circuits are merely duplications of basic circuits, it was found advantageous to use a system of wiring sheets in place of the usual full schematic circuit diagram.

The partial sheets shown in Figure 12 are samples taken from a set of six sheets which show how the input of line amplifier #11 mounted in rack #2 is connected through to the jacks mounted in rack #4. The first three sheets trace the circuit starting from the amplifier in rack #2, through the interconnects between rack #2 and rack #4, and finally to the jacks in rack #4. Sheets 4, 5, and 6 trace the same

circuit but in the opposite direction. This system of cross reference permits circuits to be traced easily from either end during the initial installation and later when searching for trouble.

In setting up such a system of wiring sheets, certain abbreviations must be adopted and the same abbreviations carried on throughout the complete set. For instance, in sheet 1 the abbreviation J-1 in Amp #11 stands for Jack #1 on the amplifier which is marked on the chassis by the manufacturer. Terminals 11 and 12 are so marked on Jack #1. The abbreviation TS-1 stands for terminal strip #1 which is one of

(Sample #1)		RACK #2		Sheet 3 of 6 sheets.		
PAIR	FROM		CABLE	TO		CIRCUIT
	EQUIPMENT	TERMINALS		EQUIPMENT	TERMINALS	
1	AMP #11	11	A	TS-1	1-1	Input to Amplifier
	J-1	12		TS-1	1-2	

(Sample #2)		RACK #2		CROSS CONNECTS		Sheet 2 of 5 sheets.
64	TS-1	1-1	A	RACK 4 TS-3	13-1	Input Ampl #11
	TS-1	1-2		RACK 4 TS-3	13-2	

(Sample #3)		RACK #4		Sheet 5 of 15 sheets.		
95	TS-3	13-1	F	JR-13	J-21-T	Input line amplifier
	TS-3	13-2		JR-13	J-22-T	

(Sample #4)		RACK #4		Sheet 8 of 15 sheets.		
95*	JR-13	J-21-T	F	TS-3	13-1	Input line amplifier
	JR-13	J-22-T		TS-3	13-2	

(Sample #5)		RACK #4		CROSS CONNECTS		Sheet 3 of 6 sheets.
64*	TS-3	13-1	A	RACK 2 TS-1	1-1	Input line amplifier
	TS-3	13-2		RACK 2 TS-1	1-2	

(Sample #6)		RACK #2		Sheet 5 of 6 sheets.		
1*	TS-1	1-1	A	AMP #11	11	Input to amplifier
	TS-2	1-2		J-1	12	

Fig. 12 — Sample wiring sheets.

the honeycomb terminal blocks mounted in the base of rack #2. Terminals 1-1 and 1-2 on TS-1 are in the top horizontal row on the block and are the first and second terminals in the row starting from the inside and counting toward the outside of the block.

Each pair of wires as it is installed is tagged with the identification number that appears in the first column of the wiring sheets. It will be noted that in sheets 4, 5, and 6 the pair numbers carry an asterisk which indicates to the installer that the pairs are already referred to in the cross-reference sheets and should not be installed twice.

The cable designations A and F which appear in column four of the wiring sheets indicate which bunched cable the individual pairs are carried in, and the bunching is worked out so that high and low level and DC pairs are not bunched in the same cable.

Sheet 3 column five shows the abbreviation JR-13 which indicates that the jack appears in the thirteenth jack row counting from the top in the jack field in rack #4. "Monitor" or "multiple" jacks are counted as separate rows of jacks. In column six the abbreviated J-21-T and J-22-T indicate that the circuit is terminated on the tip of jacks 21 and 22 counting the jacks from left to right. Actually a plug will plug into jacks 21 and 22, picking up one side of the circuit from each tip but in the wiring sheets the jacks are counted singly rather than by pairs. Jack sleeves would be abbreviated J-21-S and J-22-S, and cutoffs as J-21-C and J-22-C.

Each sheet of the number sheets is numbered and the sheets for each rack, for the console, and for the cross connections between the racks, and between the racks and console are grouped together and bound so that it is easy to refer to the sheets when it is necessary to trace out a circuit or make any changes.

CONCLUSION

Aside from the usual difficulties which are encountered in making an installation of this size, there have been no problems during six months' operation of the console and equipment in the New York Central Radio Office. Training of the technicians to operate the equipment progressed rapidly once the system and the functions of the various apparatus were explained to them.

AN ANALYSIS OF THE SAMPLING PRINCIPLES OF THE DOT-SEQUENTIAL COLOR TELEVISION SYSTEM*

A Report

BY

RCA LABORATORIES DIVISION, PRINCETON, N. J.

Summary—This paper deals quantitatively with a number of aspects of the dot-sequential color television system, namely, the influence of sampling pulse width on color cross talk, the response of standard monochrome television receivers and color television receivers to sinusoidal variations and to step functions, the manner in which the method of mixed highs combines with the sampling procedure to produce high-frequency detail, and circuit methods of eliminating cross talk.

INTRODUCTION

A QUALITATIVE description of the sampling procedure and the use of mixed highs, as well as the dot-interlacing method of increasing detail used in the RCA dot-sequential color television system, has already been published.¹ The reader is referred to that paper for background material. A quantitative discussion of a number of aspects of the system is given in the following pages.

CROSS TALK AS A FUNCTION OF THE WIDTH OF THE SAMPLING PULSE

A block diagram of the color television broadcasting station is shown in Figure 1. The studio apparatus provides three electrical signals, one for each of the primary colors (green, red and blue). Each of these signals may contain frequency components out to at least four megacycles, and in addition an average or dc component.

For one signal routing of Figure 1, each color signal passes through a low-pass filter which eliminates frequency components above a frequency f_A megacycles. Where this paper deals with numerical values, f_A will be taken as 2.0 megacycles. The green-channel signal coming out of its particular low-pass filter is designated as G_L in Figure 1, indicating that at this point the signal contains the dc component and ac components with frequencies of f_A or less. The three low-frequency

* Decimal Classification: R583.1.

¹ "A Six-Megacycle Compatible High-Definition Color Television System", *RCA Review*, Vol. X, No. 4, pp. 504-524, December, 1949.

signals, G_L , R_L , and B_L are then sent into an electronic commutator or sampler.

For the second signal routing of Figure 1, the three color signals from the camera are combined in electronic Adder No. 2 and then are passed through a band-pass filter. The output of this filter contains frequencies from f_A to f_B megacycles, with contributions from each of the three color channels. For calculation purposes, f_B has been taken as 4.1 megacycles. The signal at the output of the band-pass filter is designated as M_H , the mixed-high signal. The mixed high frequencies are fed to Adder No. 1 which is also receiving the signal from the electronic sampler.

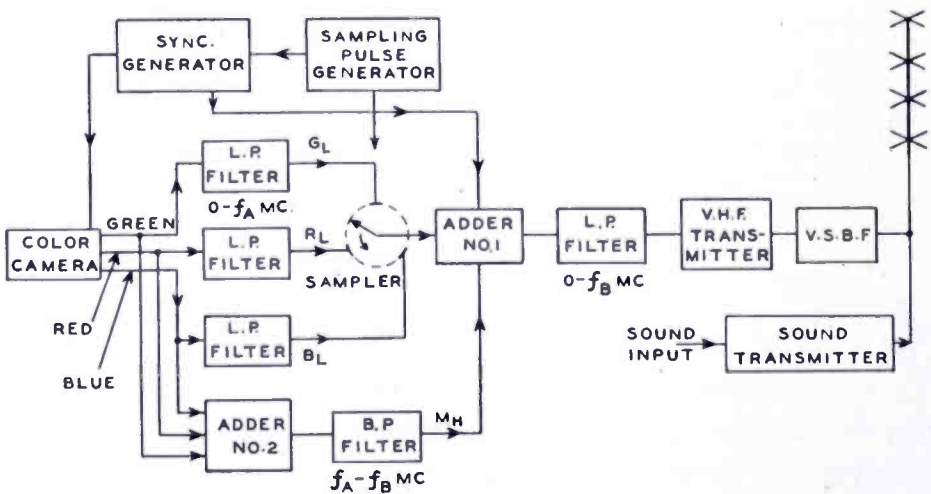


Fig. 1—Block diagram of the color television transmitter.

The frequency relationships in the system are depicted in Figure 2, with the following numerical values chosen for purposes of illustrative calculation:

- f_0 = frequency of sampling pulse generator (3.8 megacycles),
- f_A = upper limit of frequencies into the transmitter sampler and lower limit of mixed high frequencies (2.0 megacycles),
- f_B = maximum frequency component transmitted by the system (4.1 megacycles). This upper limit may be determined by the receiver or transmitter cut-off characteristic, whichever is most restrictive.
- $f_B - f_0$ = upper limit of frequencies free from inherent color cross talk without circuit devices (0.3 megacycle).

Figure 3 is a block diagram of one type of color television receiver. The output of the receiver sampler may go through separate video amplifiers to the picture reproducer, which may consist of three sepa-

rate kinescopes, as indicated in FCC Exhibit 309,² or the composite signal may go from the second detector through a single video amplifier to a point where the three kinescope grids are tied in parallel. The keying or sampling is accomplished by applying short negative pulses in sequence to the cathodes of the kinescopes, as described in FCC Exhibit 316.³

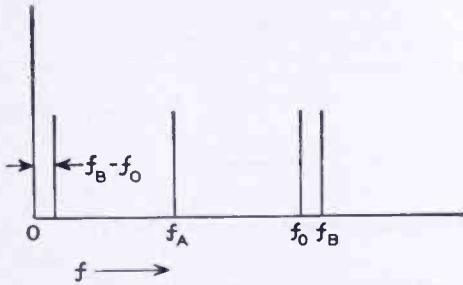


Fig. 2—Frequency relationships in the dot-sequential color television system.

f_B = upper frequency limit of system.

f_0 = frequency of sampling of individual colors.

f_A = maximum frequency of signals into the transmitter sampler (also lower frequency limit of mixed highs).

$f_B - f_0$ = upper limit of frequencies free from inherent color cross talk without circuit devices.

The sampling procedure, at either the transmitter or the receiver, may be described in mathematical terms. Suppose that a signal G is applied to one grid of an electronic tube and that the tube has such characteristics that the output signal is always proportional to the signal G . In addition, a second grid is heavily biased except for regular periodic short intervals when this grid is driven to some prescribed positive value. The signal on this second grid thus acts as a gate on the signal G , and the output signal is proportional to signal G when the second grid is positive and the output signal is zero when the second grid is heavily biased.

The output signal may then be regarded as the product of the signal G and the gating signal. A representative gating signal is shown in Figure 4. The period or time between successive gates is T , while the duration of a gate pulse is ΔT . The sampling frequency, $f_0 = 1/T$. The duty factor of the gate may be defined as $F = \Delta T/T$. Then, if the output is proportional to a signal G , the Fourier series for the gated product is

$$G(t) = G \cdot F \left[1 + 2 \sum_{n=1}^{n=\infty} a_n \cos(n\omega_0 t) \right], \quad (1)$$

where

$$a_n = \frac{\sin(n\pi F)}{n\pi F},$$

² "A Three-Color Direct-View Receiver for the RCA Color Television System", Bulletin, RCA Laboratories Division, January 9, 1950.

³ "A Simplified Receiver for the RCA Color Television System", Bulletin, RCA Laboratories Division, February 28, 1950.

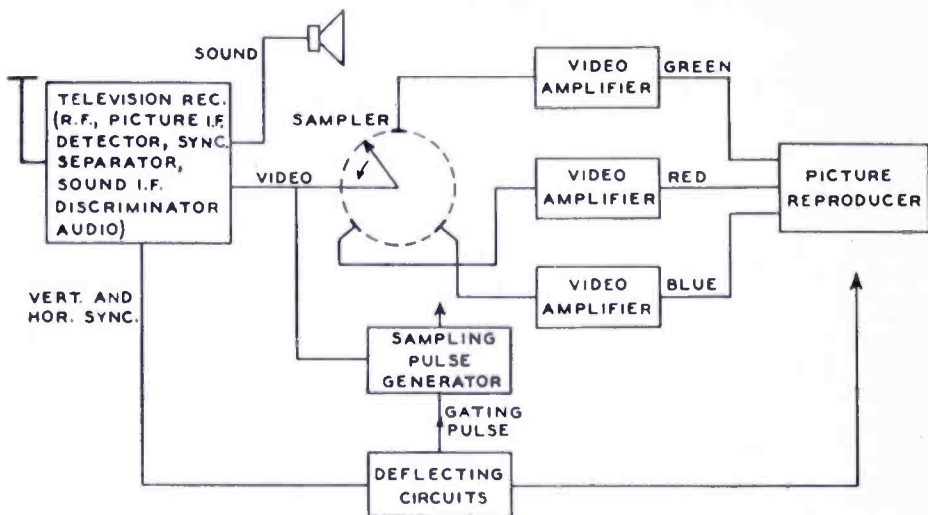


Fig. 3—Block diagram of one type of color television receiver.

and $\omega_0 = 2\pi f_0$.

The input signal G may be varying as a function of time, but for this first consideration of cross talk, G will be constant; that is, a flat green area is scanned.

The Fourier coefficients of the gating pulse shown in Figure 4 are displayed in Figure 5 for $n = 1$ and $n = 2$, as a function of the duty factor F .

Assume that the only signal from the color camera of Figure 1 is for the moment a dc signal from the green camera tube. After sampling at the transmitter, the signal at Adder No. 1 is

$$\frac{G}{3} \left[1 + 2 \sum_{n=1}^{n=\infty} a_n \cos(n\omega_0 t) \right]. \tag{2}$$

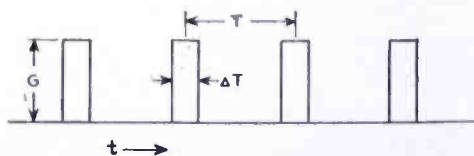


Fig. 4—Flat-top narrow sampling pulse.

$$G(t) = G \cdot F \left[1 + 2 \sum_{n=1}^{n=\infty} a_n \cos(n\omega_0 t) \right],$$

where $F = \text{duty factor} = \frac{\Delta T}{T}$,

$$a_n = \frac{\sin(n\pi F)}{n\pi F}, \quad \omega_0 = 2\pi f_0, \quad f_0 = \frac{1}{T}.$$

Since the sampling frequency is 3.8 megacycles and the upper pass limit of the transmitter is considered to be 4.1 megacycles, only the fundamental term of the summation is retained. Then the signal out of the receiver second detector is

$$\frac{G}{3} \left[1 + 2a_1 \cos(\omega_0 t) \right]. \tag{3}$$

The sampling of this signal at the receiver for a single color channel may be obtained by multiplying (3) by the Fourier series of (1), but assuming a phase displacement of θ degrees. (Green channel, $\theta = 0^\circ$; blue channel, $\theta = 120^\circ$; red channel, $\theta = 240^\circ$.) Hence the signal at a particular color kinescope is

$$\begin{aligned} & \frac{G}{9} [1 + 2a_1 \cos(\omega_0 t)] [1 + 2b_1 \cos(\omega_0 t + \theta) + 2b_2 \cos(2\omega_0 t + 2\theta) + \dots] \\ &= \frac{G}{9} [1 + 2a_1 b_1 \cos \theta \\ & \quad + 2a_1 \cos(\omega_0 t) + 2b_1 \cos(\omega_0 t + \theta) + 2a_1 b_2 \cos(\omega_0 t + 2\theta) \\ & \quad + 2a_1 b_1 \cos(2\omega_0 t + \theta) + 2b_2 \cos(2\omega_0 t + 2\theta) + 2a_1 b_3 \cos(2\omega_0 t + 3\theta) \\ & \quad + \dots]. \end{aligned} \quad (4)$$

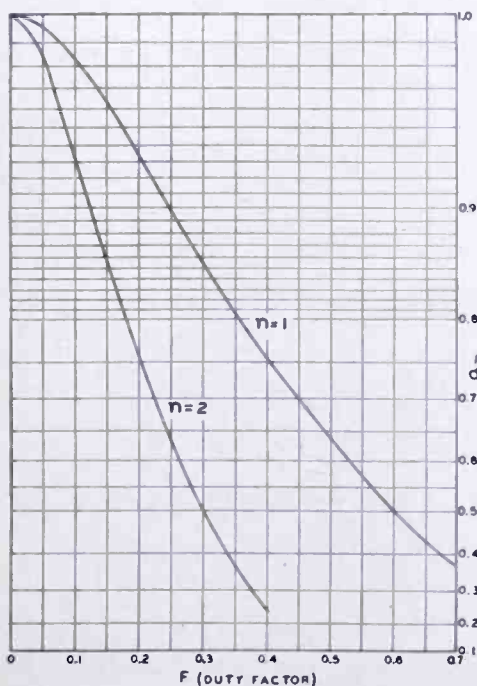


Fig. 5—Fourier coefficients of the sampling pulse of Figure 4 as a function of duty factor.

In (4), b_n has been used for the Fourier coefficients at the receiver sampling to avoid confusion with the a_n values used at the transmitter. Figure 5 applies equally well to b_1 and b_2 as it did to a_1 and a_2 .

The terms containing $2\omega_0 t$ or greater may be dropped from (4), with the result

$$\begin{aligned} & \frac{G}{9} [1 + 2a_1 b_1 \cos \theta \\ & \quad + 2a_1 \cos(\omega_0 t) + 2b_1 \cos(\omega_0 t + \theta) \\ & \quad + 2a_1 b_2 \cos(\omega_0 t + 2\theta)]. \end{aligned} \quad (5)$$

The signal on the green kinescope is obtained by setting θ equal to zero in the above expression which then becomes

$$\frac{G}{9} [1 + 2a_1 b_1 + 2(a_1 + b_1 + a_1 b_2) \cos(\omega_0 t)], \quad (6)$$

and the peak signal on the green kinescope (PS_g) is

$$PS_y = \frac{G}{9} [1 + 2(a_1 b_1 + a_1 + b_1 + a_1 b_2)]. \quad (7)$$

By setting θ equal to 120 degrees or 240 degrees, and following through the proper manipulation, one may find the peak signal on the red or the blue kinescope. Since the peak signals on the blue and the red kinescopes due to cross talk are equal in magnitude and shifted in time, it is necessary to examine only one of these signals. Cross talk (CT) may be defined as the ratio of the peak signal on the red kinescope to the peak signal on the green kinescope. Then

$$CT = \frac{1 - a_1 b_1 + 2 \sqrt{a_1^2 + b_1^2 + a_1^2 b_2^2 - a_1 b_1 - a_1^2 b_2 - a_1 b_1 b_2}}{1 + 2(a_1 b_1 + a_1 + b_1 + a_1 b_2)}. \quad (8)$$

Three combinations of duty factor choices are interesting to examine.

Case I. Duty factor of sampling at transmitter equal to duty factor of sampling at the receiver ($a_1 = b_1$).

Equation (8) then becomes

$$CT = \frac{1 - b_1^2 + 2b_1(1 - b_2)}{1 + 2b_1(2 + b_1 + b_2)}. \quad (9)$$

The attendant cross talk is shown by the top curve of Figure 6.

Case II. Duty factor of sampling at transmitter very small ($a_1 = 1$).

Equation (8) then reduces to

$$CT = \frac{1 - b_1 + 2 \sqrt{1 + b_1^2 + b_2^2 - b_1 - b_2 - b_1 b_2}}{1 + 2(1 + 2b_1 + b_2)}, \quad (10)$$

and the cross talk is shown by the middle curve of Figure 6. It may be seen that for a large duty factor at the receiver, the reduction in cross talk achieved by a short duty factor at the transmitter is small.

Case III. Duty factor of sampling at receiver very small ($b_1 = b_2 = 1$).

In this case, Equation (8) reduces to the very simple form

$$CT = \frac{1 - a_1}{1 + 2a_1}. \quad (11)$$

This cross-talk condition is shown by the lower curve in Figure 6.

The analysis displayed in Figure 6 shows the importance of maintaining a short duty factor at the receiver sampler. Since it is possible

to maintain the effect of a short duty cycle at the transmitter sampler both by gating control and circuit adjustment, it would appear that the middle curve of Figure 6 would be applicable for the actual receiver conditions. It may be seen that when the duty factor at the receiver is maintained at less than 0.15, the cross-talk signal remains at least 30 to 1 down from the desired signal.

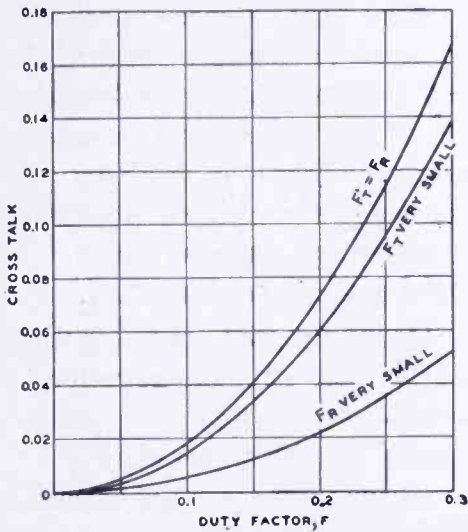


Fig. 6—Cross talk as a function of the duty factor of sampling.

Upper curve—duty factor of sampling at transmitter equal to duty factor of sampling at receiver.

Middle curve—duty factor of sampling at transmitter very small.

Lower curve—duty factor of sampling at receiver very small.

For the remainder of the analysis in this report, it will be assumed that the lessons pointed out by Figure 6 will be well learned. Hence $a_1=b_1=b_2=1$ will be used in the following analysis. To do otherwise would cloud the results in unnecessary rigor and would add little to the knowledge gained.

THE SAMPLING PROCEDURE APPLIED TO LARGE COLOR AREAS WITH A SINUSOIDAL VARIATION OF THE COLOR

a. A large green area with no variation

The green signal from the camera is assumed to be constant in magnitude, of value G . Figure 7(a) shows this fixed value, where G has been set equal to unity. Under the new assumptions ($a_1=b_1=b_2=1$), the signal to the transmitter modulator is given by Equation (3) as

$$\frac{G}{3} [1 \pm 2 \cos(\omega_0 t)], \quad (12)$$

where the plus sign applies for the first scan of the particular line and the minus sign applies to the second scan of the same line. This shift of the sampling by one half of the sampling cycle is accomplished by

the methods described in FCC Exhibit 314.⁴ The plot of Equation (12) for the two scans of the same line is shown in Figure 7(b).

The signal from the second detector or on the kinescope grid of a conventional black-and-white television receiver will also be given by

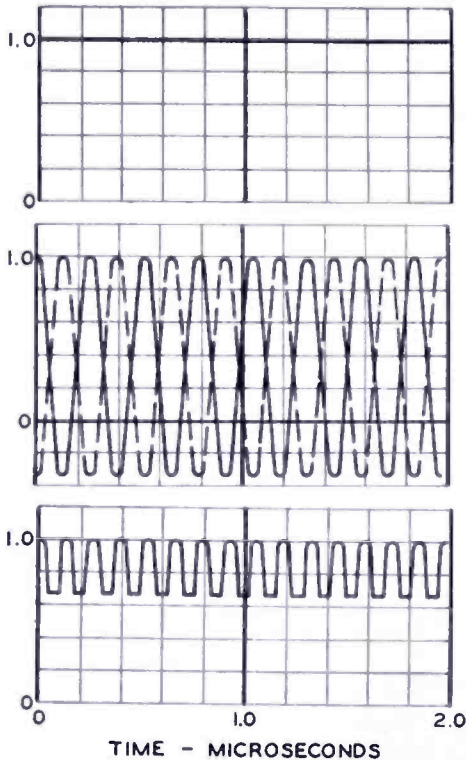


Fig. 7(a) (top)—Constant signal out of green camera tube.

(b) (middle) — Signal to transmitter modulator. Also the signal on the kinescope grid of a conventional black-and-white receiver, as well as the signal on the green kinescope grid of a color receiver.

(c) (bottom)—Combined light intensity of two successive scans of the same line on a conventional black-and-white receiver, and the combined light intensity of two successive scans of the same line on a color television receiver.

Equation (12). Hence the solid line of Figure 7(b) may be regarded as the voltage applied to the kinescope grid of a black-and-white receiver during the first scan of a particular line, while the broken line is the corresponding voltage during the second scan of the same line.

Assuming that the kinescope actually cuts off with negative applied signal, and neglecting the non-linearity of the input control-voltage versus light-output characteristic of the kinescope, the solid line above the axis may be regarded as the effective light intensity along one line scan, while the portion of the dotted line above the axis may be regarded as the effective light intensity along the same line in the next scan. Since the second scan of the same line occurs only one-thirtieth of one second after the first scan, Talbot's law indicates that the light intensities may be added as far as the effect upon the eye is concerned. Figure 7(c) was constructed from the positive values of Figure 7(b) and may be regarded as the response on a conventional black-and-white receiver.

Turning now to the color receiver of Figure 3, the signal on the green kinescope may be obtained directly from Equation (6) by letting $a_1 = b_1 = b_2 = 1$. Then Equation (6) becomes Equation (12), and Figure 7(b) may now be regarded as the voltage on the green kinescope

⁴ "Recent Developments in Color Synchronization in the RCA Color Television System", Bulletin, RCA Laboratories Division, February 9, 1950.

grid during the first and second scans of the same line, while Figure 7(c) depicts the light intensity distribution on one line of the green kinescope due to two successive scans of the line.

The signal on the grid of the red kinescope is determined by setting θ equal to 240 degrees in Equation (5), and for the assumed condition of narrow sampling which sets $a_1 = b_1 = b_2 = 1$, the result is identically zero. Similarly, by setting θ equal to 120 degrees, the signal on the grid of the blue kinescope is found to be zero. Hence, with narrow sampling of a dc signal which represents a flat field of a single color, there is no cross talk into the other two color channels.

b. $G + g \cdot \sin(\omega t)$ where $0 < f < f_B - f_o$

In this particular case, the green area is slowly varying so that the electrical signal is made up of a dc component and an ac component of frequency f where $0 < f < f_B - f_o$. This frequency region may be noted on Figure 2. For purposes of illustration, f_B has been chosen equal to 4.1 megacycles and f_o equal to 3.8 megacycles, hence the frequency of variation dealt with in this section must be less than 0.3 megacycle.

The signal out of the green camera tube is $G + g \cdot \sin(\omega t)$ where ω is $2\pi f$. This signal is sampled at the transmitter sampler in the fashion of Equation (3) so the signal at Adder No. 1 in Figure 1 is

$$[G + g \cdot \sin(\omega t)] \cdot \frac{1}{3} \cdot [1 + 2\cos(\omega_o t)]. \quad (13)$$

Equation (13) could be expanded to develop the sidebands generated by the product $\sin(\omega t) \cdot \cos(\omega_o t)$. It would be found that the sidebands have frequencies $f_o + f$ and $f_o - f$, both of which would pass through the filter and the transmitting system. Accordingly, there is no need to make the expansion for this case.

Equation (13) also represents the signal on the kinescope grid of a conventional black-and-white television receiver. Reversing the sign in the second bracket expression yields the equation for the second scanning of the same line.

When $G = 1$ and $g = 1/2$, the signal out of the green camera tube is $G + g \cdot \sin(\omega t) = 1 + 1/2 \sin(\omega t)$. The frequency has been taken as 0.2 megacycle. Figure 8(a) shows the signal out of the green camera tube for this condition.

Figure 8(b) shows a plot of Equation (13) for this same condition

and may be regarded as the voltage on the kinescope of a conventional black-and-white receiver for two successive scans of the same line. Figure 8(c) shows a summation which depicts the effective light intensity on the same line of the black-and-white receiver tube.

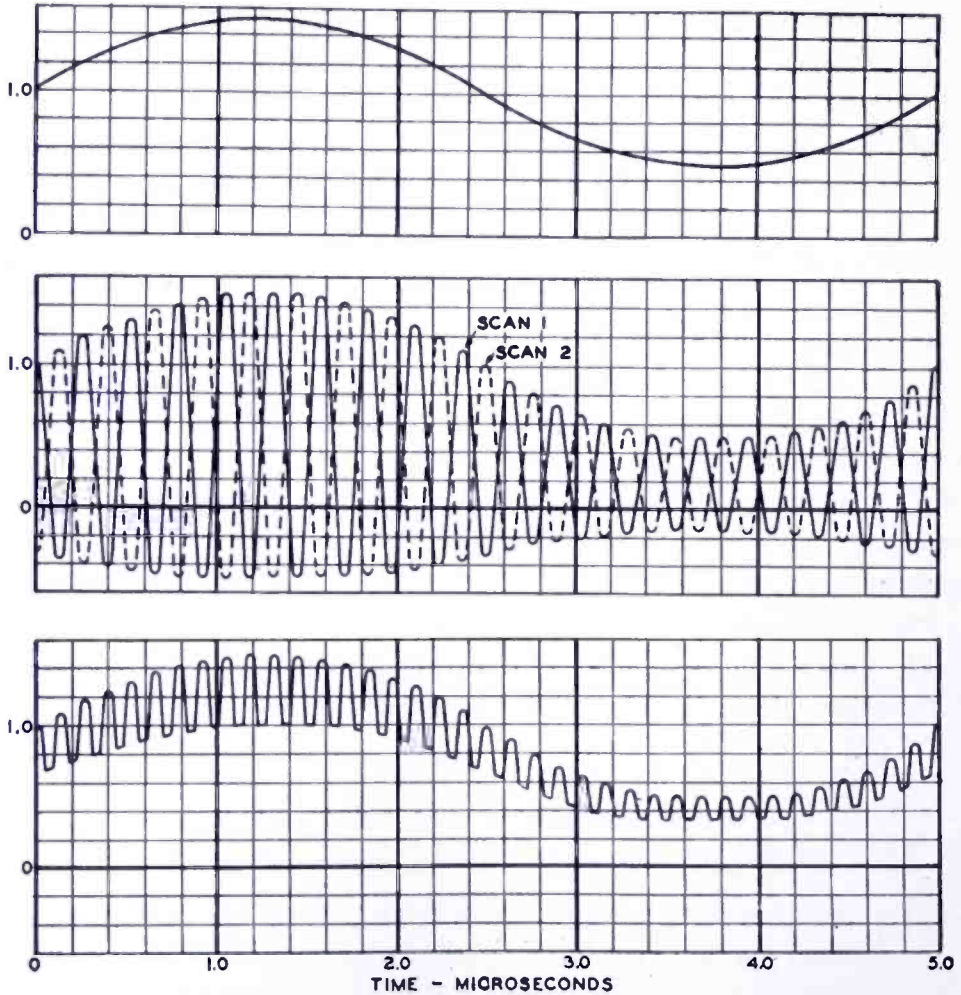


Fig. 8(a) (top)—Signal out of green camera tube; $f = 0.2$ megacycle,
 $G + g \cdot \sin(\omega t) = 1 + 1/2 \sin(\omega t)$.

(b) (middle)—Signal to transmitter modulator. Also the signal on the kinescope grid of a conventional black-and-white receiver, as well as the signal on the green kinescope grid of a color television receiver.

(c) (bottom)—Combined light intensity of two successive scans of the same line on a conventional black-and-white receiver, and the combined light intensity of two successive scans of the same line on a color television receiver.

Equation (13) is also the signal out of the second detector of the color receiver into the sampler. The sampling of this signal at the receiver for a single color channel may be obtained by multiplying (13) by the Fourier series of (1), but assuming a phase displacement of θ

degrees. Of course, a short sampling is assumed so that the Fourier coefficients are unity. Hence the signal at a particular color kinescope is

$$\begin{aligned} & \frac{1}{9} [G + g \cdot \sin(\omega t)] [1 + 2\cos(\omega_0 t)] [1 + 2\cos(\omega_0 t + \theta) \\ & \quad + 2\cos(2\omega_0 t + 2\theta) + \dots], \\ & = \frac{1}{9} [G + g \cdot \sin(\omega t)] [1 + 2\cos\theta \\ & \quad + 2\cos(\omega_0 t) + 2\cos(\omega_0 t + \theta) + 2\cos(\omega_0 t + 2\theta) \\ & \quad + 2\cos(2\omega_0 t + \theta) + 2\cos(2\omega_0 t + 2\theta) + 2\cos(2\omega_0 t + 3\theta) \\ & \quad + 2\cos(3\omega_0 t + 2\theta) + 2\cos(3\omega_0 t + 3\theta) + 2\cos(3\omega_0 t + 4\theta) \\ & \quad + \dots]. \end{aligned} \tag{14}$$

Now to find the signal on the green kinescope grid, simply let θ equal zero in (14), which reduces to

$$[G + g \cdot \sin(\omega t)] \cdot \frac{1}{3} \cdot [1 + 2\cos(\omega_0 t)]. \tag{15}$$

Since (15) is identical with (13), it is seen that Figure 8(b) may be regarded as the voltage applied to the kinescope of the green tube in the color receiver for two successive scans of the same line, and Figure 8(c) may be regarded as the equivalent light intensity variation for two scans of the same line.

To find the signal on the grid of the blue kinescope, set θ equal to 120 degrees in Equation (14) and it will be seen that the second bracketed expression goes to zero. If θ is then set equal to 240 degrees, an identical result is found, indicating no signal on the red tube.

Hence, when the frequency of variation is less than $f_B - f_0$, there is no cross talk and the single-color field is reproduced correctly in magnitude and position by the sampling procedure.

c. $G + g \cdot \sin(\omega t)$ where $f_B - f_0 < f < f_A$

In this case, the green area is varying so that the electrical signal is made up of a dc component and an ac component of frequency f , where $f_B - f_0 < f < f_A$. This frequency region may be noted on Figure 2, and for illustrative purposes lies between 0.3 megacycle and 2.0 megacycles.

The signal out of the green camera tube is $G + g \cdot \sin(\omega t)$. For purposes of illustration, f has been chosen to be 1.6 megacycles, $G = 1$ and $g = 1/2$. Figure 9(a) shows this signal, $1 + 1/2 \sin(\omega t)$.

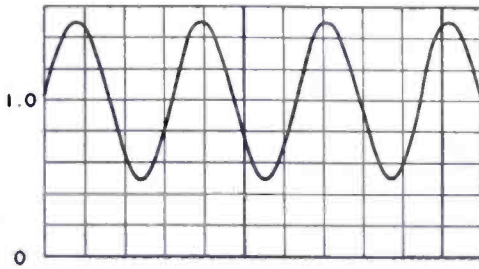


Fig. 9(a) — Signal out of green camera tube; $f = 1.6$ megacycles, $G + g \cdot \sin(\omega t) = 1 + 1/2 \sin(\omega t)$.

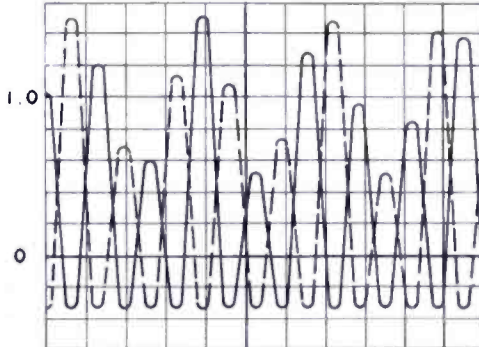


Fig. 9(b) — Signal to transmitter modulator. Also the signal on the kinescope grid of a conventional black-and-white receiver.

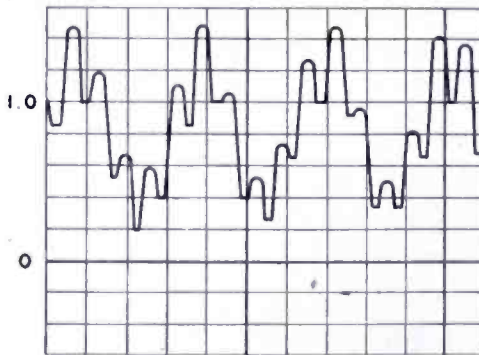


Fig. 9(c) — Combined light intensity of two successive scans of the same line on a black-and-white receiver.

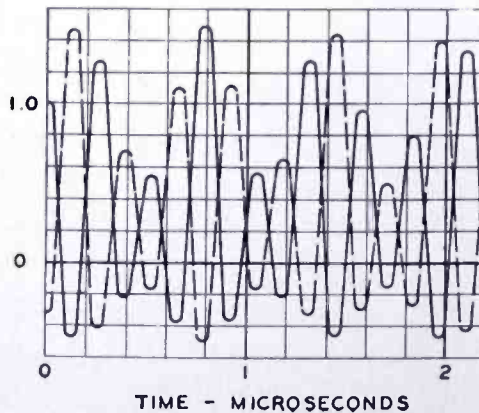


Fig. 9(d) — Signal on the green kinescope grid of a color television receiver.

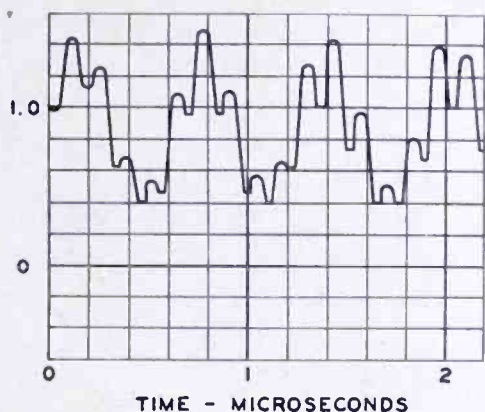


Fig. 9(e) — Combined light intensity of two successive scans of the same line on the green kinescope of a color television receiver.

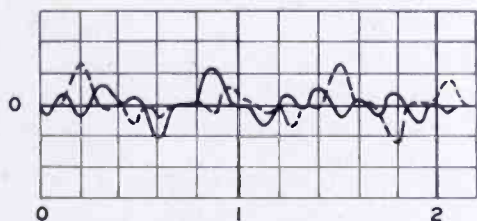


Fig. 9(f) — Cross talk voltage on red kinescope grid.

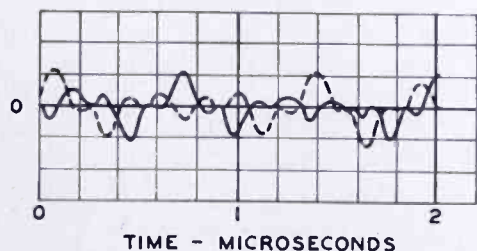


Fig. 9(g) — Cross talk voltage on blue kinescope grid

The signal from the green camera tube is sampled so that the signal at Adder No. 1 in Figure 1 is

$$[G + g \cdot \sin(\omega t)] \cdot \frac{1}{3} [1 + 2\cos(\omega_0 t)]$$

$$= \frac{g}{3} [1 + 2\cos(\omega_0 t)] + \frac{g}{3} \sin(\omega t) - \frac{g}{3} \sin(\omega_0 - \omega)t + \frac{g}{3} \sin(\omega_0 + \omega)t. \quad (16)$$

Since $f > f_B - f_0$, $f_0 + f > f_B$ and the last term in (16) is lost in going through the final filter before the transmitter in Figure 1. (This filter is not necessarily a physical reality, but serves the purpose of specifying the upper limit of frequencies that may be transmitted. It is likely that the upper frequency restriction will be imposed by the receiver rather than the transmitter.) Hence the signal at the modulator is

$$\frac{G}{3} [1 + 2\cos(\omega_0 t)] + \frac{g}{3} \sin(\omega t) - \frac{g}{3} \sin(\omega_0 - \omega)t. \quad (17)$$

Inspection of (17) shows that the loss of one of the terms with a coefficient $g/3$ has made it impossible for (17) to reproduce the desired variation in correct amplitude. This condition may be corrected by altering the response characteristics of the low-pass filters preceding the sampler in the transmitter of Figure 1. The filters should have a response in the region $f_B - f_o < f < f_A$ which is 1.5 times the gain in the region $0 < f < f_B - f_o$. Under this new condition, (17) becomes

$$\frac{G}{3} [1+2\cos(\omega_o t)] + \frac{g}{2} \sin(\omega t) - \frac{g}{2} \sin(\omega_o - \omega)t. \quad (18)$$

The condition where $G = 1$ and $g = 1/2$, computed from (18), is shown in Figure 9(b) for two successive line scans. These curves apply to the modulator signal in the transmitter and to the signal on the kinescope grid of a black-and-white receiver. Figure 9(c) shows the effective light intensity due to two scans of the same line on a black-and-white receiver.

Equation (18) may also be regarded as the signal into the sampler of the color receiver of Figure 3. The previously used expedient of multiplying by the generalized sampling function may now be resorted to just as was done in obtaining Equation (14). The result of sampling (18) is

$$\begin{aligned} & \frac{G}{9} [1+2\cos(\omega_o t)] [1+2\cos(\omega_o t + \theta) + 2\cos(2\omega_o t + 2\theta) + \dots] \\ & + \frac{1}{3} \left[\frac{g}{2} \sin(\omega t) - \frac{g}{2} \sin(\omega_o - \omega)t \right] [1+2\cos(\omega_o t + \theta) \\ & + 2\cos(2\omega_o t + 2\theta) + \dots] \\ & = \frac{G}{9} [1+2\cos(\omega_o t)] [1+2\cos(\omega_o t + \theta) + 2\cos(2\omega_o t + 2\theta) + \dots] \\ & + \frac{g}{6} [\sin(\omega t) + \sin(\omega t + \theta) \\ & + \sin([\omega_o + \omega]t + \theta) + \sin([\omega_o + \omega]t + 2\theta) \\ & - \sin([\omega_o - \omega]t + \theta) - \sin([\omega_o - \omega]t + \dots)]. \quad (19) \end{aligned}$$

Now to find the signal on the green kinescope, let $\theta = 0$ in (19) and find

$$\frac{1}{3} [G + g \cdot \sin(\omega t)] [1+2\cos(\omega_o t)]. \quad (20)$$

The condition where $G = 1$ and $g = 1/2$, computed from (20), is shown in Figure 9(d) which depicts the voltage on the grid of the green kinescope for two successive line scans. Figure 9(e) shows the effective light intensity due to two scans of the same line on the green kinescope.

The signal on the grid of the red kinescope (due to color cross talk) is found by setting $\theta = 240$ degrees in Equation (19), with the result

$$\frac{g}{6} \sin(\omega t - 60^\circ) [1 + 2\cos(\omega_0 t - 120^\circ)] \text{ (on red kinescope),} \quad (21)$$

and setting $\theta = 120$ degrees gives

$$\frac{g}{6} \sin(\omega t + 60^\circ) [1 + 2\cos(\omega_0 t + 120^\circ)] \text{ (on blue kinescope).} \quad (22)$$

The voltage on the grid of the red kinescope due to the erroneous sampling of the green signal is shown in Figure 9(f) as computed from (21), while Figure 9(g) shows the signal on the grid of the blue kinescope.

These equations show that cross talk up to fifty per cent is possible in the region where the frequency is greater than $f_B - f_0$ and less than f_A , or in the example, when the frequency lies between 0.3 megacycle and 2.0 megacycles.

At first glance, this degree of cross talk might seem intolerable. In the case shown in Figure 9, it is likely that non-linearity of the light-output versus grid-voltage characteristic of the kinescopes would make the cross talk of negligible importance. In the converse case, if the average intensity of the red tube were high, the erroneous voltage of Figure 9(f) might be enhanced to a point where cross talk produced undesirable effects. While this cross talk has not appeared to be a serious problem in the dot-sequential color television system, means for eliminating the effect will be described later in this report.

d. $G + g \cdot \sin(\omega t)$ where $f_A < f < f_B$

In this case, the green area is varying so that the electrical signal is made up of a dc component and an ac component of frequency f where $f_A < f < f_B$. This frequency region may be noted on Figure 2, and for illustrative purposes lies between 2.0 and 4.1 megacycles.

The signal from the green camera tube is $G + g \cdot \sin(\omega t)$. For purposes of illustration, f has been chosen as 3.4 megacycles, $G = 1$ and $g = 1/2$. Figure 10(a) shows this signal $1 + 1/2 \sin(\omega t)$.

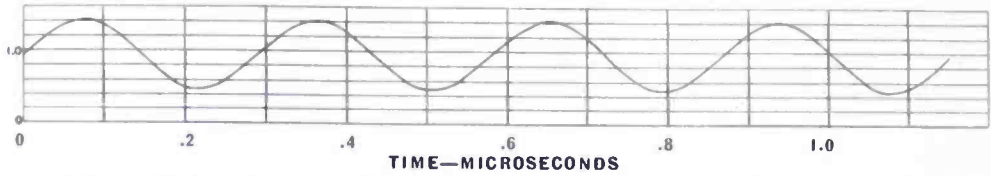


Fig. 10(a)—Signal out of green camera tube; $f = 3.4$ megacycles, $G + g \cdot \sin(\omega t) = 1 + 1/2 \sin(\omega t)$.

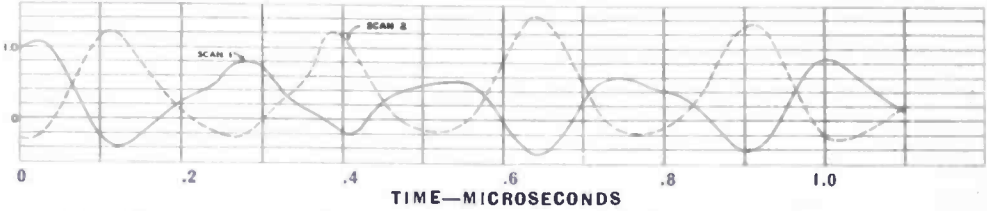


Fig. 10(b)—Signal on the green-kinescope grid of a color television receiver.

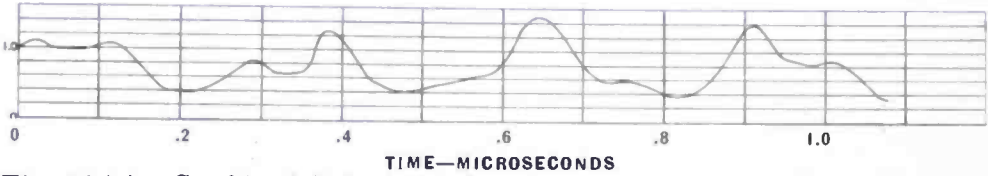


Fig. 10(c)—Combined light intensity of two successive scans of the same line on the green kinescope of a color television receiver.

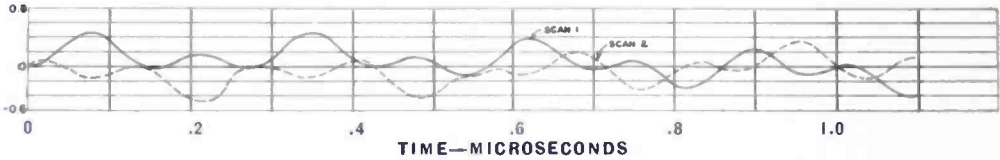


Fig. 10(d)—Voltage on the red kinescope grid.

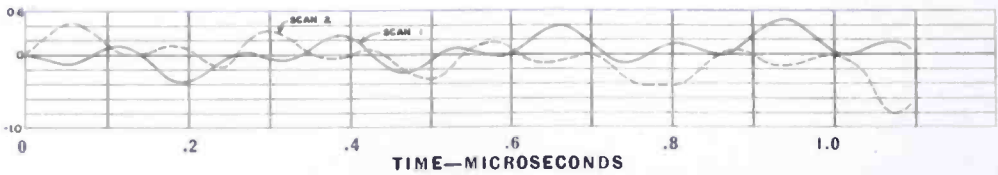


Fig 10(e)—Voltage on the blue kinescope grid.

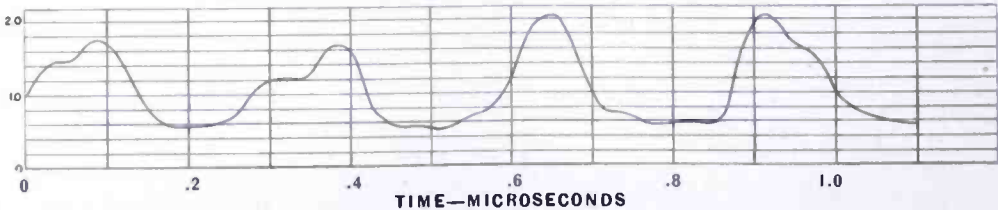


Fig 10(f)—Combined light intensity of two successive scans of the same line, obtained by adding light intensities of the green, red and blue tubes.

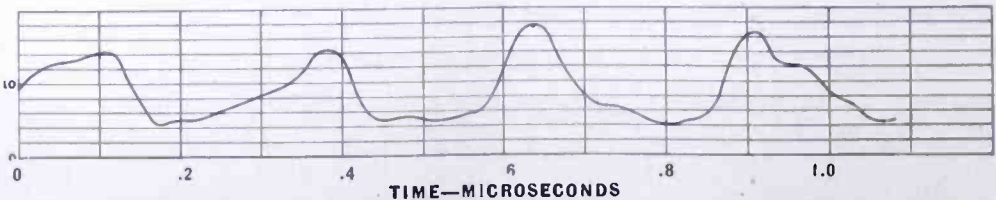


Fig. 10(g)—Combined light intensity of two successive scans of the same line, obtained by adding light intensities of the green and red tubes.

The dc signal G goes through the transmitter sampler, but since the ac term is of a frequency lying in the region committed to "mixed-highs," this latter signal goes through Adder No. 2 and the appropriate band-pass filter into Adder No. 1 of Figure 1. Hence the signal into the transmitter modulator is

$$\frac{G}{3} [1+2\cos(\omega_0 t)] + g \cdot \sin(\omega t). \quad (23)$$

Equation (23) also applies to the voltage on the kinescope grid of a black-and-white receiver. The background term is sampled while the mixed-high signal, unsampled, is superimposed to supply fine detail.

The signal out of the second detector of a color receiver also has the form of Equation (23). Sampling in the receiver results in a signal on the grid of the green kinescope of the form

$$\frac{1}{3} [G+g \cdot \sin(\omega t)] [1+2\cos(\omega_0 t)]. \quad (24)$$

A plot of this equation is shown by Figure 10(b), while Figure 10(c) shows the combined light intensity on a single line of the green tube for two successive scans of the same line. This latter plot shows the effect of the beat between the high-frequency component and the sampling frequency, so that Figure 10(c) is not a very faithful reproduction of Figure 10(a).

The output of the red sampler (the voltage on the grid of the red kinescope) is

$$\frac{g}{3} \sin(\omega t) [1+2\cos(\omega_0 t-120^\circ)], \quad (25)$$

while the voltage on the grid of the blue kinescope is

$$\frac{g}{3} \sin(\omega t) [1+2\cos(\omega_0 t+120^\circ)]. \quad (26)$$

The voltage on the red kinescope is shown in Figure 10(d), while the voltage on the blue kinescope is given by Figure 10(e).

It is obvious that the high-frequency signal mixing in this region is one hundred per cent, since the philosophy of the principle of "mixed-highs" has already been accepted, and the high frequency components of the three camera tubes have been deliberately combined at the trans-

mitter so that these signals have completely lost color identity. Because of the inability of the eye to see color in the fine detail, it is possible to combine the positive values of Figures 10(d) and 10(e) with Figure 10(c) with the result shown in Figure 10(f), which is a more satisfactory representation of Figure 10(a). However, it is well known that the resolution of the eye is very poor in blue, so it seems more fair to combine only Figure 10(d) with Figure 10(c), with Figure 10(g) resulting. The improvement in reproduction of Figure 10(a) by Figure 10(g) is striking, particularly when it is recalled that the rate of the variations in Figure 10(a) is at a high frequency, and that the differences between Figure 10(a) and Figure 10(g) represent still higher frequency components, which are beyond the limits of ordinary resolution.

THE SAMPLING PROCEDURE APPLIED TO STEP FUNCTIONS OF LIGHT INTENSITY

a. *Response of conventional black-and-white television receivers*

In the preceding pages, attention has been given to a color intensity change which produces an electrical signal consisting of a dc term and a single ac component. Such an analysis serves to demonstrate the detailed mechanism of the system. However, it is not a condition often encountered in producing an actual television image. Generally, it is more interesting to examine the action of the system near edges of objects in order to determine rise time, overshoot, and color cross talk.

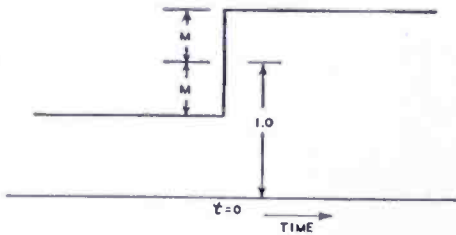


Fig. 11—Idealized step function of voltage which has a value of $1 - M$ for time less than zero and a value of $1 + M$ for time greater than zero.

For purpose of analysis, assume that the voltage coming from the green camera tube has the form shown in Figure 11, where the voltage has the value $1 - M$ for all values of time less than zero, and has the value of $1 + M$ for all times greater than zero. The function of Figure 11 may be produced exactly only when the associated circuits have unlimited frequency response. For this idealized condition, the signal from the green camera tube is given by the following Fourier Integral:

Green camera signal (G.C.S.)

$$= 1 + \frac{2M}{\pi} \int_{\beta=0}^{\beta=\infty} d\beta \int_{\omega=0}^{\omega=\infty} \sin(\omega\beta) \sin(\omega t) \cdot d\omega, \quad (27)$$

where $\beta =$ an integration variable,

$$\omega = 2\pi f,$$

$f =$ a frequency component lying between zero and infinity,

$t =$ the instant of time at which the signal is to be evaluated.

Now assume that a circuit is imposed which has unity gain for all frequencies below f_B and zero response for all frequencies above f_B , and with no appreciable phase shift. Then Equation (27) becomes

$$\begin{aligned} \text{G.C.S.} &= 1 + \frac{2M}{\pi} \int_{\beta=0}^{\beta=\infty} d\beta \int_{\omega=0}^{\omega=2\pi f_B} \sin(\omega\beta) \sin(\omega t) \cdot d\omega \\ &= 1 + \frac{2M}{\pi} \cdot \text{Si}(2\pi f_B t), \end{aligned} \quad (28)$$

where $\text{Si}(x) =$ Integral sine of $x = \int_0^x \frac{\sin u}{u} \cdot du$, a well-known and tabulated function.

Fig. 12—Response to the step function of Figure 11 ($M = 1/2$) for a circuit which has unity gain for all frequencies below 4.1 megacycles, zero response above 4.1 megacycles, and linear phase shift.

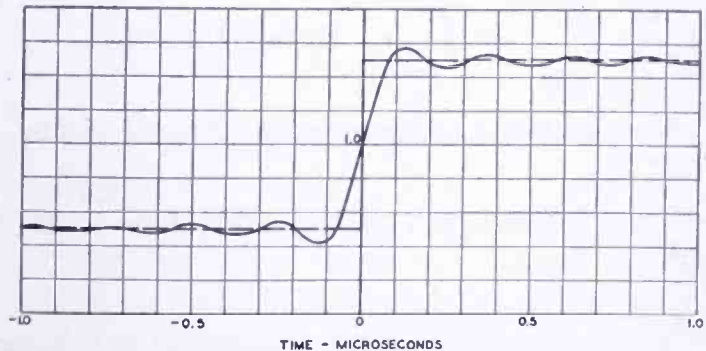


Figure 12 shows a plot of Equation (28) with $M = 1/2$ and with the upper frequency limit f_B equal to 4.1 megacycles. It should be noted that Figure 12 and not Figure 11 should be used in judging the response when other circuit factors have been added.

To find the signal at the transmitter modulator, use may be made of previously developed material to operate upon the term $\sin(\omega t)$ in Equation (28). Three frequency regions must be considered.

First, when $0 < f < f_B - f_o$, Equation (13) teaches that $\sin(\omega t)$ becomes $\frac{\sin(\omega t)}{3} [1 + 2\cos(\omega_o t)]$ at the transmitter modulator.

Secondly, when $f_B - f_o < f < f_A$, Equation (18) shows that $\sin(\omega t)$ becomes $1/2 \sin(\omega t) - 1/2 \sin(\omega_o - \omega)t$ at the transmitter modulator.

Then also in the region where $f_A < f < f_B$, Equation (23) shows that $\sin(\omega t)$ is unchanged.

Equation (12) tells that the unit value in Equations (27) and (28) becomes simply $1/3 [1+2\cos(\omega_0 t)]$.

When these operations are performed on Equation (27), the signal into the transmitter modulator (T.M.S.) is

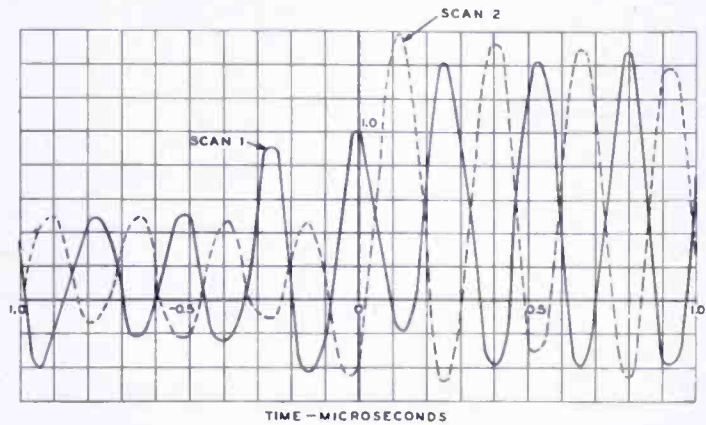
$$\begin{aligned} \text{T.M.S.} &= \frac{1}{3} [1+2\cos(\omega_0 t)] \\ &+ \frac{2M}{3\pi} [1+2\cos(\omega_0 t)] \int_{\beta=0}^{\beta=\infty} d\beta \int_{\omega=0}^{\omega=2\pi(f_B-f_0)} \sin(\omega\beta) \sin(\omega t) d\omega \\ &+ \frac{M}{\pi} \int_{\beta=0}^{\beta=\infty} d\beta \int_{\omega=2\pi(f_B-f_0)}^{\omega=2\pi f_A} \sin(\omega\beta) \sin(\omega t) d\omega \\ &- \frac{M}{\pi} \int_{\beta=0}^{\beta=\infty} d\beta \int_{\omega=2\pi(f_B-f_0)}^{\omega=2\pi f_A} \sin(\omega\beta) \sin(\omega_0 - \omega) t \cdot d\omega \\ &+ \frac{2M}{\pi} \int_{\beta=0}^{\beta=\infty} d\beta \int_{\omega=2\pi f_A}^{\omega=2\pi f_B} \sin(\omega\beta) \sin(\omega t) d\omega. \end{aligned} \quad (29)$$

Integration and combination of terms yields

$$\begin{aligned} \text{T.M.S.} &= \frac{1}{3} \{1 \pm \cos(\omega_0 t)\} \left\{ 1 + \frac{2M}{\pi} \text{Si} [2\pi(f_B-f_0)t] \right\} \\ &+ \frac{M}{\pi} \{2\text{Si}(2\pi f_B t) - \text{Si}(2\pi f_A t) - \text{Si} 2\pi(f_B-f_0)t\} \\ &\pm \frac{M}{\pi} \cos(\omega_0 t) \{ \text{Si}(2\pi f_A t) - \text{Si}[2\pi(f_B-f_0)t] \} \\ &\pm \frac{M}{\pi} \sin(\omega_0 t) \{ \text{Ci}[2\pi(f_B-f_0)t] - \text{Ci}(2\pi f_A t) \}. \end{aligned} \quad (30)$$

where $\text{Ci}(x) = \text{Integral cosine of } x = - \int_x^\infty \frac{\cos u}{u} du$. Where the \pm signs appear in Equation (30), the plus sign applies to the first scan of the line and the minus sign applies to the second scan of the same line.

Fig. 13 — Transmitter modulator signal for two successive scans of the same line. Also the signal on the kinescope grid of a conventional black-and-white receiver.



It should be noted that Equation (30) is also the voltage appearing on the kinescope grid in a black-and-white receiver. Figure 13 is a plot of Equation (30) for the following conditions:

$$M = \frac{1}{2},$$

$$f_B = 4.1 \text{ megacycles,}$$

$$f_0 = 3.8 \text{ megacycles,}$$

$$f_A = 2.0 \text{ megacycles,}$$

$$f_B - f_0 = 0.3 \text{ megacycle,}$$

and may be considered as the transmitter modulator signal for two successive scans of the same line, as well as the signal on the kinescope grid of a conventional black-and-white receiver. Figure 14 shows the combined light intensity of two successive scans of the same line on a black-and-white receiver. This latter figure, constructed graphically from Figure 13, shows close agreement with Figure 12.

b. Response of a color television receiver

To find the signal on the kinescopes of a color television receiver,

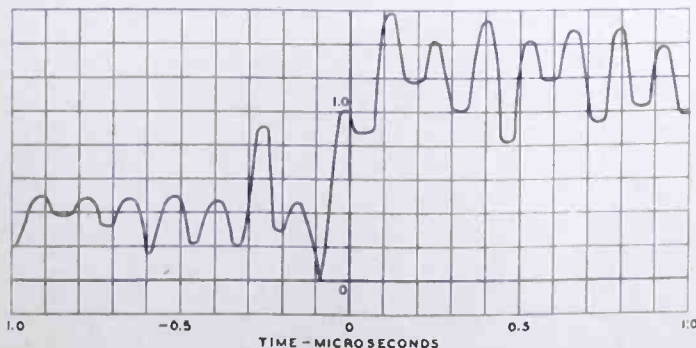
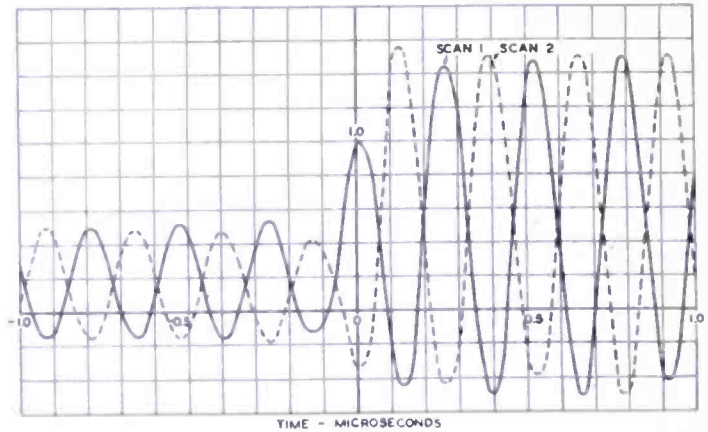


Fig. 14 — Combined light intensity of two successive scans of the same line on a black-and-white receiver.

Fig. 15 — Signal on the green kinescope grid of a color television receiver.



the operating procedure on the $\sin(\omega t)$ term of Equation (27) is determined by referring to Equations (15), (20), and (24). These equations show that $\sin(\omega t)$ is converted to $\frac{\sin(\omega t)}{3} [1 + 2\cos(\omega_0 t)]$ in all frequency regions up to f_B , so the signal on the green kinescope (G.K.S.) is simply

$$\text{G.K.S.} = \frac{1}{3} [1 \pm 2\cos(\omega_0 t)] \left[1 + \frac{2M}{\pi} \text{Si}(2\pi f_B t) \right], \quad (31)$$

where the \pm signs apply to the first and second scans of the same line.

Comparison of Equations (28) and (31) shows that the signal on the green kinescope is a perfect reproduction of the green camera signal multiplied by the sampling function. Figure 15 shows a plot of Equation (31), the signal on the green kinescope grid of a color television receiver, for the same frequency restrictions used in the previous calculations, while Figure 16 shows the combined light intensity of two successive scans of the same line on the green kinescope of a color television receiver.

The cross talk may be deduced by using Equations (21) and (25)

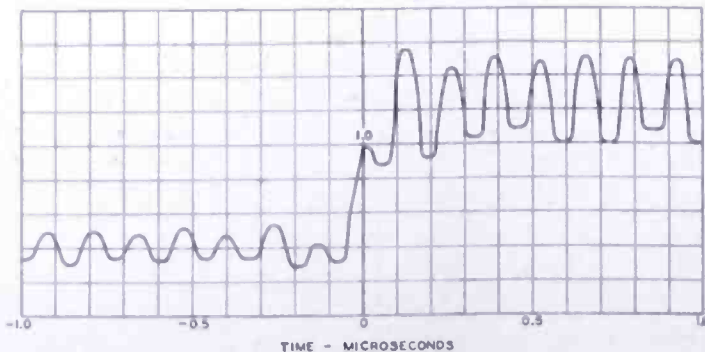


Fig. 16 — Combined light intensity of two successive scans of the same line on the green kinescope of a color television receiver.

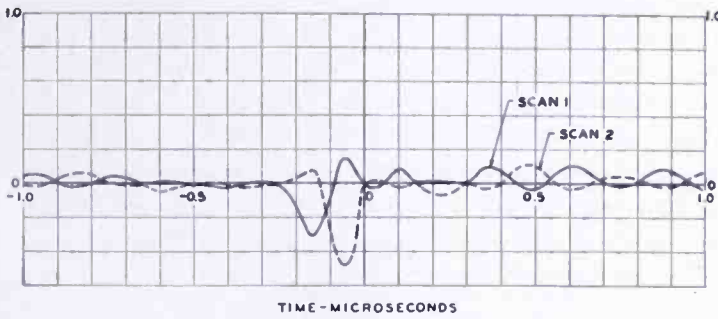


Fig. 17 — Cross-talk voltage on the red kinescope grid for two successive scans of the same line.

for the red tube cross talk and Equations (22) and (26) for the blue tube cross talk in conjunction with Equation (27). Then the red kinescope signal (R.K.S.) is

$$\begin{aligned} \text{R.K.S.} = & \frac{2M}{\pi} \{1 \pm 2\cos(\omega_0 t - 120^\circ)\} \left\{ \frac{1}{3} \text{Si}(2\pi f_B t) - \frac{1}{4} \text{Si}(2\pi f_A t) \right. \\ & \left. - \frac{1}{12} \text{Si}[2\pi(f_B - f_0)t] + \frac{\sqrt{3}}{12} \text{Ci}[2\pi(f_B - f_0)t] - \frac{\sqrt{3}}{12} \text{Ci}(2\pi f_A t) \right\}, \quad (32) \end{aligned}$$

and the blue kinescope signal (B.K.S.) is

$$\begin{aligned} \text{B.K.S.} = & \frac{2M}{\pi} \{1 \pm 2\cos(\omega_0 t + 120^\circ)\} \left\{ \frac{1}{3} \text{Si}(2\pi f_B t) - \frac{1}{4} \text{Si}(2\pi f_A t) \right. \\ & \left. - \frac{1}{12} \text{Si}[2\pi(f_B - f_0)t] - \frac{\sqrt{3}}{12} \text{Ci}[2\pi(f_B - f_0)t] + \frac{\sqrt{3}}{12} \text{Ci}(2\pi f_A t) \right\}. \quad (33) \end{aligned}$$

Figure 17 shows the cross-talk voltage on the red kinescope grid for two successive scans of the same line, while Figure 18 displays the combined light intensity of two successive line scans of the same line on the red kinescope.

Figures 19 and 20 show corresponding effects for the blue kinescope.

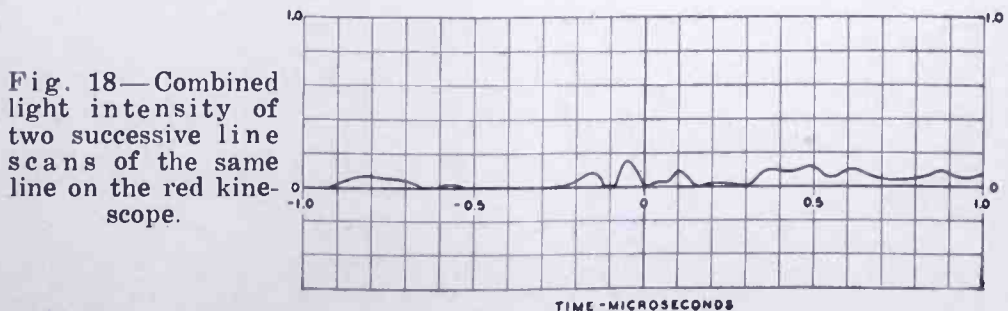
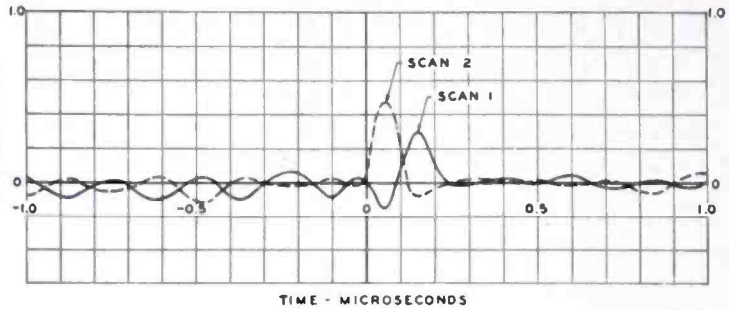


Fig. 18— Combined light intensity of two successive line scans of the same line on the red kinescope.

Fig. 19 — Cross-talk voltage on the blue kinescope grid for two successive line scans of the same line on the blue kinescope.



CROSS-TALK ELIMINATION BETWEEN THE GREEN AND RED CHANNELS WHEN $f_B - f_0 < f < f_A$

It was observed in Section III, where the frequency of the signal component lies between $f_B - f_0$ and f_A , that the color cross-talk terms may be up to fifty per cent of the desired terms. While it has not yet been clearly established that it is necessary to reduce or eliminate this cross talk, rather simple circuit expedients are possible to completely eliminate the cross talk. It should be remembered that the response in the mixed-high region has not been considered to be cross talk, since the crossing of signals in this region has been regarded as entirely legitimate.

a. *Simple modification of the transmitter sampler*

As a first step in describing a number of possibilities, a simple modification of the transmitter sampler may first be considered. Figure 21 shows the part of Figure 1 which has been changed somewhat. The mixed-high circuits have not been changed and are not shown. The low-pass filters in the red and the green channels, as before, pass frequencies up to f_A , but now have unity gain up to $f_B - f_0$ and have a gain of 2.0 from this frequency up to f_A . The low-pass filter in the blue channel may cut-off at $f_B - f_0$, since the eye is very poor in resolving power in the blue.

A band-pass filter and phase shifter connect the output of the low-pass filter in the green channel to the input of the red sampler. This

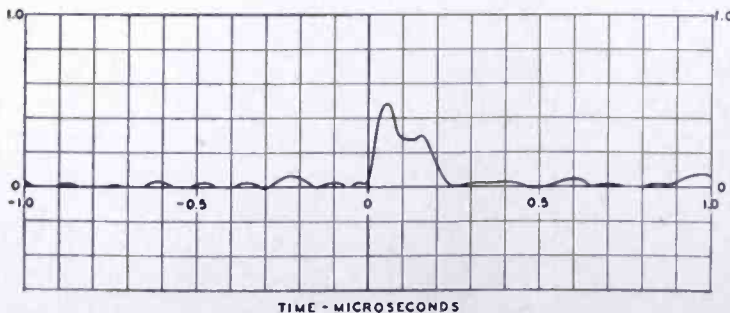


Fig. 20—Combined light intensity of two successive line scans of the same line on the blue kinescope.

channel passes frequencies between $f_B - f_0$ and f_A , the region where it is desired to eliminate cross talk. The signal from the green channel to the red sampler position is made one half of the signal going to the green sampler position. In addition, all the frequency components

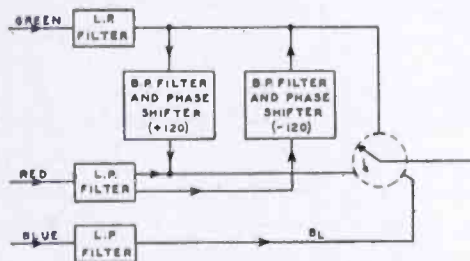


Fig. 21 — Circuit modifications at the transmitter to eliminate cross talk between the red and green channels.

are advanced 120 degrees in phase in passing through the circuit. This latter condition is quite easily brought about by a double modulating and filtering process. The corresponding element going from the red channel to the green sampling position has the same characteristics except that the phase of the components is retarded by 120 degrees.

With the signal $g \cdot \sin(\omega t)$ coming from the green camera, the signal going into the green sampler position at the transmitter is

$2g \cdot \sin(\omega t)$. This signal is sampled by the function $\frac{1}{3} [1 + 2\cos(\omega_0 t)]$

and becomes $\frac{2g}{3} \sin(\omega t) - \frac{2g}{3} \sin(\omega_0 - \omega)t$. The signal into the red sampler (from the green channel through the phase shifter) is

$g \cdot \sin(\omega t + 120^\circ)$. This signal is sampled by the function $\frac{1}{3} [1 + 2\cos$

$(\omega_0 t - 120^\circ)]$ yielding a signal out of the red sampler of $\frac{g}{3} \sin(\omega t + 120^\circ)$

$-\frac{g}{3} \sin[(\omega_0 - \omega)t - 240^\circ]$. The total signal into the modulator is

$$\frac{g}{\sqrt{3}} \{ \sin(\omega t + 30^\circ) - \sin[(\omega_0 - \omega)t + 30^\circ] \}. \quad (34)$$

When Equation (34) is sampled at the color receiver by the green sampler, using the sampling function

$$\frac{1}{3} [1 + 2\cos(\omega_0 t) + 2\cos(2\omega_0 t) + \dots],$$

the signal on the green kinescope grid becomes

$$\frac{g \sin(\omega t)}{3} [1 + 2\cos(\omega_0 t)].$$

However, when Equation (34) is sampled by the red sampler at the receiver, using the sampling function

$$\frac{1}{3} [1 + 2\cos(\omega_0 t - 120^\circ) + 2\cos(\omega_0 t - 240^\circ) + \dots],$$

the signal on the red kinescope grid becomes identically zero.

Thus a method of completely eliminating the cross talk between the red and the green channels in the frequency region above $f_B - f_o$ and below f_A has been displayed.

b. Addition of a low-pass filter to the color receiver

The additions of Figure 21 may be added to the transmitter without a single change in the receiver of Figure 3. If color receivers of this type were in operation in the field, the changes in the transmitter shown in Figure 21 could be made without altering a single receiver. The immediate effect would be an elimination of cross talk in the region in question between the green and red channels. The cross talk of red and green into the blue channel would be unchanged, but because of the high-frequency nature would probably be of no consequence. Cross talk of the blue into red or green would be eliminated by restricting the components of the blue signal to frequencies less than $f_B - f_o$ by means of the low-pass filter in the blue channel preceding the transmitter sampler.

As another experiment to investigate the matter of reduction of cross talk, a low-pass filter could be inserted in the video amplifier circuit leading to the blue kinescope in Figure 3. This filter would also remove the f_o sampling component in the blue channel.

Before proceeding with an examination of other circuit details, it may prove interesting to see what has happened to the step function response for the receiver and transmitter condition described in this section.

The desired response of the signal at the green kinescope has remained unchanged and is given by Equation (31) and by Figures 15 and 16. The cross-talk conditions have changed, however. For instance, in the red channel, the only signal mixing components are those that have been placed there deliberately by the use of mixed highs. The signal on the red kinescope grid due to the step function in the green channel is

$$\text{R.K.S.} = \frac{2M}{3\pi} [1 \pm 2\cos(\omega_0 t - 120^\circ)] [\text{Si}(2\pi f_B t) - \text{Si}(2\pi f_A t)]. \quad (35)$$

Fig. 22—Signal on grid of red kinescope due to step function in the green channel and the use of mixed highs.

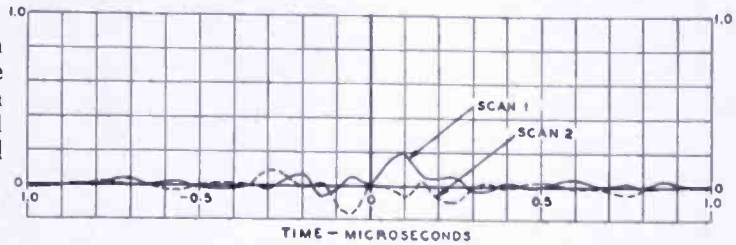


Figure 22 shows the signal corresponding to (35) for two scans of the same line, with $M = 1/2$, $f_B = 4.1$ megacycles, $f_A = 2.0$ megacycles, and $f_o = 3.8$ megacycles. Figure 23 shows the combined light intensities on the red tube for two scans of the same line, and Figure 24 has been constructed by adding Figure 23 to Figure 16, since the contribution from the red tube came entirely from the use of the mixed-highs.

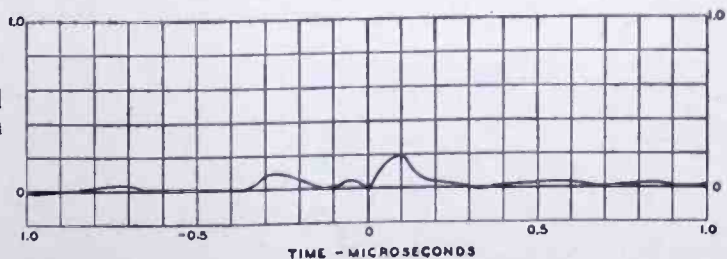
c. Increased resolution in the blue channel

In the previous example, a method of eliminating cross talk between the red and green channels has been displayed, but the resolution in the blue channel to $f_B - f_o$ (0.3 megacycle in the numerical example) has been restricted. If it should prove desirable to follow the above path of exploration and it became evident that greater resolution were desired in the blue channel, the resolution could be doubled by a simple sampling or interrupting method with dot interlacing. By this method, the resolution could be increased to $2(f_B - f_o)$, or 0.6 megacycle in the example.

Suppose that a sampler with a very broad pulse but sampling at a rate of twice the frequency $f_B - f_o$ is incorporated in the blue channel and this sampler is followed by a low-pass filter which cuts off at one half the sampling frequency. Also a simple dot interlace is introduced. Let f_s be the sampling frequency. Then suppose the signal from the blue camera tube is $B + b \cdot \sin(\omega t)$. The function $1 + \cos(\omega_s t)$ will be used for sampling. When the frequency f is less than $f_s/2$, the signal out of the sampler and the low-pass filter is simply $B + b \cdot \sin(\omega t)$. This signal at the receiver is again sampled, this time by the function $1 \pm \cos(\omega_s t)$, giving

2

Fig. 23—Combined light intensities on the red tube.



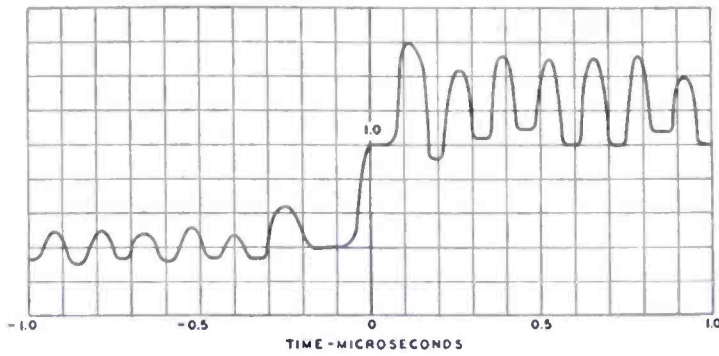


Fig. 24—Combined light intensities from red and green kinescopes.

$$[B + b \sin(\omega t)] \left[\frac{1 \pm \cos(\omega_s t)}{2} \right]$$

Figure 25 has been prepared, using

$$\begin{aligned} B &= 1, \\ b &= 1/2, \\ f &= 0.1 \text{ megacycle}, \\ f_s &= 0.6 \text{ megacycle}. \end{aligned}$$

Figure 25(a) shows the original function, while Figure 25(b) shows the effective light intensities for two scans. Figure 25(c) shows the sums of the light intensities for the two scans of Figure 25(b).

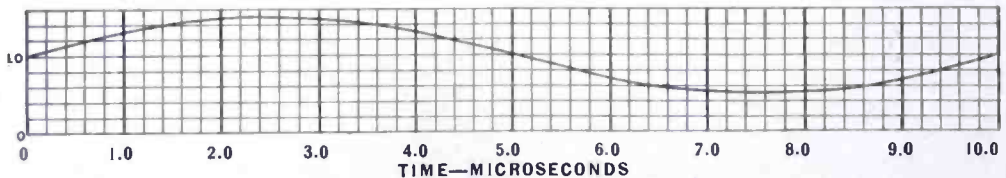


Fig. 25(a)—Signal out of the blue camera tube, $1 + 1/2 \sin(\omega t)$, with a frequency of 0.1 megacycle.

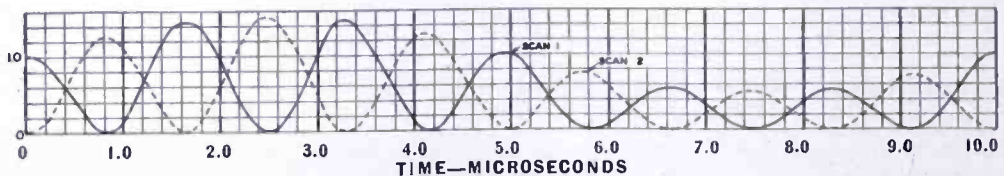


Fig 25(b)—Effective light intensities for two scans on the same line of the blue tube. Sampling frequency is 0.6 megacycle.

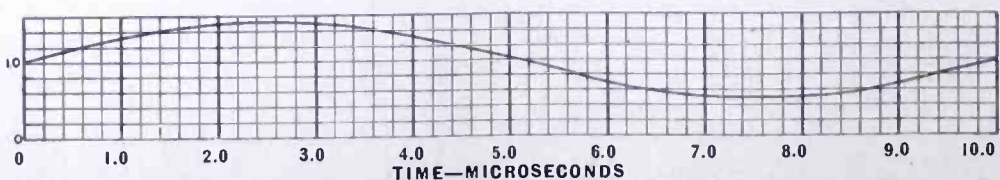


Fig. 25(c)—Sums of the light intensities for the two scans of Figure 25(b).

When the frequency f is greater than $f_s/2$, the response of the preceding circuits must be doubled. Hence the signal arriving at the sampler will be $B + 2b \sin(\omega t)$. After sampling at the transmitter by the function $1 \pm \cos(\omega_s t)$, the signal at the receiver second detector is $B \mp b \sin(\omega_s - \omega)t$. The second sampling at the receiver by the function $\frac{1 \pm \cos(\omega_s t)}{2}$ yields

$$\frac{B [1 \pm \cos(\omega_s t)]}{2} + \frac{b}{2} \sin(\omega t) \mp \frac{b}{2} \sin(\omega_s - \omega)t.$$

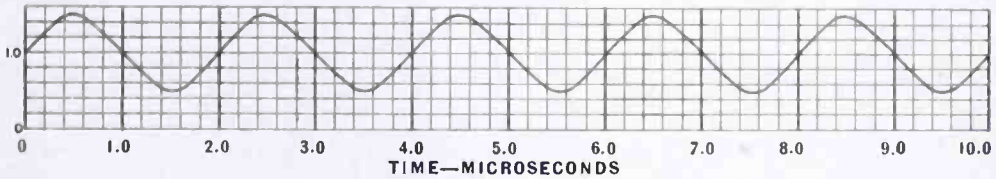


Fig. 26(a)—Signal out of the blue camera tube, $1 + 1/2 \sin(\omega t)$, with a frequency of 0.5 megacycle.

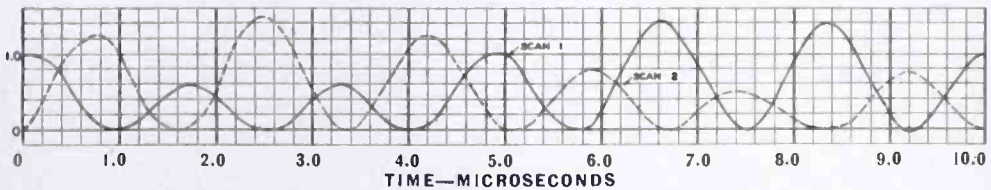


Fig. 26(b)—Effective light intensities for two scans on the same line of the blue tube. Sampling frequency is 0.6 megacycle.

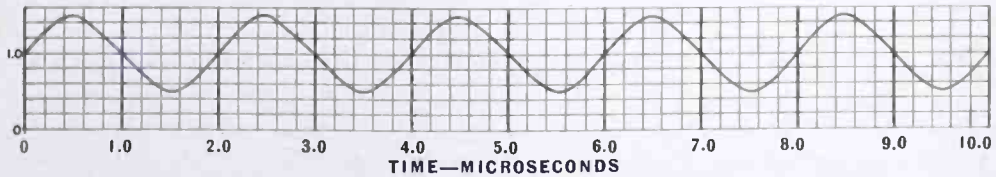


Fig. 26(c)—Sums of the light intensities for the two scans of Figure 26(b).

Figure 26 has been prepared, using

$$\begin{aligned} B &= 1, \\ b &= 1/2, \\ f &= 0.5 \text{ megacycle,} \\ f_s &= 0.6 \text{ megacycle.} \end{aligned}$$

Figure 26(a) shows the original function, while Figure 26(b) shows the effective light intensities for two scans. Figure 26(c) shows the sums of the light intensities for the two scans of Figure 26(b).

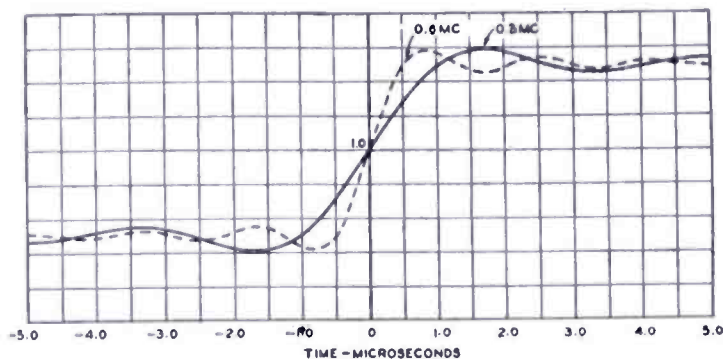


Fig. 27 — Change in step function for two frequency bands, one limited to 0.3 megacycle and the other limited to 0.6 megacycle,

This procedure illustrates the use of dot interlacing to obtain 0.6-megacycle resolution with a channel width of 0.3 megacycle.

The high-frequency sampling has been omitted from consideration in the above analysis. The signals from the blue channel are, of course, sampled at frequency f_0 just as the red and green signals, but the filter at the receiver removes all traces of this sampling on the blue tube.

Figure 27 shows the change in a step function for two cases: first, where the frequency band is limited to 0.3 megacycle, and second, where the band is restricted to 0.6 megacycle. The increased steepness due to the wider band is apparent.

The step function response on the grid of the blue kinescope is given by

$$\begin{aligned} \text{B.K.S.} &= \frac{[1 \pm \cos(\omega_s t)]}{2} \left[1 + \frac{2M}{\pi} \cdot \text{Si}(\omega_s t) \right] \\ &\pm \frac{M}{\pi} \sin(\omega_s t) \left[\text{Ci}\left(\frac{\omega_s t}{2}\right) - \text{Ci}(\omega_s t) \right]. \end{aligned} \quad (36)$$

Figure 28 shows Equation (36) plotted for two line scans, where $M = 1/2$ and f_s is 0.6 megacycle. Figure 29 shows the addition of light intensities from Figure 28. It may be seen that Figure 29 is an exact reproduction of the dotted curve of Figure 27.

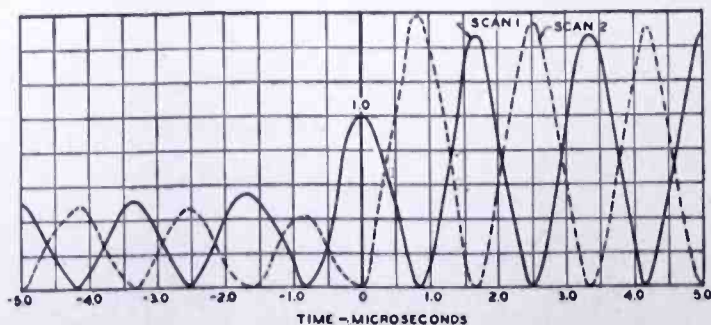


Fig. 28—Step function response on grid of blue kinescope tube with dot-interlacing and sampling.

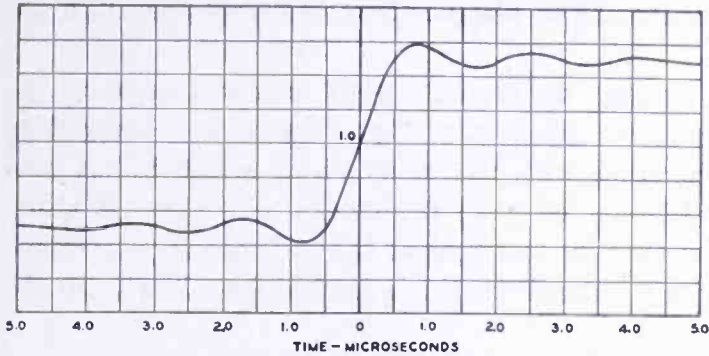


Fig. 29—Addition of light intensities on the blue tube, obtained by adding the curves of Figure 28.

CONCLUSION

Cross talk as a function of the width of the sampling pulse at both the transmitter and the receiver has been examined and limits established for reasonable cross talk. It is shown that narrow sampling at the receiver is more important than narrow sampling at the transmitter.

The sampling procedure was examined for large areas of color with a sinusoidal variation of the color. It was shown that the frequency passband was divided into three regions, the lower in which no cross talk existed, a middle region where fifty per cent cross talk was possible, and an upper region where signal mixing was expected because of the adoption of mixed highs. For the various cases, the role of dot interlacing was explained. In addition, the action on conventional black-and-white receivers as well as on color receivers was examined.

The sampling procedure was examined as it applied to step functions of light intensity. The response of a black-and-white receiver was examined and the desired and undesired responses of a color receiver were displayed.

A method of cross-talk elimination in the middle region is described. This method might be applied as an experiment in three parts. First, a simple cross-coupling and phase-shifting network is applied to the transmitter sampler. This circuit eliminates the cross talk between the red and the green channels in the middle region. No change is necessary at the receiver to take this first step. As a second improvement, a low-pass filter might be added in the blue channel at the receiver to knock out cross talk from the red and green into the blue channel. This step restricts the definition of the blue channel. A third step is suggested which doubles the resolution of the blue channel by a sampling and interlacing procedure.

The analysis and display of curves show that the sampling process in the dot-sequential color television system, together with the use of mixed highs provides a good uncoupling of the color channels together

with full resolution equivalent to black-and-white transmission in the same channel.

The construction leading to Figure 10(g) emphasizes that the output of the sampler is the *product* of input signal and the gating function. This fact, together with the principle of mixed highs, produces full detail limited only by total bandwidth available. A study of Equation (31) shows that the rise time of the envelope is determined by the highest frequency passed in the mixed-highs circuit at the transmitter.

Throughout this report, the signal under consideration originated from a single primary color. If an area is a mixture of colors, the analysis may be carried out on the basis of the superposition of the individual responses to the three primary colors. Where, in the mixture of colors, the two stronger primaries are nearly equal in intensity, the variation due to the sampling frequency shown in Figures 7(c) and 8(c) virtually disappears, particularly on a standard black-and-white receiver.

During November, 1949, the sampling frequency of the dot-sequential color television system used experimentally in Washington was reduced from 3.8 to approximately 3.6 megacycles. Many of the calculations contained in this report were already completed at that time and were made on the basis of a sampling frequency of 3.8 megacycles. Rather than repeat the many laborious computations for the slight change in sampling frequency, the remainder of the calculations were continued at a sampling frequency of 3.8 megacycles. No very major change would have been apparent in the plotted results. The region free of cross talk in the simplest form of the system ($0 < f < f_B - f_0$) would have been extended from 0.3 megacycle to 0.5 megacycle.

A STUDY OF COCHANNEL AND ADJACENT-CHANNEL INTERFERENCE OF TELEVISION SIGNALS*

A Report

By

RCA LABORATORIES DIVISION, PRINCETON, N. J.

Part II — Adjacent-Channel Studies

Summary—Included in the observer tests were color signals characteristic of the field-sequential, line-sequential, and dot-sequential systems. A standard monochrome signal was paired with a monochrome signal and the color signals in some of the tests. In all instances, the interfering sound signal was present. From the standpoint of allocation, no substantial difference in the tolerable ratios was found for the various combinations of color and monochrome signals used.

METHOD AND APPARATUS USED FOR THE DETERMINATION OF ADJACENT-CHANNEL INTERFERENCE RATIOS

Part II of this study summarizes the work with adjacent-channel interference. The approach to the problem was made through the use of subjective visual observations of a limited number of observers. The choice of personnel for the test group was made from laboratory employees with the intent of approximating a fair cross-section of the population by 15 observers. All observers were accustomed to the viewing of television pictures and had some previous acquaintance with the types of adjacent-channel interference ordinarily experienced in standard monochrome television.

Included in the tests were signals characteristic of the three proposed color television systems; the field-sequential system, the line-sequential system, and the dot-sequential system. A standard monochrome signal was paired with the color systems for certain tests to represent the coexistence of color and monochrome television on adjacent channels.

All signals were generated by low-power transmitters operating on Channels 3 and 4 within the laboratory. Attenuation of the lower sideband of an interfering signal on the upper adjacent channel was provided by a vestigial sideband filter with attenuation characteristics

* Decimal Classification: R171 × R430.11 × R583.16.

as shown in Figure 20. Synchronizing waveforms for the interfering and desired signals were generated by independent synchronizing generators not locked to a common power supply.

Significant details of the observer tests of adjacent-channel interference correspond to the conditions for cochannel interference tests as set forth in Part I of this study; namely,

Receiver	—RCA Model 9T246 modified. Video output supplied signals for monochrome and color observations.
Picture Size	—As stated in Part I.
Desired Picture	—Stationary slide, band leader and band (see Figure 12, Part I.)
Interfering Picture	—Test pattern
High-Light Brightness	—15 foot-lamberts
Ambient Room Illumination	—Up to 4 foot-candles

Observer tests of cochannel interference may ordinarily be conducted without regard for the selectivity characteristics of the receiver used, since the spectrums of both desired and interfering signals correspond and are treated equally by the receiver. On the contrary, conclusions drawn from observations of adjacent-channel interference must take account of the selectivity characteristic of the television receiver since the spectrums of the desired and interfering signals are displaced by six megacycles. In order, therefore, to place these observations on a basis independent of a particular selectivity characteristic, all interference ratios are finally referred to the detector.

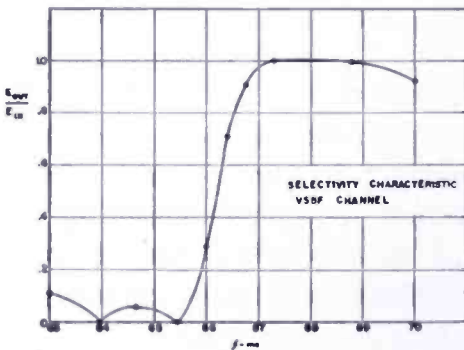


Fig. 20—Frequency-response characteristic of the vestigial sideband filter.

The over-all selectivity characteristics of the receiver used in tests at the RCA Laboratories are displayed in Figures 21 and 22.

SUBJECTIVE TESTS

In all tests, observers were instructed to inform the operator when the strength of the interfering signal corresponded (1) to interference on the threshold of visibility, and (2) to interference at the limit of tolerance. The observer was requested not to imagine that the test

slide was a favorite program, but to base judgment on the test subject as such. Hence, the ratios of desired signal to interfering signal which was obtained may be regarded as conservative values.

A fixed ratio of picture signal to sound signal equal to 3 decibels was maintained throughout.

a. Lower-Adjacent-Channel Interference

Subjective tests were conducted with the desired signal on channel 4 and the interfering signal on channel 3. There was unanimous agreement by 15 observers that the lower adjacent sound carrier was the determining factor in lower-adjacent-channel interference. That is, the

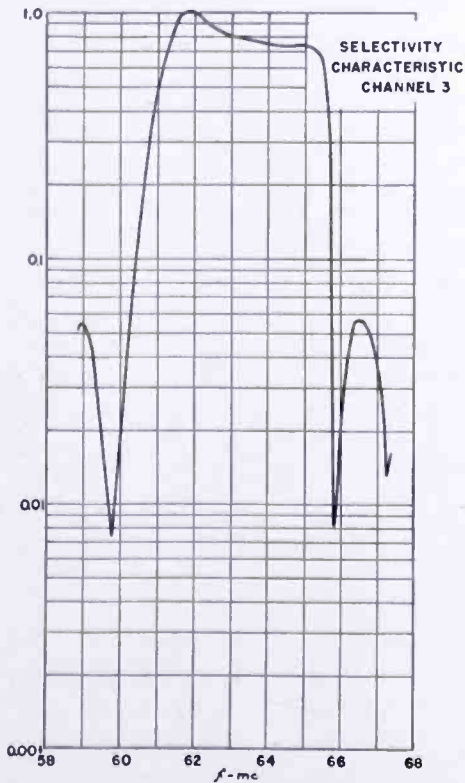


Fig. 21—Frequency characteristic of receiver on Channel 3.

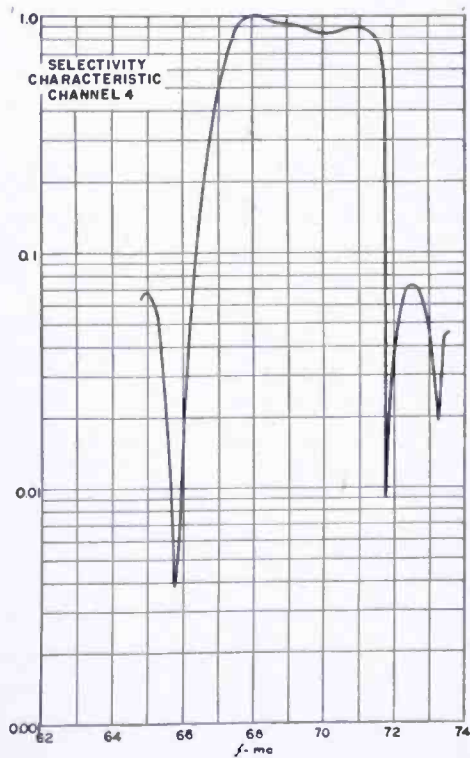


Fig. 22—Frequency characteristic of receiver on Channel 4.

presence of an interfering picture, monochrome or any of the types of color, was masked by the usual wavering fine bar pattern commonly associated in television with an interfering frequency-modulated sound carrier. Similar observations were made when a monochrome signal was on the lower adjacent channel and the desired signal was a dot-sequential picture viewed in color or monochrome or a field-sequential color picture.

In all of the foregoing observations, the average observer required a ratio of desired to interfering carriers of approximately -17 decibels

for tolerable interference and approximately -13 decibels for threshold interference. These values apply for the receiver selectivity characteristic shown in Figure 22. Since an attenuation of 48 decibels is afforded by the lower adjacent sound trap and the attenuation of the desired carrier is 5 decibels, the threshold and tolerable ratios referred to the input of the detector are 30 and 26 decibels respectively.

Table V—Summary of Tolerable and Threshold Ratios of Desired to Undesired Adjacent-Channel Television Signals

Desired Signal	Undesired Signal	Average ratio required by the observers (decibels)*	
		Threshold	Tolerable
Channel 3—desired signal			
Channel 4—undesired picture and sound signals, ratio of sound to picture = 0.71			
Standard monochrome viewed on standard monochrome receiver	Standard monochrome	-9	-14
Standard monochrome viewed on standard monochrome receiver	Field-sequential color	-9	-12
Standard monochrome viewed on standard monochrome receiver	Line-sequential color, Sequence C	-10	-14
Standard monochrome viewed on standard monochrome receiver	Dot-sequential color	-9	-13

* Ratios measured at input to receiver. Add $+33$ decibels to readings for input to detector.

b. Upper-Adjacent-Channel Interference

Measurements were made with the undesired signal on channel 4 properly restricted by the vestigial sideband filter characteristics as in Figure 20.

All observers agreed that the sound signal associated with the upper adjacent channel did not give rise to observable interference before interference due to the picture carrier exceeded the limit of tolerance. That is, the tolerable and threshold ratios were dictated by interference commonly known as "windshield wiper" effect caused by the subject matter of the nonsynchronous interfering picture.

The observer data are summarized in Tables V and VI. It is clear from Table V that the average observer did not distinguish between

sources of interference when viewing a monochrome picture. The tolerable and threshold ratios for the average observer were about -9 and -13 decibels respectively.

Table VI—Summary of Tolerable and Threshold Ratios of Desired to Undesired Upper-Adjacent-Channel Television Signals

Channel 3—desired signal
Channel 4—undesired picture and sound signals, ratio of sound to picture = 0.71

Desired Signal	Undesired Signal	Average ratio required by the observers (decibels)*	
		Threshold	Tolerable
Dot-sequential color viewed on color receiver	Standard monochrome	-5	-8
Dot-sequential color viewed on standard monochrome receiver	Standard monochrome	-6	-8
Field-sequential color viewed on color receiver	Field-sequential color	-10	-13
Field-sequential color viewed on color receiver	Standard monochrome	-15	-19
Dot-sequential color viewed on color receiver	Dot-sequential color	-11	-18
Dot-sequential color viewed on monochrome receiver	Dot-sequential color	-11	-18

* Ratios measured at input to receiver. Add $+33$ decibels to readings for input to detector.

In Table VI drawn up for the field-sequential and dot-sequential color signals as the desired signals and monochrome as the interfering signal, somewhat greater spread is recorded. It is believed, however, that more extensive observations would bring the data of Table VI into line with that of Table V.

It is reasonable to conclude that the average observer is tolerant to about the same extent of upper-adjacent-channel interference caused by a monochrome signal as color signals of any of the three types. Accepting this generalization, a ratio for threshold interference is about -9 decibels and for tolerable interference, about -13 decibels.

Since upper-adjacent-channel interference is controlled by the attenuation provided in the receiver at the frequency of the adjacent picture

carrier, the ratios may be referred to the input of the detector by reference to Figure 21. Taking values of 38 decibels and 5 decibels for adjacent picture carrier and desired picture carrier attenuations, the ratios of 24 and 20 decibels referred to the detector are deduced for threshold and tolerable interference ratios.*

Table VII—Summary of Average Threshold Ratios of Desired to Undesired Cochannel Television Signals (Decibels)

Symbols:
 BW—Standard Black and White
 FSC—Field-Sequential Color
 LSC—Line-Sequential Color
 DSC—Dot-Sequential Color

Offset—Carriers offset 10.5 kilocycles.
 Normal—Cochannel with normal frequency tolerances.

..... Undesired Signal

Desired Signal	BW		FSC		LSC		DSC	
	Offset	Normal	Offset	Normal	Offset	Normal	Offset	Normal
BW on BW Recv'r	36	55	40	57	36	57	35	56
FSC on Color Receiver	39	49	40	50	xxxx	xxxx	xxxx	xxxx
FSC on BW Recv'r	Note A	Note A	Note A	Note A	xxxx	xxxx	xxxx	xxxx
LSC on Color Receiver	Note B	46	xxxx	xxxx	Note C	Note C	xxxx	xxxx
LSC on BW Recv'r	Note B	52	xxxx	xxxx	Note C	Note C	xxxx	xxxx
DSC on Color Receiver	41	54	xxxx	xxxx	xxxx	xxxx	35	44
DSC on BW Recv'r	37	52	xxxx	xxxx	xxxx	xxxx	37	50

Note A.—No tests made.

Note B.—The coarse appearance of the scanning raster gave the same type effect as offset carrier interference so observers were unable to distinguish between interference and normal appearance of picture.

Note C.—This test would have required two sets of signal generating equipment for the line-sequential system. Only one set of equipment was available.

CONCLUSION

When the interfering signal is on the lower adjacent channel, the tolerable ratios of desired to undesired signal are very dependent upon the adjustment of the adjacent channel sound trap.

* The standard unmodified receiver type 9T246 has an adjacent picture carrier attenuation of approximately 50 decibels.

Upper-adjacent-channel interference comes mainly from the undesired picture carrier and sidebands closely associated with this carrier, and is determined by the attenuation achieved in the upper-adjacent-channel picture carrier trap.

Table VIII—Summary of Average Tolerable Ratios of Desired to Undesired Cochannel Television Signals (Decibels).

Symbols:
 BW —Standard Black and White Offset—Carriers offset 10.5 kilocycles.
 FSC—Field-Sequential Color
 LSC—Line-Sequential Color Normal—Cochannel with normal frequency tolerances.
 DSC—Dot-Sequential Color

Desired Signal	Undesired Signal							
	BW		FSC		LSC		DSC	
	Offset	Normal	Offset	Normal	Offset	Normal	Offset	Normal
BW on	29		32		30		29	
BW Recv'r		47		47		48		48
FSC on	33		33		xxxx		xxxx	
Color Receiver		42		42		xxxx		xxxx
FSC on	Note A		Note A		xxxx		xxxx	
BW Recv'r		Note A		Note A		xxxx		xxxx
LSC on	Note B		xxxx		Note C		xxxx	
Color Receiver		40		xxxx		Note C		xxxx
LSC on	Note B		xxxx		Note C		xxxx	
BW Recv'r		45		xxxx		Note C		xxxx
DSC on	33		xxxx		xxxx		29	
Color Receiver		45		xxxx		xxxx		38
DSC on	32		xxxx		xxxx		31	
BW Recv'r		45		xxxx		xxxx		43

Note A.—No tests made.

Note B.—The coarse appearance of the scanning raster gave the same type effect as offset carrier interference so observers were unable to distinguish between interference and normal appearance of picture.

Note C.—This test would have required two sets of signal generating equipment for the line-sequential system. Only one set of equipment was available.

Lower-adjacent-channel interference is more severe than upper-adjacent-channel interference by about 6 decibels when referred to the detector input.

From the standpoint of channel allocations, no substantial difference in the tolerable ratios was found for the various combinations of color and monochrome signals tested.

SUMMARY OF DATA OF PARTS I AND II*

For the convenience of the reader, the test data given in Part I of "A Study of Cochannel and Adjacent-Channel Interference of Tele-

Table IX—Summary of Average Ratios of Desired to Undesired Lower-Adjacent-Channel Television Signals (Decibels).

Interference of lower adjacent sound signal controlling for all combinations of monochrome and color signals used.

Tolerable ratio 26 decibels

Threshold ratio 30 decibels

Ratios are referred to the input of the detector.

Table X—Summary of Average Ratios of Desired to Undesired Adjacent-Channel Television Signals (Decibels).

Ratios Referred to Input of Detector
(Interfering signal on upper adjacent channel.)

Symbols:

BW—Standard Black and White

FSC—Field-Sequential Color

LSC—Line-Sequential Color

DSC—Dot-Sequential Color

Toler.—Tolerable

Thres.—Threshold

Desired Signal	BW		FSC		LSC		DSC	
	Toler.	Thres.	Toler.	Thres.	Toler.	Thres.	Toler.	Thres.
BW on BW Recv'r	19	24	21	24	19	23	20	24
FSC on Color Receiver	14	18	20	23	xxxx	xxxx	xxxx	xxxx
FSC on BW Recv'r	Note A	Note A	Note A	Note A	xxxx	xxxx	xxxx	xxxx
LSC on Color Receiver	Note B	Note B	xxxx	xxxx	Note C	Note C	xxxx	xxxx
LSC on BW Recv'r	Note B	Note B	xxxx	xxxx	Note C	Note C	xxxx	xxxx
DSC on Color Receiver	25	28	xxxx	xxxx	xxxx	xxxx	15	22
DSC on BW Recv'r	25	27	xxxx	xxxx	xxxx	xxxx	15	22

Note A.—No tests made.

Note B.—The coarse appearance of the scanning raster made it difficult and meaningless to make observations.

Note C.—This test would have required two sets of signal generating equipment for the line-sequential system. Only one set of equipment was available.

* "A Study of Cochannel and Adjacent-Channel Interference of Television Signals—Part I," *RCA Review*, Vol. 9, No. 1, pp. 99-120, March, 1950.

vision Signals" together with additional data pertaining to cochannel interference is summarized in Table VII for threshold interference and in Table VIII for tolerable interference.

Tables IX and X repeat the data for adjacent-channel interference with ratios referred to the input of the detector.

STABILIZATION OF WIDE-BAND DIRECT-CURRENT AMPLIFIERS FOR ZERO AND GAIN*

BY

EDWIN A. GOLDBERG

Research Department, RCA Laboratories Division,
Princeton, N. J.

Summary—A method for automatically stabilizing direct-current amplifiers against zero offset voltage and voltage drift is described. Stabilization is obtained through the application of a mechanical chopper to detect any zero offset error voltage. The circuit is such that the stabilization device does not alter the high-frequency response characteristics of the amplifier. Primary application has been in the field of analogue electronic computers.

A MAJOR OBSTACLE in the application of direct-current (dc) amplifiers has been their inherent dc voltage offset and drift which, in general, has been compensated by means of manual adjustments. This difficulty has been overcome for the case of narrow band amplifiers by utilizing a mechanical chopper to change the dc voltage into an alternating-current (ac) voltage, amplifying the resultant with an ac coupled amplifier, and rectifying the output of the

ac amplifier.¹ The available bandwidth of such a system is a function of the frequency of the mechanical chopper. This paper will describe an amplifier which utilizes a mechanical chopper for stabilizing with respect to dc without affecting the high frequency response.

Figure 1 is a block diagram of one form of the stabilized amplifier. It consists of a normal dc coupled feedback amplifier plus a mechanical chopper, an ac coupled amplifier, and a synchronous rectifier. The chopper samples the potential which appears at the summing point, A.

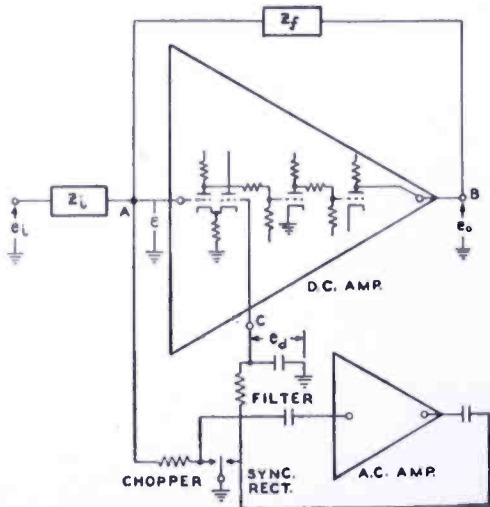


Fig. 1—Basic diagram of the stabilized dc amplifier.

* Decimal Classification: R363.3.

¹ A. J. Williams, Jr., R. E. Tarpley and W. R. Clark, "D-C Amplifier Stabilized for Zero Gain," *A.I.E.E. Transactions*, Vol. 67, pp. 47-57, 1948.

This voltage is amplified and rectified, and the output voltage of the rectifier is applied to the amplifier at some point, C , where a zero setting voltage may be inserted provided this point is not the summing point A . The rectifier is provided with a long time constant filter in order that components of the chopper frequency will not appear on the output of the dc amplifier. The input to the chopper is provided with a filter for reducing error voltage components of chopper frequency in order that ac input voltages synchronous with chopper frequency will not cause a dc voltage to be developed by the synchronous rectifier which would cause the dc amplifier to have a dc offset.

The operation principle of the amplifier may best be understood from the following mathematical analysis. Assume that the internal gain of the dc amplifier is equal in magnitude for signals inserted either at point A , the summing point, or at point C , the place where the zero set voltage is normally applied.

Let $G_1(\omega)$ = Gain of dc amplifier.

$G_2(\omega)$ = Gain of chopper, amplifier, rectifier chain.

k = Zero set voltage which would normally be necessary to cause e_o to be zero when ϵ is zero. This is the normal offset voltage of the amplifier referred to the input.

e_i = Input voltage to amplifier.

e_o = Output voltage of amplifier.

ϵ = Voltage at summing point.

e_d = Voltage at zero set point.

Z_i = Input impedance.

Z_f = Feedback impedance.

$$e_o = (\epsilon - e_d + k) G_1(\omega) \quad (1)$$

$$e_d = \epsilon G_2(\omega) \quad (\text{Note that } e_d = 0 \text{ when } \epsilon = 0. \text{ The chopper insures this for dc}) \quad (2)$$

$$\frac{e_i - \epsilon}{Z_i} = \frac{\epsilon - e_o}{Z_f} \quad (3)$$

$$\epsilon = \frac{Z_f}{Z_f + Z_i} e_i + \frac{Z_i}{Z_f + Z_i} e_o \quad (4)$$

$$e_d = \frac{Z_f}{Z_f + Z_i} e_i G_2(\omega) + \frac{Z_i}{Z_f + Z_i} e_o G_2(\omega). \quad (5)$$

By eliminating ϵ and e_d in the above equations, the following expression is obtained for the output voltage of the amplifier.

$$e_o = \frac{e_i \left[\frac{Z_f}{Z_f + Z_i} G_1(\omega) - \frac{Z_f}{Z_f + Z_i} G_1(\omega) G_2(\omega) \right] + k G_1(\omega)}{1 - \frac{Z_i}{Z_f + Z_i} G_1(\omega) + \frac{Z_i}{Z_f + Z_i} G_1(\omega) G_2(\omega)}. \quad (6)$$

If $\frac{Z_i}{Z_f + Z_i} G_1(\omega)$ is made very large relative to unity, the unit term in the denominator will have negligible effect and may be omitted. The expression for the output voltage as a function of the input voltage may then be written:

$$e_o = -e_i \frac{Z_f}{Z_i} + k \frac{Z_f + Z_i}{Z_i \{G_2(\omega) - 1\}}. \quad (7)$$

The first term on the right-hand side is desired, and the second term is the zero offset voltage term. Note that in order to reduce the zero offset voltage, it is only necessary to make $G_2(\omega)$ large at dc. $G_2(\omega)$ may be made large enough so that the second term of (7) is negligible, in which case the gain is

$$e_o = -e_i \frac{Z_f}{Z_i} \quad (8)$$

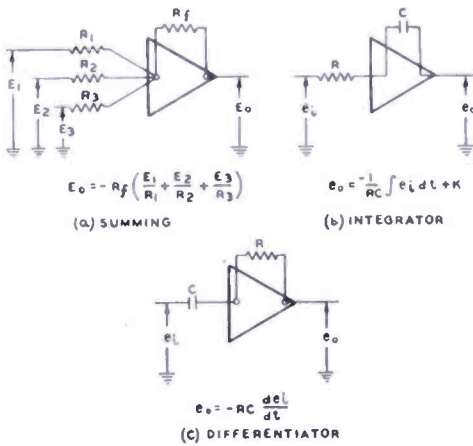
which states that the gain is the ratio of the feedback impedance to the input impedance, and that there is no dc offset.

The zero stabilizing circuit not only eliminates the zero and drift problems common to dc amplifiers, but also effectively increases the loop gain. The expression for the loop gain is

$$\mu\beta = \frac{Z_i}{Z_f + Z_i} \{G_1(\omega) - G_1(\omega) G_2(\omega)\}.$$

When Z_f and Z_i are equal (gain of unity), the feedback factor is 75,000,000, which is quite high. At dc, this amplifier is capable of producing a swing from -200 volts to +200 volts across a load resistance of 100,000 ohms.

The frequency response of this amplifier depends on the input and feedback networks. When these networks are identical (say equal resistances) the amplifier has a gain of unity and is flat at least out to 100 kilocycles. This amplifier was developed specifically for application in electronic analogue computers, and may be used as a summing amplifier, integrator, or differentiator, dependent on the input and feedback networks used. Figure 3 shows how the amplifier is adapted for these specific applications. The



stabilizer makes the frequent manual zero adjustment of dc computer amplifiers entirely unnecessary, and holds the offset to a much lower value than can ever be done practically through manual adjustments.

When used for the integrator application, the drift rate is extremely small, and when used as a summing amplifier or differentiator the spurious dc offset is held to a very low value. In the actual amplifiers

Fig. 3—Diagrams illustrating several basic computer applications for the dc amplifier.

constructed, the offset is generally less than 50 microvolts referred to the input when the input and feedback networks have impedances in the megohm range. The small offsets encountered are due to (1) spurious potentials developed within the chopper itself due to contact potential, thermals, etc., (2) grid current in the first stage of the dc amplifier (which would cause an output voltage of $Z_f \times$ grid current, (3) lack of infinite gain in the ac amplifier. Item (3) would cause an offset referred to the input of

$\frac{e_{do}}{G_2(0)}$ to first approximation where e_{do} is the voltage normally required at point C to zero the amplifier. Should the resulting small offset from these causes be greater than desired for some particular application, it could of course be reduced by a manual zero adjustment.

A FEEDBACK-CONTROLLED CALIBRATOR FOR PHONOGRAPH PICKUPS*

BY

J. G. WOODWARD

Research Department, RCA Laboratories Division,
Princeton, N. J.

Summary—The phonograph pickup calibrator is an electromechanical device for imparting known and controllable lateral motions to the stylus of a pickup under test. The calibrator employs a dynamic driving system, and electromechanical feedback is used to secure a uniform response between 20 and 20,000 cycles per second. The absolute as well as the relative response of a pickup can be conveniently and quickly measured within this frequency range.

INTRODUCTION

THE response-frequency and distortion characteristics of phonograph pickups are usually measured by means of tone records. One of the commercially available tone records is played in the conventional manner and measurements of the voltage generated by the pickup give the desired information. This method is convenient, particularly when the test must be made with the pickup *in situ* in some particular installation. Moreover, such tests are useful in giving an integrated picture of the reproducing system from record groove to amplifier output. On the other hand, when the characteristics of a large number of pickups are to be measured, tone record methods become unduly time-consuming. If it is desired to make prolonged measurements at some particular frequency, or intensive measurements within a narrow band of frequencies, or measurements at various amplitudes, tone records are inconvenient, to say the least. High-quality tone records of frequencies below 50 cycles per second and above 10,000 cycles per second are not readily available. Characteristics of a pickup at the extremes of its working range of frequency are often obscured by the relatively high noise level of the test record. Measurement of harmonic distortion in the output of a pickup is rendered difficult by wows and other undesirable changes in frequency. Perhaps most serious of all is the impossibility of separating the distortions (amplitude as well as nonlinear) introduced by the pickup itself from those initially present in the groove of the tone record,

* Decimal Classification: R391.12×621.372.

those caused by compliance of the groove walls, and those due to stylus tracking phenomena.

For the reasons enumerated, a device capable of imparting an accurately known and controllable mechanical vibration to the stylus of a phonograph pickup should be useful to those engaged in phonograph development programs. One such device, consisting of an electromagnetically driven reed and having a working range up to about 9000 cycles per second, has been reported.¹ In the following discussion a phonograph pickup calibrator having a useful working range from 20 to 20,000 cycles per second will be described.

DESCRIPTION OF CALIBRATOR

The phonograph pickup calibrator comprises two major parts, namely, an electromechanical driving system and an amplifier especially designed to energize the driving system. The electromechanical system

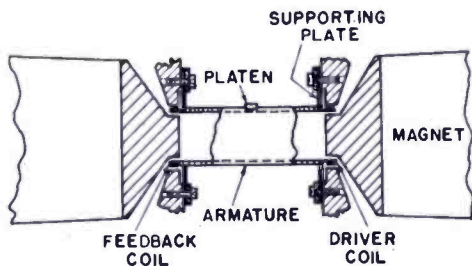


Fig. 1—Principal elements of calibrator driving system.

employs a dynamic drive. The available power of the amplifier is used to best advantage, while maintaining substantially uniform response throughout the useful frequency range, by placing the primary mechanical resonance of the driving system in the mid-audio range, and using electromechanical feedback to reduce the response at

resonance. The principal elements of the mechanical system are sketched in Figure 1. The armature consists of a circular, dural tube having a diameter of $\frac{5}{8}$ inch and a length of $1\frac{7}{8}$ inches. Coils wound on flanges at each end of the armature are centered in the annular air gaps of the magnetic structures. One coil acts as the driver coil, the other as the feedback coil. Alternating current supplied by the amplifier and passing through the driver coil reacts with the permanent magnetic field to set the armature tube into lateral oscillation parallel to its axis. Motion of the armature generates, in the feedback coil, a voltage which is returned to the driving amplifier in the proper phase to reduce the driving current over most of the audio range.

The armature is supported near each end by a thin, circular plate clamped at its outer edge. These plates have their central areas cut away to allow them to fit on flanges just inside the driver and feedback

¹ H. A. Pearson, R. W. Carlisle and H. Cravis, "Vibrators for Measurement of Response and Compliance of Phonograph Pickups," *Jour. Acous. Soc. Amer.*, Vol. 20, pp. 830-833, November, 1948.

coils. They are fastened to the armature tube with a thermosetting cement. The supporting plates also provide the restoring force for the resonant mechanical system. On the top side of the armature tube, midway between the ends, a $\frac{1}{8}$ -inch wide slot has been milled. A small platen of suitable material may be wedged and cemented in this slot. Grooves in the face of the platen receive the stylus of the phonograph pickup under test and impart to it the motion of the armature.

The circuitry of the driving amplifier is, for the most part, conventional. Two 6L6 tubes in push-pull in the output stage furnish adequate power to drive the calibrator. The voltage generated by the feedback coil is amplified and mixed with the main signal voltage at the grid of the phase inverter preceding the output stage. A potentiometer connected across the feedback coil terminals permits adjustment of the amount of feedback from zero to a maximum set by stability considerations. A compensation network is included in the feedback loop to correct the loop transmission for uniform armature response in the upper audio range. Additional compensation outside the feedback loop serves to make the armature response, with the feedback control at its maximum setting, approximately that prescribed by the standard recording characteristic, i.e., constant amplitude of motion below and constant velocity above 500 cycles per second. A meter jack on the amplifier chassis furnishes convenient access to the voltage generated by the feedback coil. A high-impedance vacuum-tube voltmeter connected at this point gives readings directly proportional to the velocity of the armature at any frequency within the working range of the calibrator regardless of the amount of feedback used.

Connections between the amplifier chassis and the driving unit are made through two flexible, shielded cables. The calibrator as it appears in use is shown in Figures 2 and 3.

OPERATIONAL CHARACTERISTICS

The armature velocity versus frequency characteristics of the calibrator in the audio range for various amounts of feedback are shown in Figure 4. The principal resonance at 1800 cycles per second is evident. With the maximum available feedback the velocity curve agrees with the standard recording characteristic within ± 2 decibels. This is probably as close an agreement as is possible in this system with simple R-C compensation. A closer fit can be secured, of course, by the use of more complicated L-C networks. With the feedback control at its maximum setting the feedback is seen to be negative over most of the audio range. However, it becomes positive, or regen-

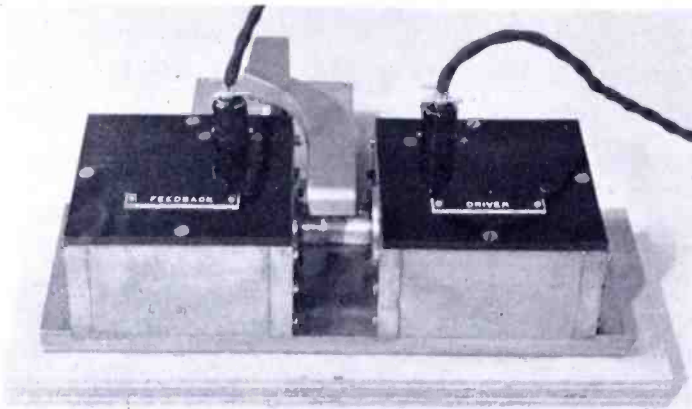
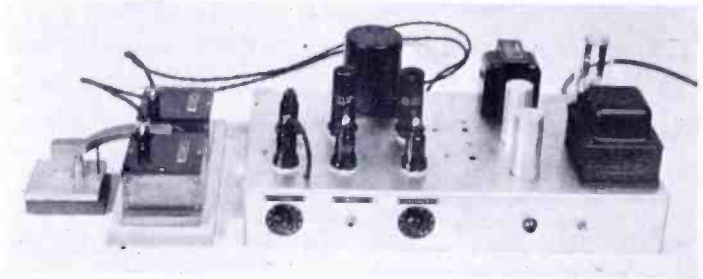


Fig. 2 — Calibrator driving system with a phonograph pick-up in the test location.

erative, below 75 and above 7600 cycles per second. Reasons for this change will be considered in the following section.

The feedback voltage versus frequency characteristics for frequencies between 10 and 100 kilocycles, with and without feedback, are shown in Figure 5. Above about 30 kilocycles the voltage generated by the feedback coil is no longer an accurate measure of the armature

Fig. 3 — Calibrator driving system and amplifier.



velocity since, at these higher frequencies, the armature length is an appreciable fraction of a wave length of the transmitted vibrations, and all parts of the armature may not move with the same amplitude and phase. With excessive amounts of feedback, the calibrator oscillated in the neighborhood of 65 kilocycles. The tendency for this high-

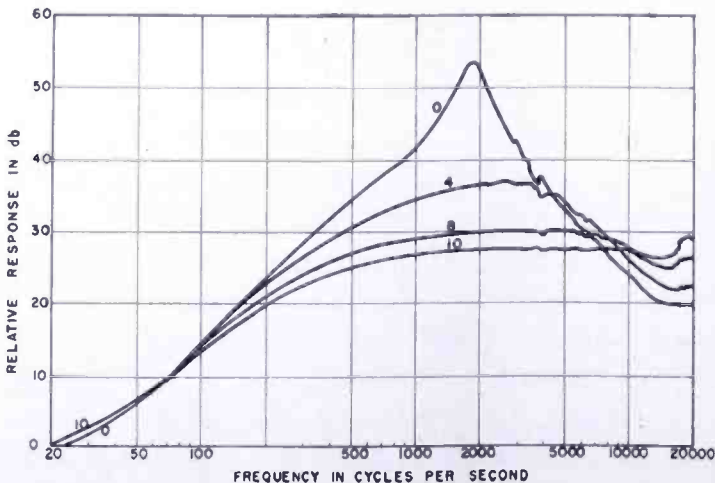


Fig. 4—Armature velocity vs. frequency for various amounts of feedback. Numbers on curves are feedback control settings.

frequency oscillation was considerably reduced by applying mechanical damping to the armature and was made entirely negligible by inserting the proper compensation in the feedback loop and keeping the amount of feedback within reasonable bounds. Some instability persists in the region between 18 and 22 kilocycles. This is not surprising in view of the relatively large amount of positive feedback effective at these frequencies and in view of the fact that the armature supporting plates exhibit mechanical antiresonances in this region. The instability is manifested by a dependence of the response upon the level of operation

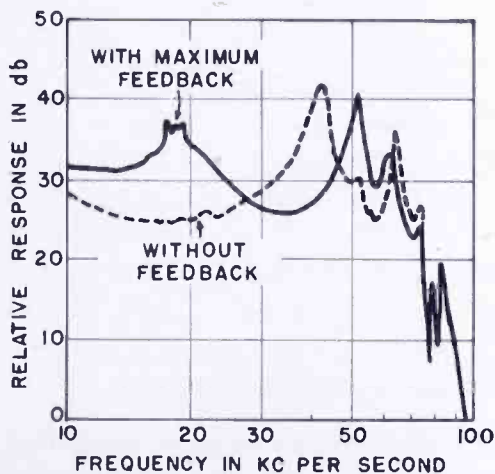


Fig. 5—Voltage generated by feedback coil as a function of frequency.

and by the occasional absence of the four or five decibel rise in response shown at 18 kilocycles with maximum feedback. Since these variations are rather small and have no effect upon the response below 15 kilocycles, the usefulness of the calibrator is not seriously impaired. In all other respects the calibrator has proved to be stable in operation and has yielded highly reproducible results on successive tests. The mechanical loading imposed by the stylus of a pickup under test does not alter the motion of the armature in any measurable degree.

With maximum feedback, armature velocities of 0.5 centimeter per second in the constant velocity portion of the response are easily obtained. Much higher levels of operation result in amplifier overloading or in excessive heating of the driver coil except when operating with reduced feedback and in the neighborhood of mechanical resonance. Armature velocities were established by measuring amplitudes with a microscope having a calibrated eyepiece. It was found that the root-mean-square armature velocity was equal to 5.98 times the root-mean-square voltage generated by the feedback coil.

The results of measurement of harmonic distortion are shown in Table I. The measurements were made on the voltage generated by the feedback coil and represent the distortion existing in the armature motion.

The voltage generated in the feedback coil due to induction by the current in the driver coil was found to be at least 30 decibels below the voltage generated by motion of the feedback coil. With a ratio this great no difficulty was experienced in controlling the feedback because

of the direct coupling between coils. However, the proximity of the driver coil to a phonograph pickup under test caused voltages to be induced in most magnetic and electronic pickups of sufficient magnitude to be troublesome. Crystal pickups, being electrostatic devices, were not affected in this way. Refinements in construction of the calibrator are contemplated to extend its use to magnetic and electronic pickups.

Table I—Total Root-Mean-Square Harmonic Distortion*

Frequency (cycles per second)	Armature Velocity (centimeters per second)		
	.25	.50	.75
500	.30%	.63%	.98%
5000	.51%	.97%	1.40%

* With maximum feedback.

ELECTROMECHANICAL FEEDBACK CONSIDERATIONS

Only a very few attempts to control electromechanical devices over a wide frequency range by means of feedback have been reported. The application of feedback to loudspeakers^{2, 3} and microphones⁴ evidently has not progressed beyond the experimental stage. Phonograph recorders are now available in which feedback effectively reduces distortion and improves the transient response and stability.^{5, 6} Regardless of their particular configuration, all electromechanical feedback devices present certain characteristic problems which are associated with higher order resonances, or "breakup," of the vibrating system. These are of a fundamental nature. They arise from the fact that the dimensions of the moving parts of any practical electromechanical device are comparable to the wave length of the vibrations being transmitted at audio or slightly higher frequencies. Stated otherwise, the mechanical system has distributed rather than lumped parameters at these

² H. F. Olson, *ELEMENTS OF ACOUSTICAL ENGINEERING*, Second Edition, pp. 158-159; D. Van Nostrand Company, Inc., New York, 1947.

³ D. N. T. Williamson (letter to editor), *Wireless World*, Vol. 53, p. 402, October, 1947.

⁴ Jan de Boer and Gerrit Schenkel, "Electromechanical Feedback," *Jour. Acous. Soc. Amer.*, Vol. 20, pp. 641-647, September, 1948.

⁵ L. Vieth and C. F. Wiebusch, "Recent Development in Hill and Dale Recorders," *Jour. Soc. Mot. Pict. Eng.*, Vol. 30, pp. 96-103, January, 1938.

⁶ G. R. Yenzler, "Lateral Feedback Disc Recorder," *Audio Eng.*, Vol. 33, pp. 22-26, 44-45, September, 1949.

frequencies. This situation is not ordinarily encountered in audio-frequency circuitry except in the case of very long transmission lines. It is a major factor in limiting the use of electromechanical feedback.

Effects of the short wave length of mechanical vibrations are well illustrated in the behavior of the phonograph pickup calibrator by the pronounced higher order resonances between 10 and 100 kilocycles. The armature tube can be treated as a mechanical transmission line in longitudinal vibration, driven through the mass of the driver coil and loaded with the mass of the feedback coil. When this is done, calculated resonances are found in agreement with those observed at 42 and 85 kilocycles. Other high-frequency resonances can be attributed to higher order coupling between the armature tube and the supporting plates. Transverse vibrations in a sheet of dural .010 inch thick have a quarter-wavelength of the order of .5 centimeter at 10 kilocycles. The armature supporting plates are cut from such a sheet, so it is not surprising to find them giving rise to minor perturbations in the response at audio frequencies. Mathematical analyses of mechanical members in transverse vibration—and every vibrating system has at least one—are so involved that useful results cannot be obtained except in a few highly idealized cases. Consequently, it is virtually impossible to predict completely the behavior of a wide-band system when even the simplest mechanical device is included in the feedback loop. This is true even though feedback network theory is well understood and general equations in terms of the loop transmission can be written.

In the neighborhood of a principal resonance, an ideal mechanical vibrating system can be represented by lumped parameters. At resonance the phase shifts through 180 degrees, and somewhat above and below resonance the velocity-frequency characteristic falls off at a 6-decibel-per-octave rate for increasing and decreasing frequency respectively. The electrical components of the driving amplifier contribute to the transmission characteristic to give a response which, in general, falls off at a rate considerably greater than 6 decibels per octave. Bode⁷ has shown that positive feedback at high and low frequencies, in a system having negative feedback in the mid-range, is a consequence of a greater than 6-decibel-per-octave slope in the loop transmission. This phenomenon is frequently evidenced in feedback amplifiers by peaking of the response at frequencies near the limits of the transmission band. The situation can be ameliorated somewhat by making the pass-band of the electrical components of the amplifier

⁷ H. W. Bode, NETWORK ANALYSIS AND FEEDBACK AMPLIFIER DESIGN, p. 285; D. Van Nostrand Company, Inc., New York, 1945

as wide as possible and by including, in the feedback loop, tailor-made compensation to partially match the characteristics of the mechanical system. In this way the positive feedback can be reduced in magnitude by spreading it out over a wider range of frequencies. This, of course, calls for control of the transmission for frequencies far beyond the nominal working range of the system. In view of the high degree of complexity of the mechanical system at high frequencies this is a difficult feat, indeed.

The above discussion points out some of the problems encountered in the construction of electromechanical feedback systems. It has been demonstrated in at least a few instances that successful systems can be built in spite of the fundamental nature of the problems. It should be evident, however, that feedback is not a cheap cure-all for the shortcomings of electromechanical systems. The design problems and the requirements of precision in manufacture for a system employing feedback are likely to be even more severe than for a system having the same nominal working range of frequency but without feedback. This is the price that must be paid for the advantages afforded by feedback, namely, improved stability, linearity, and uniformity of response.

APPLICATION OF CALIBRATOR

The phonograph pickup calibrator has been used to measure the response-frequency characteristics of a number of crystal pickups. Results for a pickup supplied with a common type of record player will be given here. For purposes of comparison, the upper half of Figure 6 shows a pickup response curve obtained by playing a standard tone record with the pickup mounted on the record player. The lower half of the figure gives the response obtained with the calibrator. In this case the pickup cartridge was mounted on a special, adjustable tone arm. In both cases the pickup was connected to a 500,000-ohm load. The calibration curve giving the armature velocity is also shown. The traces obtained with the calibrator become fuzzy below 70 cycles per second because of hum in the automatic curve-tracing equipment. The small variations between 400 and 560 cycles per second in the calibrator curves are caused by a parasitic resonance in the frame of the calibrator. A tone-arm resonance at 27 cycles per second and a stylus-arm resonance at 12 kilocycles are evident.

At 1500 cycles per second, the output of the feedback coil was .076 volt. This, multiplied by 5.98, gives a root-mean-square armature velocity of .455 centimeters per second. At 1500 cycles per second, the corresponding output of the pickup was .0515 volt. By using these figures and referring to the curves of Figure 6, the absolute sensitivity

of the pickup may be calculated for any frequency between 20 and 20,000 cycles per second.

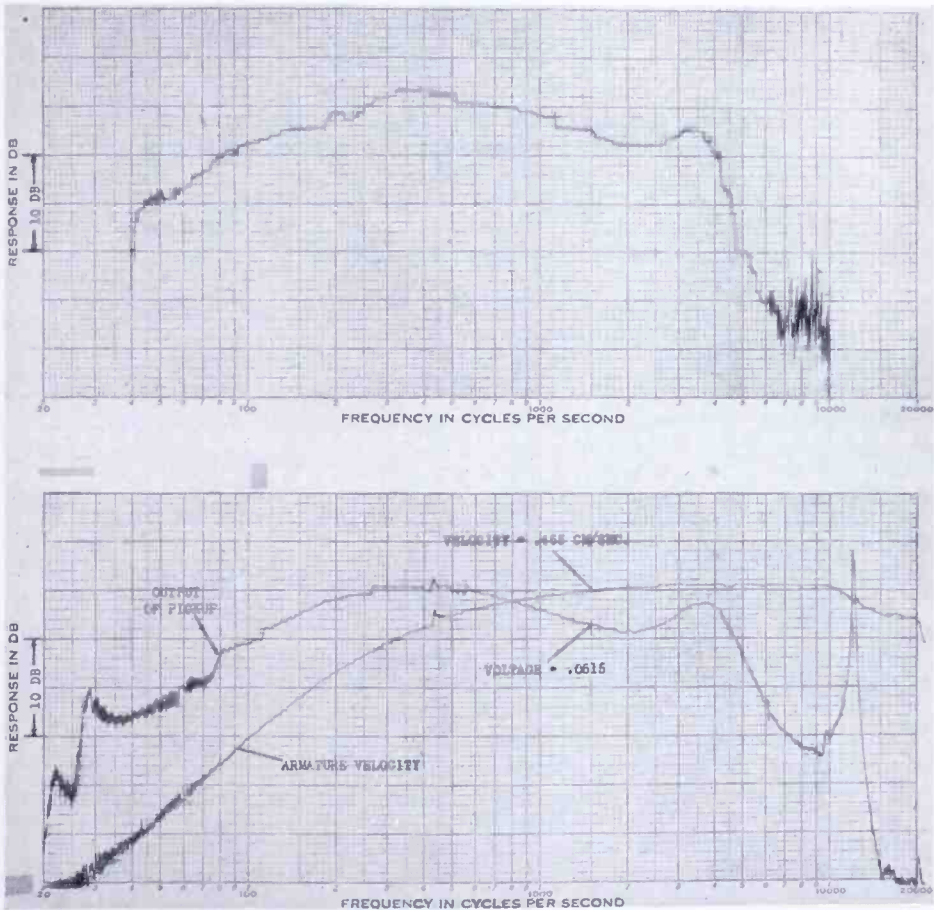


Fig. 6—Above: Response of pickup playing a standard tone record.
Below: Response of same pickup measured with calibrator.
The velocity of the calibrator armature is also shown.

In most tests the platen was a piece of material cut from a vinylite record. Other materials have been used, however. The material of the platen seems to make little difference in the response curves obtained except at the low-frequency tone-arm resonance where the pickup stylus offers a high impedance to the driving force. Any compliance of the platen material is in parallel with the compliance of the stylus arm and therefore lowers the frequency of the tone-arm resonance. Since it provides a convenient means of measuring this effect, the calibrator may prove to be useful in studying the dynamic properties of record materials.

ACKNOWLEDGMENT

In conclusion, the writer wishes to express his appreciation for many helpful suggestions arising from discussions with A. R. Morgan of these laboratories.

RCA TECHNICAL PAPERS†

First Quarter, 1950

Any request for copies of papers listed herein should be addressed to the publication to which credited.

"Adjustments for Obtaining Optimum Performance in Magnetic Recording", A. W. Friend, <i>RCA Review</i> (March)	1950
"Answers to Questions about Color Television", Pamphlet, RCA Department of Information (March 30)	1950
"An Automatic Plotter for Electron Trajectories", David B. Langmuir, <i>RCA Review</i> (March)	1950
"The 'Bantam' Mike — KB-2C", L. J. Anderson and L. M. Wigington, <i>Broadcast News</i> (March-April)	1950
"The Bantam Velocity Microphone", L. J. Anderson and L. M. Wigington, <i>Audio Eng.</i> (January)	1950
"Behind the Scenes at a Television Show", Milton Brown, <i>Rad. & Tele. News</i> (March)	1950
"A Broadband Transition from Coaxial Line to Helix", C. O. Lund, <i>RCA Review</i> (March)	1950
"Characteristics of High-Efficiency Deflection and High-Voltage Supply Systems for Kinescopes", O. H. Schade, <i>RCA Review</i> (March)	1950
"Characteristics of High-Efficiency Deflection and High-Voltage Supply Systems for Kinescopes", O. H. Schade, <i>RCA Licensee Bulletin LB-791</i> (February 10)	1950
"Colorimetric Analysis of RCA Color Television System", Bulletin, RCA Laboratories Division (February 15)	1950
"Derivation of Thermal Emittance Equation", A. D. Power, <i>Amer. Jour. of Phys.</i> (March)	1950
"Design of Absorption Traps", Jack Avins, <i>Electronics</i> (January)	1950
"Design of 41.25-MC Video I-F Amplifiers", J. Avins, <i>RCA Licensee Bulletin LB-790</i> (January 10)	1950
"Directional Antenna Systems", C. A. Rosencrans, <i>Broadcast News</i> (March-April)	1950
"Directional Antenna Systems for Microwave TV — Part I", C. A. Rosencrans, <i>Tele-Tech</i> (February)	1950
"Directional Antenna Systems for Microwave TV, Part II", C. A. Rosencrans, <i>Tele-Tech</i> (March)	1950
"The Electron Coupler", C. L. Cuccia and J. S. Donal, Jr., <i>Electronics</i> (March)	1950
"An Experimental Determination of the Sideband Distribution in the RCA Color Television System", Bulletin, RCA Laboratories Division (January 17)	1950
"An Experimental UHF Television Converter", Bulletin, RCA Laboratories Division (January 30)	1950
"Experimental Ultra-High-Frequency Television Station in the Bridgeport, Connecticut Area", R. F. Guy, J. L. Seibert and F. W. Smith, <i>RCA Review</i> (March)	1950
"An Experimental Ultra-High-Frequency Television Tuner", T. Murakami, <i>RCA Review</i> (March)	1950
"First UHF TV Transmitter Shipped", <i>Broadcast News</i> (January-February)	1950

† Report all corrections or additions to *RCA Review*, Radio Corporation of America, RCA Laboratories Division, Princeton, N. J.

- "The Genlock for Improved TV Programming", J. H. Roe, *Broadcast News* (March-April) 1950
- "Giving TV a New Meaning", V. K. Zworykin, *Televiser* (February) 1950
- "High Efficiency Deflection and High Voltage Circuits for Short Metal Kinescope RCA-16GP4", *RCA Application Note AN-142*, RCA Tube Department, Harrison, N. J. (March 31) .. 1950
- "High-Efficiency Loud Speakers for Personal Radio Receivers", H. F. Olson, J. C. Bleazey, J. Preston and R. A. Hackley, *RCA Review* (March) 1950
- "High Gain and Directional Antennas for Television Broadcasting", L. J. Wolf, *Broadcast News* (March-April) 1950
- "How to Adjust Frequency Response in Video Amplifiers for TV", J. H. Roe, *Broadcast News* (March-April) 1950
- "How to Use Standard Filters with New Flat Magnetic Pickup", H. E. Roys, *Broadcast News* (March-April) 1950
- "How to Use the TM-5A Monitor to Check Sync Signals by the 'Pulse Cross' Method", H. J. Markley, *Broadcast News* (January-February) 1950
- "International Allocation of Radio Frequencies", T. L. Bartlett, *Signals* (January-February) 1950
- INTRODUCTION TO LUMINESCENCE OF SOLIDS, H. W. Leverenz, John Wiley & Sons, Inc., New York, N. Y. (January) 1950
- "Laboratory Modifications in the RCA Model EMC Electron Microscope", S. G. Ellis, *Rev. Sci. Instr.* (March) 1950
- "Manufacture of Electron Tube Parts by the Rubber-Die Technique", W. J. Bachman, *Elec. Eng.* (March) 1950
- "Mixing Local and Remote Television Signals", W. E. Wells and J. M. Weaver, *Tele-Tech* (January) 1950
- "Mobile Radio Sets on 152-174 Megacycles", R. A. Beers, W. A. Harris and A. D. Zappacosta, *Elec. Eng.* (March) 1950
- "Phototube Controls R-F Welding", H. H. Wittenberg, *Electronics* (January) 1950
- "Radiophoto Practices and Problems", R. E. Hammond, *Elec. Eng.* (March) 1950
- "Radio and Television in 1949-1950", David Sarnoff, *Broad. Eng. Jour.* (January) 1950
- "Reducing Radiation from Heat Equipment", G. W. Klingeman, *Elec. Eng.* (January) 1950
- "Receiving Tubes Employing Secondary Electron Emitting Surfaces Exposed to the Evaporation from Oxide Cathodes", C. W. Mueller, *Proc. I.R.E.* (February) 1950
- "Recent Developments in Color Synchronization in the RCA Color Television System", Bulletin, RCA Laboratories Division (February 8) 1950
- "Recording Dilatometer for Measuring Thermal Expansion of Solids", John C. Turnbull, *American Ceramic Society Journal* (February) 1950
- "Resonant Frequencies and Characteristics of a Resonant Coupled Circuit", C. L. Cuccia, *RCA Review* (March) 1950
- "A Simplified Receiver for the RCA Color Television System", Bulletin, RCA Laboratories Division (February 28) 1950
- "A Single Tube A.F.C. Circuit for TV Deflection Systems", J. A. Cornell, *Radio & Tele. News* (January) 1950
- "Stabilizing the VFO", C. A. West, *CQ* (February) 1950
- "Studies of the Action of Sodium Fluoride on Human Enamel", D. B. Scott, R. G. Picard and R. W. S. Wyckoff, *Journal of Dental Research* (January) 1950

- "A Study of Cochannel and Adjacent-Channel Interference of Television Signals, Part I—Cochannel Studies", *RCA Review* (March) 1950
- "A Study of Co-Channel and Adjacent Channel Interference of Television Signals, Part I", Bulletin, RCA Laboratories Division (January 17) 1950
- "A Study of Co-Channel and Adjacent Channel Interference of Television Signals, Part II", Bulletin, RCA Laboratories Division (January 30) 1950
- "Supplemental Data on UHF Tuner Described in Bulletin 'An Experimental UHF Television Tuner'", Bulletin, RCA Laboratories Division (January) 1950
- "Television Service. Part IX—Blanking and Synchronizing Signals", J. R. Meagher, *RCA Rad. Serv. News* (Spring) .. 1950
- "A Three-Color Direct-View Receiver for the RCA Color Television System", Bulletin, RCA Laboratories Division (January 9) 1950
- "The Trend in Drive-In Theaters", C. R. Underhill, Jr., *Jour. S.M.P.T.E.* (February) 1950
- "TV Remote Control Switching", W. E. Tucker and C. R. Munro, *Broadcast News* (March-April) 1950
- "Use of Sharp-Cutoff Miniature Pentode RCA 6CB6 in Television Receivers", *RCA Application Note AN-143*, RCA Tube Department, Harrison, N. J. (March 31) 1950
- "A Variable Speed Turntable and Its Use in the Calibration of Disk Reproducing Pickups", H. E. Haynes and H. E. Roys, *Proc. I.R.E.* (March) 1950
- "What Procurement Expects from Standardization", V. deP. Goubeau, *Standardization* (January) 1950
- NOTE—Omissions or errors in these listings will be corrected in the yearly index.

Addendum:

"Adjustments for Obtaining Optimum Performance in Magnetic Recording", by A. W. Friend, pp. 38-54, March, 1950.

It has come to the attention of the author that the following two references, which should have been included in the above paper, were inadvertently overlooked:

J. W. Gration, "Noise in Magnetic Recording System as Influenced by the Characteristics of Bias and Erase Signals", *Jour. Acous. Soc. Amer.*, Vol. 21, No. 2, pp. 74-81, March, 1949.

Lynn C. Holmes, "Techniques for Improved Magnetic Recording" *Elec. Eng.*, Vol. 68, No. 10, pp. 836-841, October, 1949.

AUTHORS



JOSEPH R. BENNETT received the B.S. degree in Electrical Engineering in 1943 and the B.S. degree in Industrial Engineering in 1947, both from the University of Washington. From 1943 to 1946 he was on active duty with the United States Army Signal Corps in Europe. He joined the RCA Student Training Program in 1948 and since October of that year he has been with the Television Transmitter Section of the Engineering Products Department.

O. O. FIET received the B.S. degree in Electrical Engineering from the University of Utah in 1940 and the M.S. in Electrical Engineering from the University of Pennsylvania in 1947. He is, at present, engaged in further part time graduate work at the University of Pennsylvania. Since 1940, he has been a member of the Engineering Section, Engineering Products Department of the RCA Victor Division at Camden, N. J. He has worked on FM and AM broadcast transmitters, communication transmitters, radar transmitters, antennas and receivers. Since the war, most of his work has been on the design and development of FM and TV broadcast transmitting antennas and filter circuits. During 1947 to 1948, he was instructor in "Radio Receiver Design" for the RCA Victor Technical Training Program in Camden. Mr. Fiet is an Associate Member of the Institute of Radio Engineers.



EDWIN A. GOLDBERG received the degrees of B.S. in E.E. and M.S. in E.E. in 1938 and 1940 at the University of Texas. From 1938 to 1939 he was employed on a field seismograph crew by the Magnolia Petroleum Co. He joined the RCA Manufacturing Co. in 1940 as a student engineer, and was assigned to the Research Division in 1941. He was transferred to Princeton in 1942 with RCA Laboratories Division. Mr. Goldberg is a Member of Eta Kappa Nu, Tau Beta Pi, Sigma Xi, and the American Institute of Electrical Engineers.

RUSSELL E. HAMMOND joined the operating staff of RCA Communications, Inc. in 1932. In 1936 he transferred to the Program-Radiophoto Department where he served as a technician until 1945. During the period 1945-1946 he entered foreign service as Assistant Manager of the RCA Manila station which was rehabilitated in June 1945 after its destruction during the Philippine campaigns. After returning to New York he served as Manager, Program-Radiophoto until 1949 when he became an Engineering Assistant in the Office of the Traffic Engineer.





EDWARD O. JOHNSON received the B.S. degree in Electrical Engineering from Pratt Institute of Brooklyn in 1948. From 1941-1945 he served as an electronic technical in the U. S. Navy. In 1948 he joined the RCA Laboratories Division, Princeton, N. J., where he is now engaged in work on gaseous electronics. Mr. Johnson is a member of the Institute of Radio Engineers.

LESTER S. LAPPIN received the B.S. degree in Communications from the Massachusetts Institute of Technology in 1935. From 1935 to 1937 he was an engineer at the Cornell-Dubilier Electric Corporation. In 1937 he joined the Federal Telegraph Company where he was engaged in the design of radio transmitters and the installation of radio range equipment. In 1940 he joined Harvey-Wells Electronics, Inc. as a transmitter engineer. Since 1941 he has been associated with the RCA Victor Division in Camden, N. J., as a design engineer in the Industrial Heating and Broadcast Transmitter Divisions. Mr. Lappin is a Senior Member of the Institute of Radio Engineers.



LOUIS MALTER received the B.S. degree from the College of the City of New York in 1926 and the M.A. and Ph.D. degrees in Physics from Cornell University in 1931 and 1936, respectively. He taught Physics at the College of the City of New York from 1926 to 1928. He was with the Acoustic Research and Photophone Divisions of Radio Corporation of America from 1928 to 1930, and during the Summer of 1931. From 1933 to 1942 he was with RCA Manufacturing Company at Camden, N. J., and from 1942 to 1943 with RCA Laboratories Division at Princeton, N. J. From 1943 to 1946, he was in charge

of the Special Development Division of RCA Manufacturing Company at Lancaster, Pa. From May 1946 to December 1947 he was in charge of the Vacuum Tube Research Section of the Naval Research Laboratory, Washington, D.C. In December 1947 he returned to the RCA Laboratories where he is now engaged in research on gaseous electronics. Dr. Malter is a Fellow of the American Physical Society, a Senior Member of the Institute of Radio Engineers, a Member of the American Association for the Advancement of Science, and a Member of Sigma Xi.

MADISON P. REHM graduated from RCA Institutes in 1923. In the same year he joined the RCA Engineering Department in New York City. From 1924 to 1928 he was with the Design Laboratory in New York, and from 1928 to 1930 he was at the experimental radiophoto station at New Brunswick, N. J. From 1930 to 1940 he was at the Frequency Measuring Laboratory of RCA Communications, Inc., at Riverhead, L.I., N.Y. and from 1940 to 1943 with the Program Radiophoto Services of that company in New York City. In 1943 he took Military Leave and served with the Communication Branch Office of Strategic Services until 1946. Mr. Rehm is now Supervisor of Technical Facilities, Program Radiophoto Services in New York.





S. H. SIMPSON, JR. received the B.S. degree in Electrical Engineering from Texas A & M College in 1928, when he joined RCA working in the Technical and Test Department. From 1930 to 1933 he was with RCA Communications, Inc. in Riverhead, L.I., transferring in 1933 to the New York central office as Manager of Program and Radiophoto Services. From 1941 to 1945 he served in the armed forces, first in the Censorship Bureau for International Communications, and later as Deputy Chief of the Communications Branch O.S.S., of the E.T.O., also heading a special intelligence unit. In October 1945 he

returned to RCA Communications, Inc. and is now Traffic Engineer in the Office of the Executive Vice President. Mr. Simpson is a Member of the Institute of Radio Engineers and the American Institute of Electrical Engineers.

J. G. WOODWARD received the B.A. degree from North Central College in 1936, the M.S. degree in Physics from Michigan State College in 1938, and the Ph.D. degree in Physics from the Ohio State University in 1941. He held Graduate Assistantships at Michigan State College from 1936 to 1939 and at the Ohio State University from 1939 to March 1941. In March 1941 he joined the Research Division of the RCA Manufacturing Company at Camden, N. J., and later that year transferred to the RCA Laboratories Division at Princeton, N. J. where he has been engaged in research in acoustics. Dr. Woodward is a member of the Acoustical Society of America and Sigma Xi, and is a Fellow of the American Association for the Advancement of Science.



